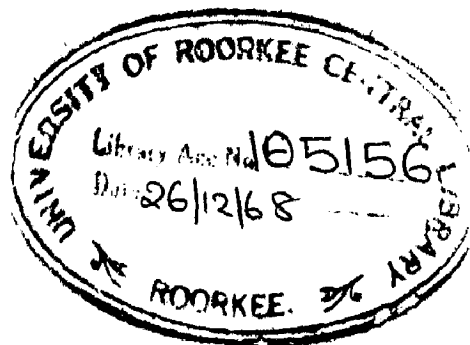


ANALYSIS OF THE PERFORMANCE OF BUNDLE CONDUCTORS ON EHV TRANSMISSION LINES

A Dissertation
submitted in partial fulfilment
of the requirements for the Degree
of
MASTER OF ENGINEERING
in
POWER SYSTEM ENGINEERING

By
H. CHANDRA GUPTA



DEPARTMENT OF ELECTRICAL ENGINEERING
UNIVERSITY OF ROORKEE
ROORKEE
August, 1968

A_B_S_T_R_A_C_T.

With the increase in the voltage of transmission many problems arise. Of them the two important problems are Corona losses and Radio interference. Unless the voltage gradient is limited, the losses can become very high and the interference to radio listeners can become excessive. Bundle conductors, if used decrease the operating voltage gradient and thus bring the above two factors under control.

In addition to the above two advantages, power transmission capability and the permissible voltage of operation, increase substantially. The above advantages are obtained largely by changing from one conductor to two conductors per phase. These points are discussed in detail. Extensive tables of the electrical parameters have been prepared.

An introductory investigation of the unbalance evaluation has been presented. A thorough study of unbalances is time consuming as the number of variables to be studied is too large. Calculations of the unbalances are done with the help of the digital computer IBM 1620.

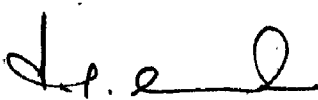
Bundle conductors have also been used for DC power transmission. A comparison of the operation of bundle conductors on AC and DC systems is presented.


CERTIFICATE

Certified that the dissertation titled "Bundle Conductors on EHV Transmission Lines" which is being submitted by Sri H.Chandra Gupta, in partial fulfilment for the award of the degree of Master of Engineering in Electrical Power Systems of University of Roorkee, is a record of candidate's own work carried out by him under our supervision and guidance. The matter embodied in this dissertation has not been submitted for the award of any other Degree or Diploma.

This is further to certify that he has worked for a period of 8 months from December 1967 to July 1968 for preparing dissertation for Master of Engineering Degree at the University.

Dated: 17. 8. 68
ROORKEE


(T.S.M. RAO)
Prof. & Head of the
Elect. Engg. Department,
University of Roorkee,
ROORKEE.


(K.B. MISRA)
Lecturer,
Elect. Engg. Department,
University of Roorkee,
ROORKEE

ACKNOWLEDGEMENTS

The author expresses his sincere thanks to Dr.T.S.M. Rao, Prof.& Head of the Elect.Engg.Deptt., University of Roorkee, Roorkee for initiating this topic for the dissertation and for his able guidance and suggestions in preparation of this work.

Sincere thanks are also due to Mr. K.B. Misra, Lecturer in Electrical Engineering for his guidance and encouragement throughout this work.

Dated: 15 Aug '68

ROORKEE



H. Chandra Gupta

CONTENTS

	<u>Page</u>
ABSTRACT	I
CERTIFICATE	II
ACKNOWLEDGEMENTS	III
NOMENCLATURE	VI
CHAPTER - 1 BUNDLE CONDUCTOR TRANSMISSION LINES	1
1.1. Introduction	1
1.2. Development of bundle conductor lines	2
1.3. Cost analysis	5
1.4. Transmission capability	7
1.5. Voltage gradients	8
1.6. Corona losses	9
1.7. Radio interference	10
1.8. Special features of bundle conductor lines	11
1.9. Some aspects of mechanical behaviour of bundle conductor lines	12
1.10. Design of bundle systems	13
1.10.1. Choice of number and size of conductors	13
1.10.2. Optimum intra-conductor spacing	15
1.11. Advantage of bundle conductor lines	17
CHAPTER - 2 VOLTAGE GRADIENT STUDIES	18
2.1. Introduction	20
2.2. The case of a single conductor	20
2.3. The case of the n conductors arranged on the circumference of a circle	21
2.4. Equivalent radii and gradient determination	21
2.5. Gradient distribution around the circumference	23
2.6. Effect of conductor cross section on gradient	24
2.7. Effect of conductor height	25
2.8. Effect of phase separation and intra-conductor separation	25

		Page
	2.9. Comparison of the methods of gradient determination.	26
CHAPTER 3	ELECTRICAL CHARACTERISTICS OF BUNDLE CONDUCTOR LINES	27
	3.1. Introduction	27
	3.2. Method of Calculation and assumptions	27
	3.3. Sequence impedances	30
	3.4. Reactances of single and bundle conductor lines	30
	3.5. Effect of number of conductors and intra-conductor spacing on reactances	31
	3.6. Tables for quick estimation of Reactances	32
CHAPTER 4	CORONA ON BUNDLE CONDUCTORS	33
	4.1. Corona phenomenon	33
	4.2. Theory of AC Corona	34
	4.3. Corona in foul weather	36
	4.4. Corona initiation voltage	37
	4.5. Effects of Corona	39
	4.6. Corona loss calculations	40
	4.7. Bundle conductor efficiency coefficients.	40
	4.8. Methods of Corona loss measurement	43
	4.9. Corona loss results from test projects.. . . .	45
	4.9.1. Factors that influence	45
	4.9.2. Hourly loss variations	46
	4.9.3. Losses and system variables	48
CHAPTER 5	RADIO INTERFERENCE FROM BUNDLE CONDUCTOR LINES	50
	5.1. Introduction	50
	5.2. Noise generation and propagation	50
	5.3. Adam's theory and analytical determination of RI-	52
	5.4. Design factors	55

	<u>Page</u>
5.6. Measurement of RI	59
5.7. Frequency Spectrum	60
5.8. RI and System variables	61
5.9. The case of a distribution line crossing the EHV line	63
5.10. Reduction of RI	64
CHAPTER 6 UNBALANCES OF UNTRANSPOSED BUNDLE CONDUCTOR LINES	66
6.1. Introduction	66
6.2. Investigation of unbalances	66
6.3. Electrostatic unbalance to ground	68
6.3.1. Outline of the method	68
6.3.2. General solution	69
6.3.3. Line with no ground wires	70
6.3.4. Negative and zero sequence unbalances	71
6.3.5. Line with two ground wires	72
6.4. Electromagnetic unbalance	74
6.4.1. Line with no ground wires	74
6.4.2. Line with two ground wires	75
6.5. Reduction of unbalances	77
6.6. Conclusions	78
CHAPTER 7 BUNDLE CONDUCTORS FOR DC TRANSMISSION	79
7.1. Introduction	79
7.2. Voltage gradients	79
7.3. Corona phenomenon	79
7.4. Corona losses on DC lines	80
7.4.1. Effect of weather on corona losses	81
7.4.2. Effect of voltage on corona losses	82
7.5. RI from DC lines	83
7.5.1. RI Generation	83

	7.5.3. Short line test results and long line prediction	84
	7.5.4. SNR on DC and AC lines		..	84
	7.5.5. RI and weather	85
	7.5.6. Influence of the line voltage		..	85
	7.6. Conclusions	86
CHAPTER 8	CONCLUSIONS AND PROPOSALS FOR FURTHER STUDY		..	88
	8.1. Conclusions	88
	8.2. Proposals for further study	92
	APPENDIX A	94
	APPENDIX B	95
	REFERENCES	97

NOMENCLATURE

- A_1, B_1, C_1 .. elements of eigen vectors of line equation
 a .. complex operator $1 / \underline{120^\circ}$
 b .. construction coefficient Kg/Km/sq.cm.
 c .. conductor cost Rs./Kg.
 D .. Phase separation
 D_{nn} .. distance from the centre of n^{th} conductor to its image
 D_{nm} .. distance between centres of n^{th} conductor and image of m^{th} conductor
 d .. conductor diameter
 d_{nm} .. distance between centres of n^{th} and m^{th} conductor of a system
 d_o .. ground displacement factor
 d_2, d'_o .. negative and zero sequence electrostatic unbalance factors, respectively.
 E .. line to neutral voltage, KV
 E_o .. neutral displacement voltage
 e .. energy cost Rs./Kwhr.
 F_2, F_o .. negative and zero sequence magnetic unbalance factors, respectively.
 f .. frequency, Hz
 f_1 .. plant factor
 G .. gradient factor KV/cm./KV_{ground}
 GD .. generation density
 GMD .. geometric mean distance
 GMR .. geometric mean radius of the conductor
 g or E_{av} .. average surface gradient KV_{rms}/cm.
 h .. conductor height above ground
 I_{a1}, I_{a2}, I_{ao} .. positive, negative and zero sequence currents respily.
 I .. equivalent current generator for a section of line of length l

- J .. noise current density
 j .. complex operator
 M .. geometric mean intra conductor spacing
 M_s .. surface factor
 m .. intra-conductor separation
 $m_{12} \dots m_{1n}$.. distance between centres of conductor 1 and conductors 2....n of the phase considered.
 n .. number of conductors in the bundle
 P .. three phase corona loss, KW/Km.
 Q .. Charge per unit length
 R .. conductor resistance, ohms/km.
 RI .. Radio interference
 RN .. radio noise
 R_m .. bundle circle radius, cm.
 R_c .. equivalent radius for same total capacitance of a bundle
 R_g .. equivalent radius for same maximum gradient of a bundle
 r .. conductor radius, cm.
 SNR .. signal to noise ratio
 T_3 .. number of fair weather hours in a year
 t .. financial coefficient
 t_3 .. number of foul weather hours in a year
 X .. inductive reactance ohms/km.at 50 Hz
 X' .. capacitive reactance, Meg ohms/km.at 50 Hz
 X_a .. conductor component of inductive reactance
 X_d .. separation component of inductive reactance
 X'_a .. conductor component of capacitive reactance
 X'_d .. separation component of capacitive reactance
 x .. lateral distance from a transmission line, unless specified.

Z_1, Z_2, Z_0 .. positive, negative and zero sequence impedances
ohms/km, respectively.

Z_{11}, Z_{12} etc. sequence self and mutual impedances

α .. twice the corona angle, degrees, unless specified

β .. propagation constant, unless specified.

$\gamma^{(m)}$.. field factor for m^{th} mode, meters⁻¹

δ .. relative air density factor

θ .. angle between the point considered and that of maximum
gradient point.

ϕ .. power factor angle

ϵ_0 .. permittivity of free space.

CHAPTER I

BUNDLE CONDUCTOR TRANSMISSION LINES

1.1. Introduction:

An idea about the rapidly increasing demand of electrical power can be had from the fact that in our country, during the last decade the demand has increased four times. This holds good in other countries also, ofcourse at varying degrees.

To cope up with this ever-increasing demand of electrical power the generating capacities of the existing systems should correspondingly be increased. Often, the generating stations are located away from the load centers of the system. Such as hydro-electric stations, which are located where geographical features permit them.

Thus large blocks of power are to be transmitted to the consumers far away from the generation point. It is an established fact that the use of high voltages gives rise to large savings, especially for long distance and large block power transmission. But, operation at higher voltage has many problems associated with it, such as proper conductor selection etc.

To successfully design a transmission line and adequately solve the associated problems, a design engineer may find the use of single conductors, in steadily increasing diameters reaching a practical limit. Consequently, a multiple number of smaller conductors per phase, spaced short distances apart, but metallicly connected, is gaining increasing prominence. This arrangement popularly called as bundle conductor system, or synonymously as split-conductor system or multi-conductor system or grouped conductor system, offers many advantages over single conductor per phase arrangement.

1.2. Development of Bundle Conductor Lines:

The application of bundle conductors to transmission lines was first proposed in 1909 by P.H. Thomas. A more complete consideration of the electrical characteristics of bundling was done by E. Clarke⁽⁴⁴⁾, and recently by many others.^(28,43,98,110) Chapter 3 of this work discusses the electrical characteristics in some detail. At about the same time as in America investigations were carried out in Europe on electrical characteristics and economics of bundle conductor lines. The plethora of literature available on bundle conductors is itself the proof of the suitability of bundle conductors for EHV lines. As a result of these investigations, one can say, that the reliability and advantages were proved very often and many lines have been constructed or are being constructed with this type of overhead line arrangement throughout the world. Table 1.1 shows the development of bundle conductor lines in a nutshell⁽⁶²⁾.

Considerable work has been done on bundle conductors in Sweden⁽⁵⁷⁾. It is generally concluded that bundle conductors are not economical at 220KV, but, for voltage ranges 400KV and above, they are the best solution possible⁽⁶⁰⁾. Whereas, Rusk and Rathsmann⁽³⁾ declare that the economics of duplex system (two conductors per phase) is amply justified by the corresponding increase in transmission line capability. However, there are cases where bundle conductors have been used mostly two per phase, at as low voltage as 69KV, for many reasons^(12,53). The author supports the opinion that⁽³⁾ bundle conductors can be used at 220KV and above after a sufficient justification is obtained about their economy. However, at higher voltages the author feels they are inevitable.⁽⁸⁵⁾

In short the advantages of Bundle conductors can be stated as follows. They have lower inductive reactance, thus reducing surge impedance resulting in a higher capability. They have higher disruptive critical voltages, allowing for an increase in voltage of operation. And, the increase in corona loss and radio interference is lower when the operation voltage is raised. However, before deciding upon the design of the line, it remains to weigh these advantages against the increased investment. These aspects will be discussed in detail, some of them at present and the rest in the chapters that follow.

TABLE 1.1

Development of Bundle Conductor Transmission Lines.

Country	Year of installation	Voltage KV	No. of conductors	Intra-condr. spacing.cms.
Sweden	1950	380	2	45
		380	3	45
		200	2	45
		130	2	45
Japan	1951	275	4	40
		275	2	40
		110	2	40
		77	2	40
Great Britain	1953	400	4	30
		275/400	2	30
		275	2	30
		132	2	30
Italy	1953	380	2	38
		220	2	38

Country	Year of installation	Voltage KV	No. of conductors	Intra-condr. spacing cms.
Germany	1954	380	4	40
		220/380	2	45
		220	2	45
France	1957	380	2	40
Spain	1957	380	4	40
		380	2	40
		220	2	40
		220	2	30
USSR	1959	500	3	40
		± 400 DC	2	40
USA	1959	500	4	45
		500	3	45
		500	2	45
		345	2	45
Canada	1959	500	4	45
		345	2	40
Czechoslovakia	1959	400	3	40
		220	2	40
Rhodesia	1959	330	2	45
Zambia	1959	330	2	45
Australia	1959	330	2	19
Argentina	1959	380	2	20
Newzealand	1960	220	2	35
		500DC	2	43
Finland	1960	400	2	45
Denmark	1961	400	2	40

Country	Year of installation	Voltage KV	No. of conductors	Intra-condr. spacing cms.
South Africa	1964	400	2	38
		275	2	35

1.3. Cost Analysis:

The bundle conductor lines cost more. The extra cost is due to the fact that they experience heavier wind and ice loads, need bigger transmission towers, sophisticated and expensive hardware, and above all have maximum stringing costs. This cost increases with the increase in number of conductors used per phase. But on the contrary it is believed that, these lines are less vulnerable to aeolian vibrations and swinging action when subjected to lateral force.⁽⁵¹⁾ A figure of 13-20 percent higher cost is given^(1,12) for a duplex line of same conductor cross-section per phase as that of a single conductor line. As indicated earlier this excessive cost is justified against the increase in circuit capability by some experts in this field^(53,94). Exact figures of increase in transmission line investment for triplex and quadruplex lines are not available. However, the absolute cost increase depends upon many other uncontrolled factors such as location of the line, availability of material etc.

A method of cost estimation has been proposed, which considers the effect of all the factors influencing the design of transmission lines.⁽⁷²⁾ It consists in evaluating the annual cost of the conductor and the cost due to joule losses viz. c_1 and c_2 respectively.

$$c_1 = k_1 r^2 \quad \dots \quad \dots (1)$$

where,

$$k_1 = tcb$$

t financial coefficient, considering annual charges on investment.

c cost of the conductor including transport and construction (Rs. per kg.).

b construction coefficient kg/km./sq.cm.

$$c_2 = \frac{k_2}{r^2} \dots \dots (2)$$

where,

$$k_2 = \frac{m_1^2 E f_1 I_n e}{\sqrt{3} v \cos \phi . n^2} k'_0$$

$m_1 = 1.05$ to 1.1 depending on $f_1 \leq 0.5$ respectively.

E_1 energy transmitted, kw hrs.

f_1 plant factor

I_n rms current/phase, Amps.

e energy cost Rs./kw.hr.

v Line voltage, volts.

ϕ power factor angle

n number of conductors

$k'_0 = 0.04$ for ACSR conductors.

In the above method, corona losses have not been considered.

By taking into account the effects of all pertinent variables, the corona loss cost equation can be given as⁽⁷⁵⁾

$$c_3 = k_3 r^2 g^3 (T_3 + t_3 g^3) \dots (3)$$

where,

$$k_3 = k'_3 e = (15 \times 10^{-6}) e$$

e energy cost Rs./kw.hr.

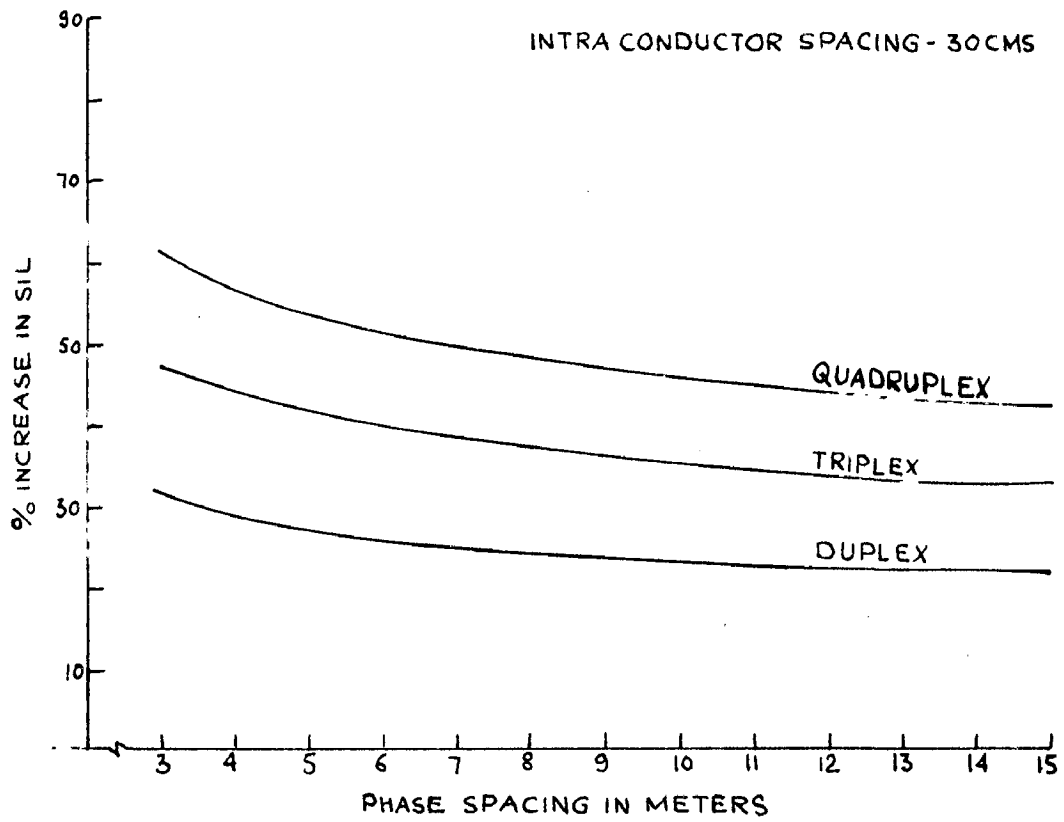
- T_3 number of fair weather hours in year
 t_3 number of foul weather hours in a year.

The total annual cost per unit length then will be the sum ($c_1 + c_2 + c_3$). For a single conductor line c_1 & c_2 are lower where-as c_3 may substantially be large when compared with bundle conductor line.

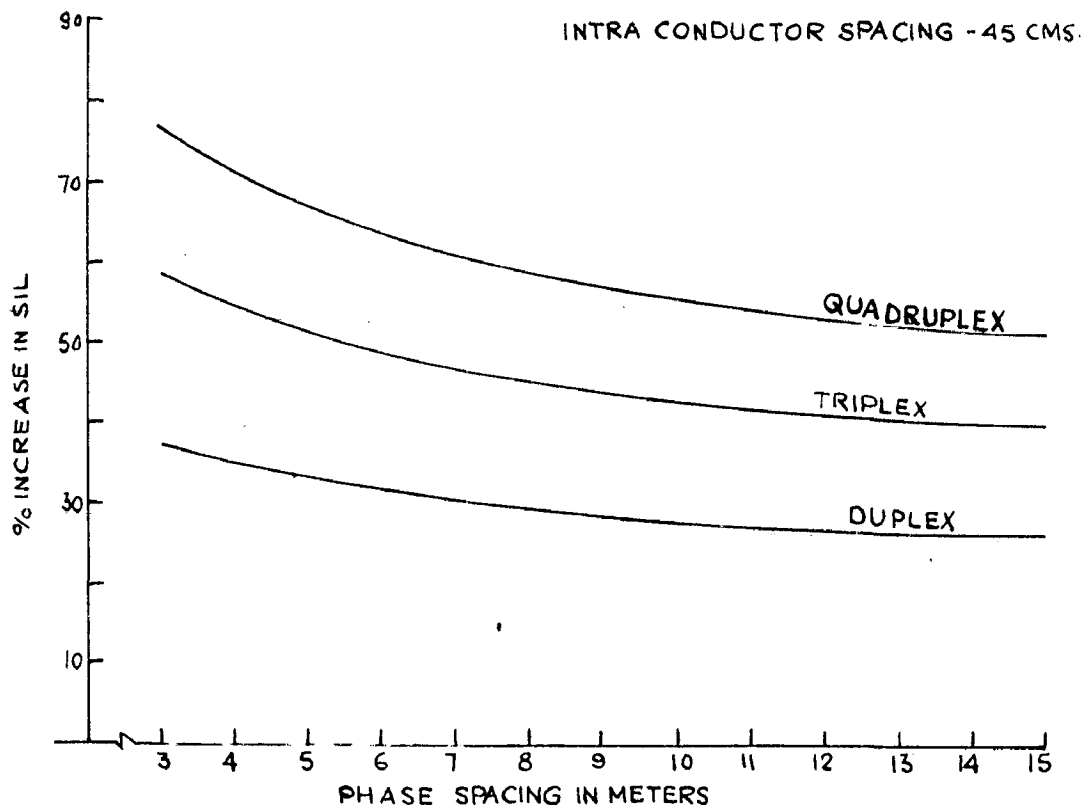
1.4. Transmission Capability:

Bundle conductor transmission lines are undoubtedly capable of transmitting high power compared to single conductor lines of same total conductor area of cross section per phase. (Mathematically treated in Chapter 3). Transmission capability is dependent upon various factors (i) conductor size (ii) intra-conductor spacing (iii) conductors per phase and (iv) phase separation.⁽²⁸⁾ Fig.1.1 shows the percentage variation in capability with phase spacing and intra-conductor spacing, when the total conductor area is held constant practically. Fig.1.2 clearly shows the possible increase in transmission voltage with 2, 3 and 4 conductors per phase. For overall optimisation of the transmission line design a careful consideration of both line reactances and conductor cross-sections is necessary. An advantage of bundle conductor transmission lines is clear from Table 1.2,⁽⁶²⁾ that, judicious use of bundle conductors results in obtaining the advantages of higher transmission voltages without incurring the extra cost of insulation, switchgear and transformers, which otherwise would have been essential. The following are the effects of the variables listed above on transmission capability.

(1) Unless conductor current carrying capacity is increased conductor dimension does not alter the transmission



(A)



(B)

FIG.11 PERCENT INCREASE IN SIL WITH BUNDLED CONDUCTORS
(HORIZONTAL ARRANGEMENT SINGLE CKT.)

capacity.

(ii) Intra-conductor spacing has significant effect on transmission capacity. It is seen from Fig.1.1. that an increase in conductor separation from 30 to 40 cm. results in capacity increment of 10%.

(iii) With increase in number of conductors per phase a small incremental capability is obtained, but this compared with the increased capacity obtainable by n different circuits is very less. For example, the resulting capacity increase of 25-30 percent with duplex system is considerably less when compared to 100% capability obtainable with that of a double circuit line. Approximate increase in capability for 2,3, and 4 conductor bundles is respectively 30, 40 and 50 percent.

(iv) Increased phase separation decreases the circuit capacity. This clearly is an additional advantage.

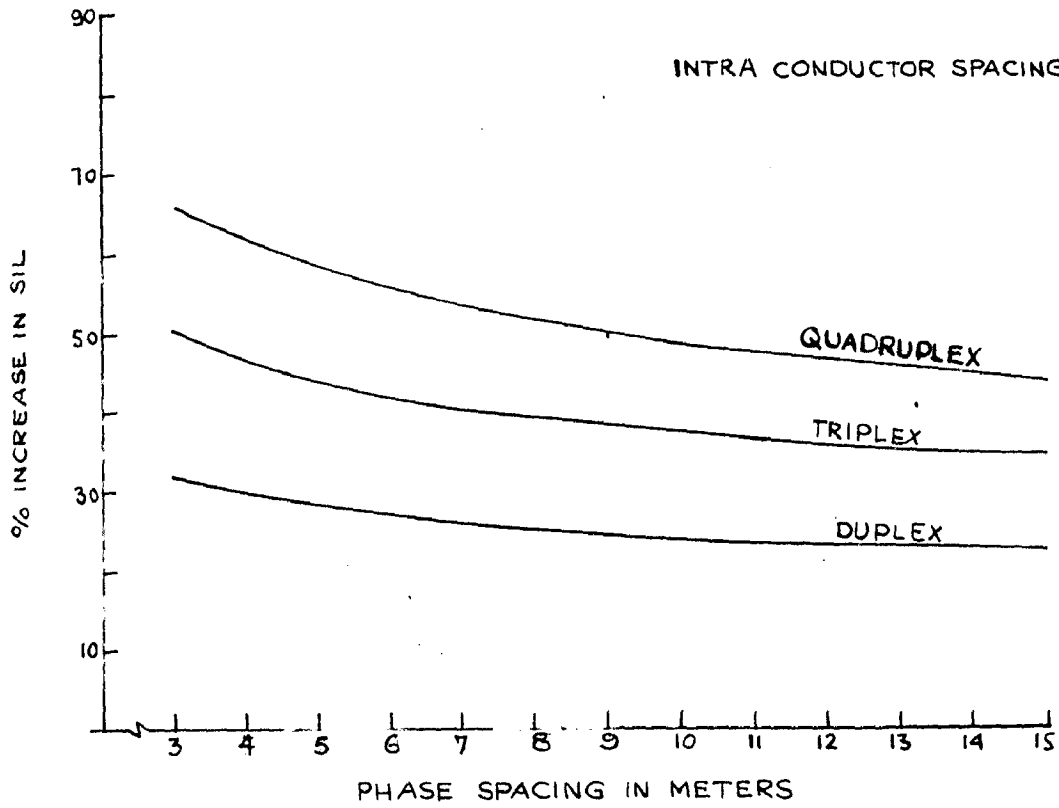
TABLE 1.2

Equivalent Operating Voltages (KV) for Various Bundles

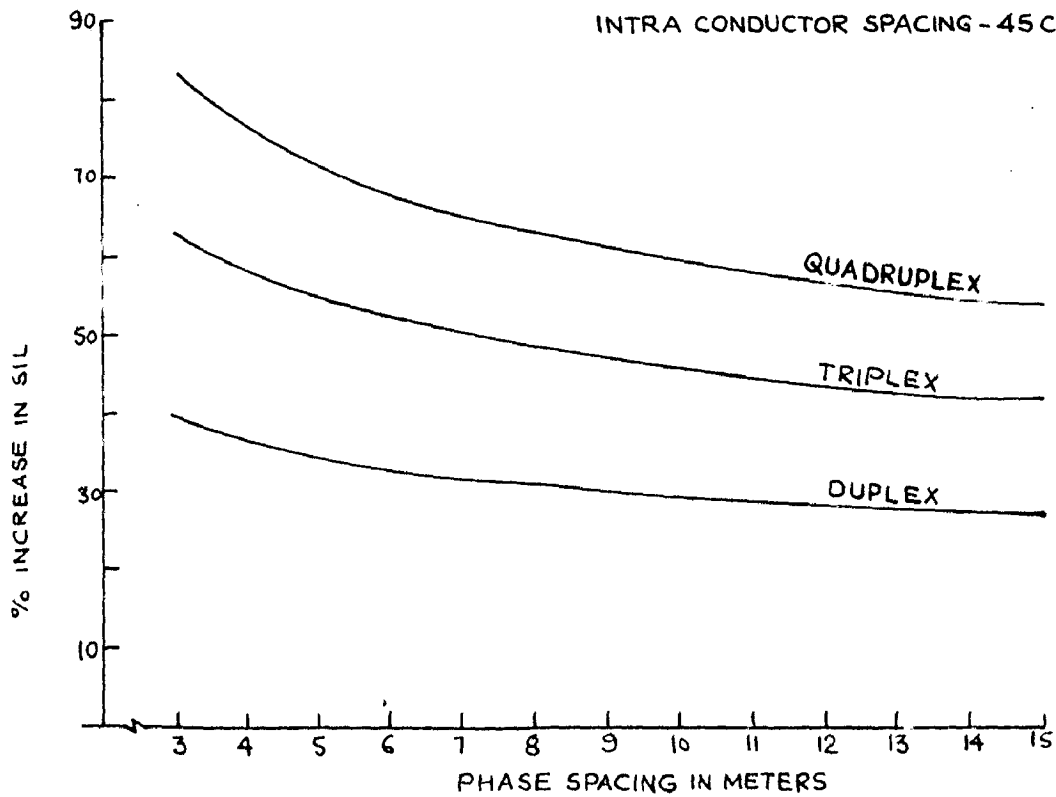
Simplex	Duplex	Triplex	Quadraplex
69	80	85	90
138	158	168	176
230	260	275	286
345	390	410	425

1.5. Voltage Gradients:

At extra high voltages, voltage gradient or electrical stress on dielectric surrounding the conductor becomes of paramount importance. The characteristic feature of the voltage gradients, around bundle conductors is its non-uniformity, which makes its determination a little tedious. But the tedium can be overcome



(C)



(D)

FIG.1.1 PERCENT INCREASE IN SIL WITH BUNDLED CONDUCTORS
(TRIANGULAR ARRANGEMENT SINGLE CKT.)

capacity.

(ii) Intra-conductor spacing has significant effect on transmission capacity. It is seen from Fig.1.1. that an increase in conductor separation from 30 to 40 cm. results in capacity increment of 10%.

(iii) With increase in number of conductors per phase a small incremental capability is obtained, but this compared with the increased capacity obtainable by n different circuits is very less. For example, the resulting capacity increase of 25-30 percent with duplex system is considerably less when compared to 100% capability obtainable with that of a double circuit line. Approximate increase in capability for 2,3, and 4 conductor bundles is respectively 30, 40 and 50 percent.

(iv) Increased phase separation decreases the circuit capacity. This clearly is an additional advantage.

TABLE 1.2

Equivalent Operating Voltages (KV) for Various Bundles

Simplex	Duplex	Triplex	Quadruplex
69	80	85	90
138	158	168	176
230	260	275	286
345	390	410	425

1.5. Voltage Gradients:

At extra high voltages, voltage gradient or electrical stress on dielectric surrounding the conductor becomes of paramount importance. The characteristic feature of the voltage gradients, around bundle conductors is its non-uniformity, which makes its determination a little tedious. But the tedium can be overcome

with the help of a digital computer as is done in Chapter 3. For the same area of conductor cross section per phase the maximum voltage gradient decreases in order, for duplex, triplex and quadruplex systems. This is evidently an advantage. A gradient reduction of about 20 percent is obtained by bundling. The gradient further reduces with increase in the number of sub-conductors. Mangoldt's equation⁽⁵⁷⁾ is being extensively used in industry. It can be used with equal facility for determination of gradient on centre as well as on outer phases, at any point around it.

Gradient varies sinusoidally around the circumference of a sub-conductor. It is minimum at a point on the conductor nearest to the bundle centre and maximum at a point circumferentially opposite to this. Of interest, usually is the value of maximum surface gradient for determination of corona disruptive critical voltage etc.

1.6. Corona Losses:

Since the operating gradient on a bundle conductor line is less than that for single conductor line, corona initiation is (in fair weather) further delayed to higher line voltage^(15,26). In foul weather the losses are definitely less than those for single conductor lines⁽⁶⁴⁾ (discussed in detail in Chapter 4). While, fair weather losses⁽⁶⁾ may be maintained low or negligibly small by suitably selecting the conductor and hardware⁽¹⁰²⁾, foul weather losses⁽⁴⁾ form a few percent of the power transmitted. The case will be worse if foul weather were to exist at the peak load period. Even more important and interesting case is that of the losses during over voltages of say twice or so, the order of operating voltage. This aspect of corona loss needs further investigation.⁽⁸⁸⁾

The simplest possible method of measuring corona losses on operating transmission lines is to install wattmeters in every phase at both ends and measure the loss. This after deduction of copper losses gives the actual corona losses. A line should be designed such that fair weather losses are zero or negligible. The other methods of measurement are discussed later.

1.7. Radio Interference:

The problem of RI is of little importance at low transmission voltages, of the order of 220 KV. The study of RI becomes important over and above this value, and is often of a major concern to the line designer.^(15,26) Strictly speaking, RI is a nuisance factor, which should not dictate at all, the design of a transmission line.⁽²¹⁾

Design criteria⁽⁷³⁾ are developed by classifying the type of broadcast reception and limiting the radio noise produced by the transmission line by the criteria. One such criteria developed⁽⁹²⁾ indicates a SNR (Signal to noise ratio) of 24 dB as the acceptance level, as measured by Stoddart NM-20 meter. With any other meter this value should be ^{modified} accordingly depending on its parameters.

The radio noise attenuates rapidly, lateral to the transmission line.⁽³⁹⁾ This defines the distance between the residential areas and transmission line, for a given class of reception.⁽⁹²⁾ This again depends on the locality through which the line is passing viz., urban or rural. Whereas in urban areas the probability of a radio receiver being nearer and that of high signal strength is high, but in rural areas it is quite probable that the receivers may be farther away from the line and the signal

strength quite low. To maintain same class of reception the line design should be done accordingly. (71)

1.8. Special Features of Bundle Conductor Lines:

Increasing ^{the} number of conductors per phase involves many mechanical problems unknown hitherto in the construction of single conductor transmission lines. One such is the maintenance of constant separation distance between the subconductors. For this purpose spacers are used. These spacers along with maintaining the required separation distance also connect electrically all the subconductors of the phase. This ensures that each subconductor is at the same potential practically. Rigid spacers are apt to be damaged under short-circuit conditions and are apt to tear out the conductor strands practically. (62) During which period the electro-mechanical forces developed force all the conductors towards bundle centre. Investigations on this problem reveal that spring type spacers are best suited for bundle conductor transmission lines, since, they allow a limited motion in a vertical plane, and some longitudinal motion. (1) Each country has developed its own research projects to optimise the design of bundle conductor spacers and all seem to accept the above type of spacer. The spacers are located at every 50-80 meter distance, a minimum of 4 per span depending upon the terrain and the atmospheric conditions such as wind, frost etc., The spacers should have a life period of atleast 25 years, which also holds good for other accessories.

Bundle conductors can avoid grading rings around the insulators. The top two conductors in a quadruplex system can be centered in such a manner that they provide the necessary grading. With duplex and triplex systems a similar approach is possible.

Even though the modern practice is to avoid transpositions, it will be economical to provide at least one or two cycles of transpositions as indicated in Chapter 6, at the compensating series capacitors located at every one third of the total distance. This has been proved to reduce the unbalances greatly.⁽³²⁾

In almost all transmission lines the intra-conductor spacing is of the order of 40 cms. A slightest difference in sag of sub-conductors will be very conspicuous. A slight difference in length of cables will result in difference of sag. It is necessary to make the tendency of permanent set of the individual conductors same by providing a uniform history of stress from their production to final stringing. For this purpose all the individual conductors per phase should be selected from the same production run. This assures uniform internal stress and temperature to be same during the production period. Wiring is made by uniforming the tension in each sub-conductor.

1.9. Some Aspects of Mechanical Behaviour of Bundle Conductor Lines:

With bundle conductor transmission lines the accidental contact of conductors in the same bundle is given rise to by (a) aero-dynamic forces and (b) electro-dynamic forces. These accidental contacts may result in clinging together of conductors even after the release of the forces just as in the case of severe short circuits.^(51,93) Such clinging of subconductors is apt to cause damage to the outer conductors, this necessitates location of flexible spacers at intervals as may be dictated by the above two forces.

It is interesting to study and compare horizontal or other circuit arrangements with vertical arrangement. Movement towards

forces or aerodynamic forces is zero or quite less in the case of vertical arrangement. Theoretically spacers can be dispensed with. But horizontal and other arrangements are vulnerable to these and require spacers at intervals as mentioned earlier.

The following comments can be made with regard to vibration and dancing on bundle conductor transmission lines.⁽⁵⁶⁾ With spacers located at distances as discussed, reduce effectively the vibration as compared with the single conductor.

The transmission line is found to become practically immune to dangerous vibration when 3 or 4 conductors are employed as is the case at EHV. On the contrary bundle conductor transmission lines experience a greater degree of dancing as compared to single conductor lines. And if rigid spacers are employed, the transmission line is prone to torsional oscillations. Dancing becomes an important factor deciding the spacings of the transmission line, in places where icing is accompanied by winds of moderate velocity. Dancing can be avoided by melting the ice formed on the lines before vibrations set in.

1.10. Design of Bundle Systems:

1.10.1. Choice of Number and Size of Conductors:

The factors controlling the conductor choice were elucidated hitherto, and will be discussed further. The choice of conductor⁽⁷⁾ always an important factor in transmission line design, assumes added significance in the design of modern EHV lines.⁽⁸⁾ As the voltage levels increase, a conductor choice based on the classical economic approach, i.e. Kelvin's Law, will result in conductor sizes that will have an increased voltage gradient at the conductor surface. Because of the effect of higher surface gradient on corona loss and RI performance, as well as the

considerable expense of all elements of an EHV line, an optimum choice requires careful study of the performance characteristics of conductor alternatives. (21)

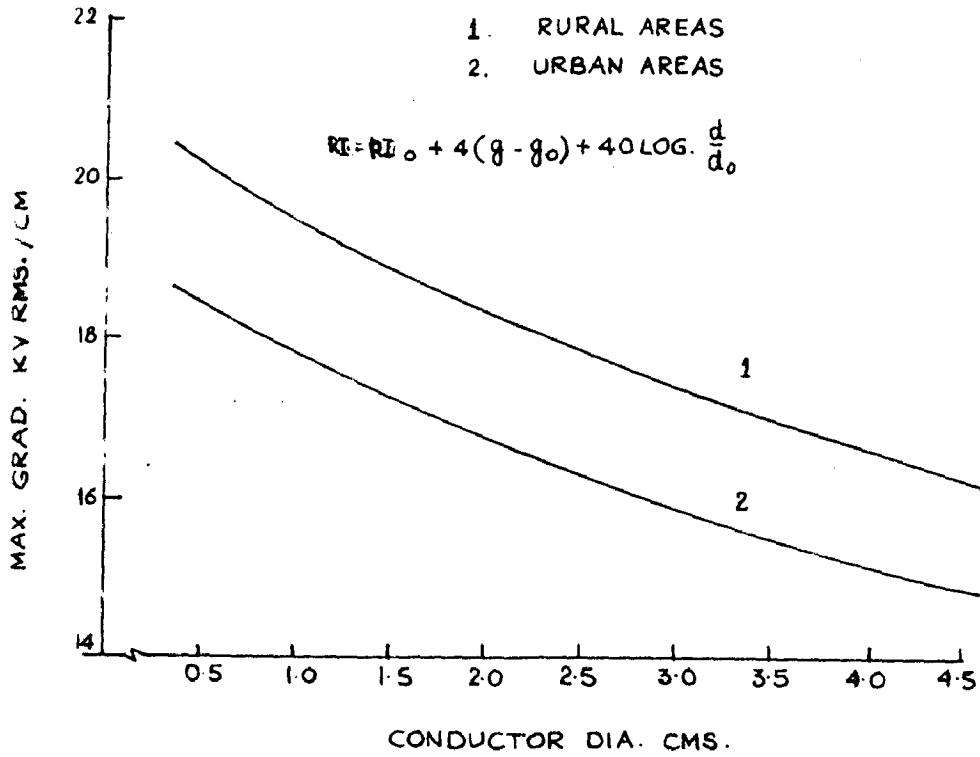
A method of preliminary selection is suggested. (72) Such a selection should provide minimum annual costs. The total annual costs are given by the sum of the equations (1), (2) and (3). Differentiation of such an expression to get optimum conductor cross section would be a tedious job. If however the corona losses are neglected an easy rough estimate can be done. Then we get after differentiating and equating to zero.

$$r = \sqrt[4]{\frac{k_2}{k_1}}$$

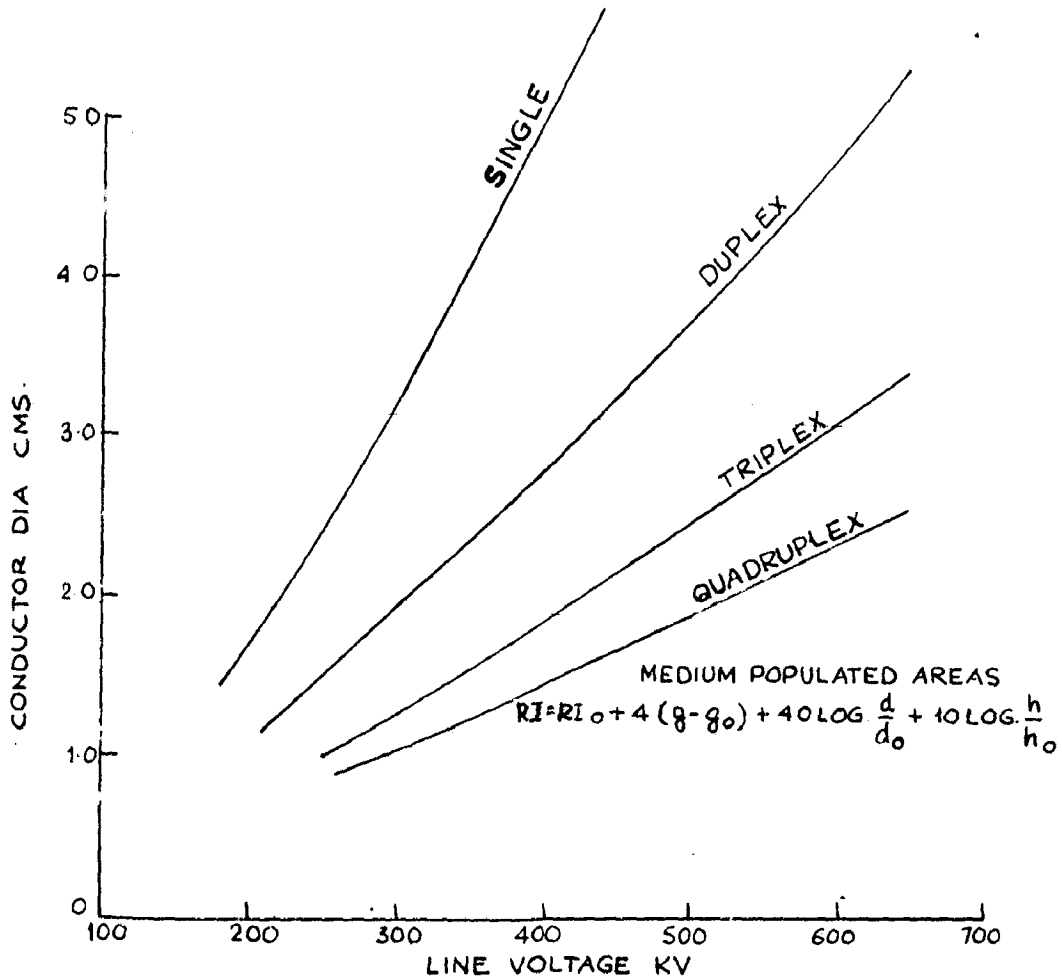
This radius can be checked against corona by calculating the critical corona voltage.

Where as corona losses seem to be a factor restricting the reserve capacity, they do not have a major influence over conductor choice as compared to high frequency disturbance. (37) The permissible radio disturbance depends upon the type of location- urban or rural. Based on the experience on the existing lines, it is possible to predict the performance of other lines (75,92) curves representing such predictions are shown in fig.(1,2). The two graphs (A) and (B) show typical practices in Canada and Italy. The curves can be approximately represented by the respective equations inserted in each graph. These graphs can be used as a check against the radius of the conductor calculated on the lines outlined in the previous paragraph.

It is generally recognised that for a given total cross section of conducting material per phase, both RI and Corona loss



A:- CONDUCTOR DIAS FOR ACCEPTABLE RIL - CANADA & U.S.A



B:- CONDUCTOR DIAS. FOR ACCEPTABLE RIL - ITALY

decrease as the material is subdivided into successively more conductors. However many of the costs of achieving this subdivision are difficult to assess, such as the increased cost of stringing and the rather intangible cost accompanying the overall mechanical performance. The number of conductors in a bundle is decided by the voltage of operation. However, before selecting a larger number of conductors in a bundle it is good to have a check on the accompanying increase in cost and the mechanical arrangements. Circuit reliability is however increased with the number of conductors per phase. It has been usual practice to have duplex or quadruplex systems. So at lower voltages say 220 to 500 KV a duplex system may be employed and at 400KV and above a quadruplex system is suggested.

1.10.2. Optimum Intra-Conductor Spacing:

All characteristic features which decide the design of a EHV line are dependent upon the maximum surface gradient. While determining the optimum intra-conductor spacing the surface gradient equation should be considered. Mangoldt in 1942 presented an equation to determine the surface gradient on bundle conductor lines. The equation is⁽⁵⁷⁾

$$G = \frac{1 + \{2(n-1)r \sin(\theta/n) \cos \theta\}/n}{n r \log_e \{2h/r^{1/n} M^{(n-1)/n} / \sqrt{(2h/D)^2 + 1}\}} \dots (4)$$

WHERE,

- G gradient factor, KV/cm/KV to ground or neutral
- n number of conductors in the bundles.
- θ angle from point of maximum gradient.
- m distance between nearest subconductors.
- r conductor radius, cm.
- h conductor height above the ground plane

M geometric mean intra conductor spacing = $n-1 \sqrt{m_1 m_2 m_3 \dots m_{n-1}}$
 is m for $n = 2$ & 3 , $1.12m$ for $n = 4$.

D geometric mean phase spacing.

The bundle arrangements/as shown in Fig.(1.3). The notations conform to those used in the above equation. Equation (4) for maximum gradient at $\theta = 0$ can be written as,

for $n=2$

$$G = \frac{1 + 2r/m}{2r \log_e \left[2h / \sqrt{rm} \left(\frac{4h^2}{D^2} + 1 \right) \right]} \text{ KV/cm./KV}_{\text{ground}} \dots (5)$$

for $n=3$

$$G = \frac{1 + 3.464 r/m}{3r \log_e \left[2h / \left\{ 3 \sqrt{rm^2} \sqrt{\frac{4h^2}{D^2} + 1} \right\} \right]} \text{ KV/cm./KV}_{\text{ground}} \dots (6)$$

and lastly for $n = 4$

$$G = \frac{1 + 4.242 r/m}{4r \log_e \left[2h / \left(4 \sqrt{r(1.12m)^3} \sqrt{\frac{4h^2}{D^2} + 1} \right) \right]} \text{ KV/cm./KV}_{\text{ground}} \dots (7)$$

Differentiating equations (5), (6) and (7) w.r.t. m and equating to zero, an equation involving all geometrical parameters is obtained. Solution of this equation provides the optimum intra conductor spacing. For example equation (5) is considered.

Denoting $\frac{2h}{\sqrt{\frac{4h^2}{D^2} + 1}} = A,$

$$\begin{aligned} \frac{\partial G}{\partial m} = 0 &= \left(2r \log_e \frac{A}{\sqrt{rm}} \right) \left(-\frac{2r}{m^2} \right) - \left(1 + \frac{2r}{m} \right) (2r) \left(\frac{\sqrt{rm}}{A} \right) \left(-\frac{1}{2m^{1.5}} \right) \\ &= \frac{m}{2A\sqrt{r}} + \log_e m = 2 \log_e \frac{A}{\sqrt{r}} - \frac{\sqrt{r}}{A} \dots (8) \end{aligned}$$

for $n = 3$

... 1/3

and for $n = 4$

$$\left| \frac{1.0887}{Ar^{\frac{1}{4}}} \right| \left| \frac{m}{5.7} \right|^{\frac{3}{4}} \log_e m = \log_e \left| \frac{A}{1.0887 r^{\frac{1}{4}}} \right|^{-0.75} \left| \frac{1.0887 r^{\frac{1}{4}}}{A} \right| \dots (10)$$

The values of optimum intra-conductor spacing obtainable from equations (8), (9) and (10) are- less than those used in practice.

1.11. Advantage of Bundle Conductor Lines:

From the foregoing discussions the advantages of bundle conductor transmission lines can be stated as follows in the order of importance,

- i) increase in operating voltage
- ii) improved circuit reliability
- iii) increase in circuit capability
- iv) reduction in reactance of the circuit
- v) decrease in RI level
- vi) decrease in corona losses
- vii) reduction in required circuit compensation, due to increased line capacitance
- viii) Facility in handling due to light and smaller hardware and accessories.
- ix) lighter supporting structures.

On the other hand, there are some disadvantages such as increased investment, mechanical problems, added accessories such as spacers etc.

The design of bundles conductor lines should take into account RI generated by the line. Intra conductor spacing used in practice is usually greater than the optimum spacing, due to mechanical limitations.

CHAPTER 2 VOLTAGE GRADIENT STUDIES

2.1. Introductions

Whenever a conductor is maintained at a potential the dielectric surrounding the conductor is electrically stressed. The electric stress decreases, as the distance from the conductor increases, in a rapid manner. This electric stress is called voltage gradient. surface voltage gradient is defined as the electric intensity of the electrostatic field surrounding the conductor as measured at its' surface in a direction perpendicular to the axis of the conductor under the assumption that there is no corona present. With the advent of the extra-high voltage transmission for various reasons pointed out in Chapter-1, the voltage gradient and its' studies have gained importance for the reason that with voltage gradient are associated a loss factor and a nuisance factor. With increase in gradient the surrounding air will break down at its' critical value, which gives rise to a charged envelope around the conductor, virtually increasing the diameter of the conductor. This dielectric break down is associated with a power loss termed "corona-loss", and a nuisance factor which is high frequency interference such as ⁱⁿ the Radio and Television broad-cast band. The electromagnetic waves from the overhead conductor interfere with the signal transmission and if due care is not taken in the design, the noise may even over-ride the signal itself. Chapter 4 and 5 discuss these two important factors of a EHV bundle conductor lines.

Studies of voltage gradient^(5,7,13,15) have been made since the beginning of the power transmission. However, bundle conductors appeared in the transmission field only a few years ago and since then attempts are being made to study thoroughly the voltage

involved in the calculation of the voltage gradients due to its inherent ^{non}uniformity, certain assumptions are necessary, which when made with a sound reasoning preserve the accuracy of the calculations.

The following are the assumptions made in the analytical studies:

1. The charge distribution on each conductor of an individual phase is uniform, throughout the length of the transmission line. So a charge per unit length is considered in the calculations. This assumption is based on the fact that a transmission line is always considered to be at a constant average height above the ground, unless specified.
2. The line is perfectly balanced i.e., the transmission line is assumed to be transposed at regular intervals.
3. Spacings, intra-conductor and intra-phase are respectively from centre to centre of the conductors in one phase and between bundle centres of the phases. It is assumed further that these distances same throughout the length.
4. The conductor surface is smooth and the radius of the conductor is that of the outer circumscribing circle.
5. The transmission towers and other accessories have negligible effects on the voltage gradients.
6. The effect of the fields on other phases on a particular bundle has been neglected while the effect of the capacitances on fields produced has been considered.

Calculations of Temoshok⁽⁵⁾ indicate that the influence of the factors such as ground wires (one or two) and finite

and can be neglected altogether. In the case of transmission lines using one conductor per phase gradient distribution around the periphery is uniform. Where as, in the case of bundle conductor transmission lines the gradient distribution is essentially non-uniform. By the use of conventional method, using maxwell's coefficients it is possible to obtain only the surface gradient, which ofcourse, is sufficient sometimes to predetermine the corona loss and RI characteristics of the line. (7,15,26) But for a study of gradient distribution around and away from the bundle, conformal mapping will be very useful. This was formerly tried by Poritsky⁽⁴⁴⁾ developed by Sreenivasan⁽⁹⁵⁾ and recently throughly studied by Timaschef.⁽⁹⁶⁾ The same principle of conformal mapping is used to outline the procedures for gradient determination.

2.2. The Case of a Single Conductor:

A thin conductor of infinite length and carrying a uniform charge Q per unit length, gives rise to a potential ϕ at any point P , x meters away from the conductor as given by the following equation,

$$\phi = - \frac{Q}{2 \pi \epsilon_0} \text{Log}_e(x) + k \quad \dots \quad (1)$$

where,

k , is a constant

Equation (1) reveals that equipotential lines (on which ϕ is constant) are given by circles. A circular conductor such as used on transmission lines, can be superposed to coincide with one of the equipotential lines of an imaginary infinitessimally thin conductor, which essentially does not alter the field pattern given by (1). This approach is further developed to meet the requirements of bundle conductor lines.

2.3. The case of the n Conductors arranged on the Circumference of a Circle:

Potential at a point due to n infinitesimally thin conductors of charge Q per unit length is given by

$$\phi = - \frac{Q}{2\pi\epsilon_0} \text{Log}_e(x_1 \cdot x_2 \cdot \dots \cdot x_n) + K' \quad \dots \quad (2)$$

where, k' is a constant and x_1, x_2, \dots, x_n are distances to the point P from conductors 1, 2, ..., n respectively. Just as in the case of a single conductor all the n conductors of finite radius can be superposed to coincide with the appropriate equipotential lines. Equipotential lines are given by-

$$x_1 \cdot x_2 \cdot \dots \cdot x_n = \text{constant} \quad \dots \quad (3)$$

Fig. 2.1 shows the arrangement of conductors and the usual nomenclature. Now by taking a transformation such that $W = Z^n$, the actual conductor system in W plane can be mapped into Z plane. In Z plane it is necessary to consider only the field due to a single conductor, which when mirrored a suitable number of times depending on n , the actual field system is obtained. The transformation for a simple case of $n=2$ is indicated in Appendix A. Extending for a case of n conductors,

$$R_m = 0.5 (n\sqrt{1+\tau} + n\sqrt{1-\tau}).$$

$$r = 0.5 (n\sqrt{1+\tau} + n\sqrt{1-\tau}) \quad \dots \quad (4)$$

where τ is the radius of the circle undergoing transformation from W -plane to Z plane, and in this case it is the actual conductor radius to a scale. From Fig. (2.1) and equation (4)-

$$2\left(\frac{R_m}{m}\right) \sin\left(\frac{\pi}{n}\right) \quad \dots \quad (5)$$

and
 2.4. Equivalent Radii and Gradient Determination:
 For convenience, two quantities are defined viz., (i) a

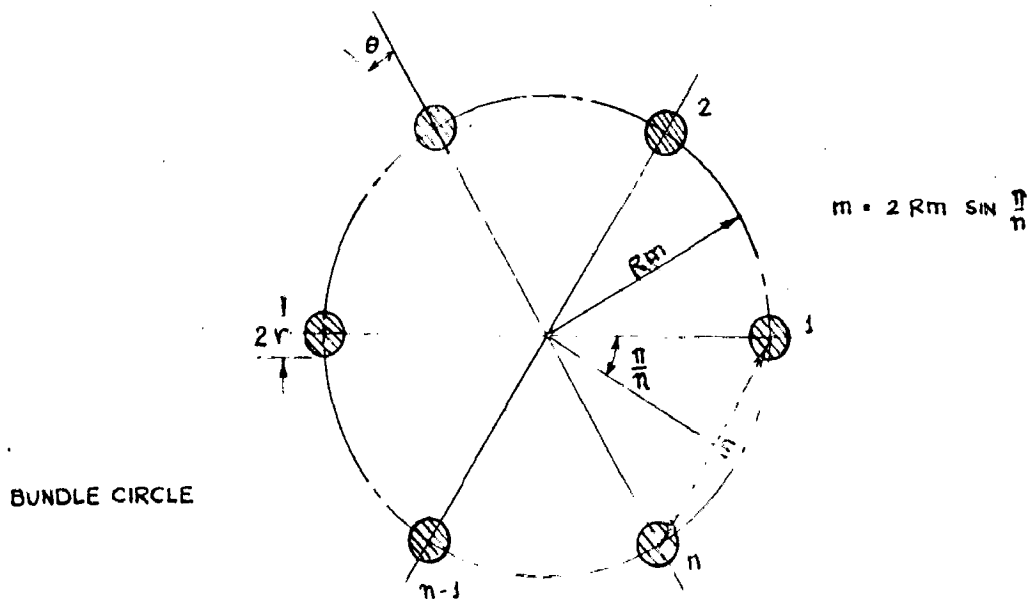


FIG.21 ARRANGEMENT OF THE n CONDUCTORS

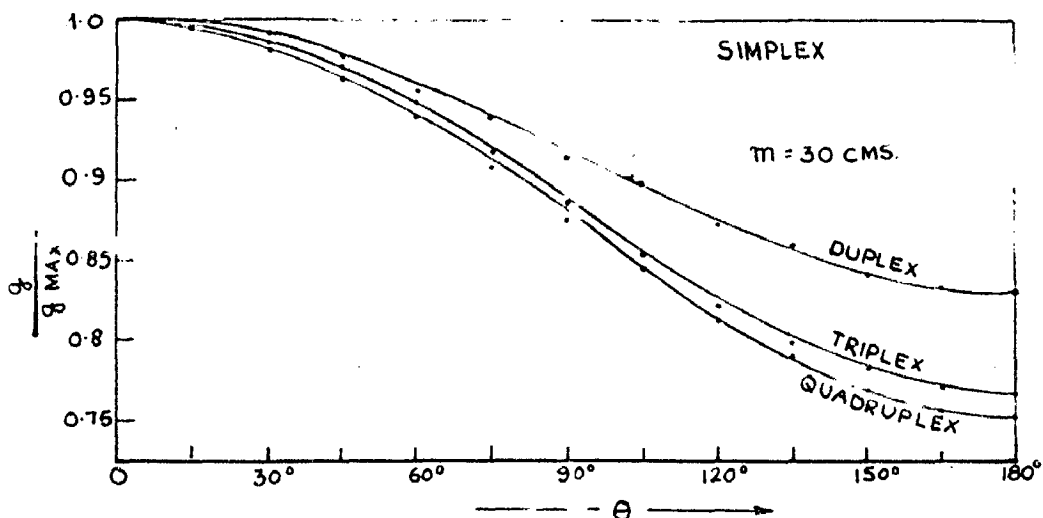


FIG.22 GRADIENT DISTRIBUTION AROUND THE CIRCUMFERENCE

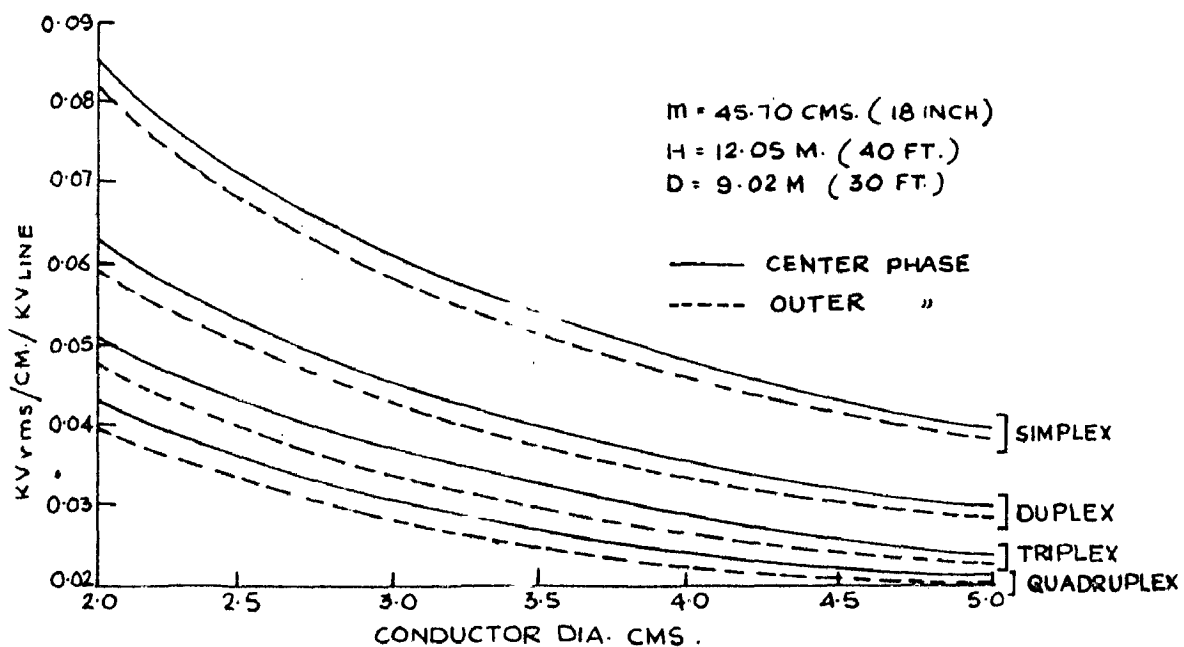


FIG. 2.3 EFFECT OF CONDUCTOR CROSS-SECTION

(i) a single conductor of same capacitance as the bundle and
 (ii) a single conductor of maximum gradient as that of bundle,
 both located at bundle centre. The radii of these conductors
 respectively is given by⁽⁶⁸⁾

$$R_c = r \cdot \left(\frac{m}{2r \sin \frac{\pi}{n}} \right)^{\frac{n-1}{n}} \cdot n \cdot \frac{1}{n} \quad \dots \quad (6)$$

$$\text{and } R_g \text{Log}_e \left(\frac{D}{R_g} \right) = r \cdot \frac{m \cdot n}{m + 2r(n-1) \sin \left(\frac{\pi}{n} \right)} \text{Log}_e \frac{D}{R_c} \quad (7)$$

It is worth noting here that the two equations (6) and (7) would have been same if the gradient distribution around the bundle conductors were uniform. However, the gradient distribution is nonuniform, the radius of equivalent conductor representing maximum surface gradient is $(1 + \beta)$ times smaller than that for uniform field distribution [from (7)].

$$\text{where } \beta = \frac{2(n-1)r}{m} \sin \left(\frac{\pi}{n} \right) \quad \dots \quad (8)$$

$$\text{Therefore } \epsilon_{\max} = \epsilon_{\text{uni}} (1 + \beta) \quad \dots \quad (9)$$

$$\epsilon_{\text{uni}} = \frac{Q'}{2\pi \epsilon_0 n r}; \quad Q' = \text{Total charge on equivalent conductor.}$$

Since the variation of gradient around the conductor in a bundle has been proved to be sinusoidal, gradient at any point at a reference angle θ (Fig.2.1) is given by

$$\epsilon = \epsilon_{\text{uni}} (1 + \beta \cos \theta) \quad \dots \quad (10)$$

ϵ_{\max} , on the otherhand can be obtained directly by solving for R_g in (7) and is given by-

$$\epsilon_{\max} = \frac{E}{R_g \text{Log}_e \frac{D}{R_g}} \quad \dots \quad (11)$$

where E line to neutral voltage KV

D phase separation in meters.

There however exists a difference in the value of maximum surface gradients between the centre phase and the outer phases, e.g. as in the case of a horizontal single circuit. There however also exists a difference though slightly in the maximum surface grad. between the subconductors themselves in any particular phase (Ref. Appendix B). Since the calculations are carried out with the help of a single equivalent conductor of maximum surface gradient the results are safe. Equation (11) can be corrected for finite height above ground by using a factor nearly 0.97 according to Timaschef, and the effective phase distances can be taken into ^{account} by the factors $(D/3\sqrt{2})$ and $(3\sqrt{2}.D)$ for center and outer phases respectively. However in the opinion of the author values $(\sqrt{2}.D)$ and (D) are the values that should be used for centre and outer phases, since these represent the actual geometric mean distances.

2.5. Gradient Distribution Around the Circumference:

Since the ^{gradient} ~~applied voltage~~ is a function of applied voltage, it varies sinusoidally at a point. The investigations reveal that a sinusoidal variation around a conductor in a bundles can be assumed. (10,21,98) Fig.2.2 gives a graphical picture of this variation around the conductor periphery, in the case of each of the arrangements viz., Simplex, duplex etc. It is evident that at a point 180° from the reference line the gradient is minimum, at 0° it is maximum and at 90° it has the average value. A graphical estimation to a good degree of accuracy has been presented by Schmidt, which gives the values of gradient on the

surface and in the near vicinity at all possible angles and also the determination of the corona angle.⁽²²⁾ The chart construction is based on the conformal mapping principle. A recent paper⁽⁹⁶⁾ presents a computer plotted equigradient line arrangement for specific examples of duplex, triplex and quadruplex lines.

Fig.(2.2) gives the gradient values for intra-conductor spacing indicated, for subconductor diameters listed in Table 2.1. In all further calculations throughout this work the conductor diameters are essentially these values unless otherwise specified.

Table 2.1

Sub-conductor Diameters of same cross section per phase.

Arrangement	Conductor dia.cms.
Simplex ..	3.924
Duplex ..	2.776
Triples ..	2.355
Quadruplex ..	1.989

2.6. Effect of Conductor Cross Section on Gradient:

Conductor cross section has a direct effect upon the gradient. Fig.2.3 shows the variation in gradient factor for the various arrangements of a single horizontal circuit without ground wires. The gradient is inversely related to the conductor diameter. The figure also illustrates the difference in gradients on centre and outer phases. The following facts are evident from the figure, (1) the gradient on bundle conductors is lower. The greatest difference occurs when changing from simplex to duplex systems; (2) the gradient on centre and outer phases may be almost a constant ratio in all arrangements.

and (3) as the conductor diameter increases the difference in gradient between the arrangements is reduced.

Appendix B, lists the variations of gradients on sub-conductors of centre and outer phases for the system referred therein.

2.7. Effect of Conductor Heights:

The conductor height has very little effect on the gradient. In fact a correction factor of the order of 0.97 can be used for the heights used in practice on EHV lines⁽⁶⁸⁾ However the gradient varies slightly from point to point in a span. The calculations show the difference as listed in Table 2.2.⁽⁹¹⁾

TABLE 2.2

Gradient Variation in a Normal Span.

525 KV Line; $D = 10.52\text{m}$; $m=45.67\text{ cm.}$; $2 \times 4.07\text{ cm.}$
Two ground wires, 16.5m apart, 41.2m high at tower and 31.7m high at mid span.

Conductor or height meters	Max.gradient on outside phase KV rms./cm.	Max.gradient on center phase KV _{rms} /cm
11.74 Mid.span	16.76	17.82
18.30 AV.height	16.44	17.73
29.70 Tower	16.30	17.75

Maximum variation occurs on outer phase and is about .0275 for about 18 meters height difference. Temoshok's calculations also indicate this fact.⁽⁵⁾

2.8. Effect of Phase Separation and Intra-conductor Separation:

Phase separation has significant effect upon the conductor gradient. The calculations show that with decrease in phase spacing the gradient increases largely.⁽⁵⁷⁾

Intraconductor separation was discussed in Chapter 1. Equations for the optimum intra-conductor spacing were derived. The gradient is minimum for the optimum spacing and increases greatly for values less than or above this value. It is to be noted that the values used in practice are little higher than the optimum values for facility in construction. It is very difficult to maintain small intra-conductor spacings and, under mechanical vibrations contacts between conductors will be numerous resulting in abrasions, spacer and conductor damage.

2.9. Comparison of the Methods of Gradient Determination:

The conventional method of gradient determination using Maxwell's equations is tedious and requires digital calculation. The standard gradient calculation procedure can be fitted into the system design programs, to study the alternative solutions^(42,46) This method considers all the variables and system features viz. height and ground wires, and gives accurate results.

The method of conformal mapping is useful in the study of gradient pattern around the subconductors and so can be developed to study more clearly the phenomena such as corona and RI that are associated with EHV lines. This method involves some assumptions which altogether neglect the effects-finite height and ground wires, which as known are of secondary in nature.

Mangoldt's equation used in Chapter 1 neglects the secondary effect due to ground wire and provides quick determination of the gradient. This equation is widely used in industry.⁽⁵⁷⁾ Calculations done by the author show a good agreement among the methods within acceptable limits.

CHAPTER 3

ELECTRICAL CHARACTERISTICS OF BUNDLE CONDUCTOR LINES:

§.1. Introduction:

The presence of conductors in the close vicinity reduces the inductance, while increasing the capacitance. This led the pioneers in the transmission field to adopt bundle conductor transmission lines. The calculation of the parameters has been revised about three decades ago which once again established the advantages of bundle conductor lines.⁽⁴⁰⁾ Since then many others^(28, 100, 101) have attempted presenting all the parameter in a ready-to-use form. A recent paper deals with the method of calculation for all arrangements of simplex, duplex, triplex and quadruplex lines⁽¹¹⁰⁾ Exhaustive tables have been prepared which allow ready estimation of the parameters at very close intervals of the different variables. In the design of transmission line it may be necessary to incorporate a program which can calculate all the sequence-self and mutual parameters for each conductor.^(42, 109)

3.2. Method of Calculation and Assumptions:

The inductance and capacitance can be split up into two components, conductor component and separation component. The conductor component is same for all circuit configurations viz., horizontal etc., depending only upon the number of subconductors, radius of subconductor and intra-conductor separation.

In addition to the assumptions made in the voltage gradient calculations, it is also assumed that the transmission line is perfectly transposed and that the current distribution between subconductors is equal. The calculation procedure can also be extended to untransposed transmission lines provided the unbalances are compensated by terminal impedances.

$$X = X_a + X_d \text{ ohms/phase/km. at 50 cycles.} \quad (1)$$

where, X_a is inductive reactance due to both, flux inside the conductor and that external to the conductor out to one meter radius, is called conductor component.

$$= \frac{0.1446}{n} \text{ Log } \frac{1}{\text{GMR} \cdot m_{12} \cdot m_{13} \cdot \dots \cdot m_{1n}}$$

GMR conductor geometric mean radius, meters

$m_{12} \cdot m_{1n}$ distance between conductor 1 and conductors 2...n, meter.

and X_d inductive reactive reactance due to flux external to the conductor out from one meter radius, to a radius of equivalent phase spacing, called as line component, or separation component.

$$= 0.1446 \text{ Log (GMD).}$$

GMD geometric mean distance between phases

$$= \frac{3}{\sqrt{2}} D \text{ for Horizontal arrangement}$$

$$= D \text{ for triangular arrangement.}$$

capacitive reactance of a n conductors/phase line is given

$$\text{by } X' = X'_a + X'_d \text{ megohms/phase/km. at } 50 \text{ cycles.} \quad \dots (2)$$

where, X'_a is capacitive reactance due to both electrostatic flux inside the conductor and that external to the conductor out to one meter radius, called as conductor - component.

$$= \frac{0.05094}{n} \text{ Log } \frac{1}{r \cdot m_{12} \cdot m_{13} \cdot \dots \cdot m_{1n}}$$

r radius of the conductor, meters

and X'_d is capacitive reactance due to electrostatic flux external to the conductor out from one meter radius, to a radius of equivalent phase spacing.

The proof for these expressions, based on the geometric mean distance principle, is given the reference. (28)

3.3. Sequence Impedances:

The positive and negative sequence impedances are equal and are given by-

$$Z_1 = Z_2 = \frac{R}{m} + j0.1446 \text{ Log } \left(\frac{\text{GMD}}{\text{GMR} \cdot m_{12} \dots m_{1n}} \right) \text{ ohms/km.} \quad (3)$$

Zero sequence impedance with earth return is given by-

$$Z_0 = \frac{R}{n} + 0.1489 + j(1.3030 + 0.1446n \text{ Log } (\text{GMD}^2 \cdot \text{GMR} \cdot m_{12} \dots m_{1n})) \text{ ohms/Km.} \quad (4)$$

where,

R Resistance of the subconductor ohms/Km.

The equations (3) and (4) are modified and are presented in Chapter 6.

3.4. Reactance of Single and Bundle Conductor Lines:

Table 3.4 lists the values of conductor components for simplex, duplex, triplex and quadruplex line, essentially with the same area of cross section per phase. Evidently, the inductance decreases with bundling and with increasing number of conductors. On the other hand capacitance increases with increase in number of conductors, and capacitive reactance in effect decreases.

TABLE 3.1

Effect of Bundling on Reactances:

Number of condrs.	(Sub)condr. diameter cms.	Intra-condr. spacing cms.	Conductor component of Inductive React- ance ohms/km.	Capacitive React ance MOhms/km.
1	3.924	-	0.26023	0.08695
2	2.776	30	0.17880	0.06062
3	2.355	30	0.14779	0.05926
4	1.989	30	0.12692	0.04355

From the table it is evident the bundle conductor lines, offer great advantage by reducing the inductive reactance. This leads to reduced surge impedance and increased line capability. Curves for percent increase in line capability have been presented in Chapter 1.

3.5. Effect of Number of Conductors and Intra-conductor Spacing on Reactances:

Fig. (3.1) and (3.2) illustrate the effect of number of conductors in a bundle and the intra-conductor separation, on inductive reactance and capacitive susceptance. For comparative purposes the value for single conductor line is also indicated. Table 3-1 and these two figures show only the conductor component; the separation component for a given phase separation is constant for all systems (simplex, duplex etc.). There exists a uniform decrease in inductive reactance with increase in number of sub-conductors, from 2 to 4. The intra-conductor spacing further decreases the inductive reactance. However, at practical intra-conductor spacings comparatively large reduction is obtained. By increasing the number of conductors per phase from 1 to 2 or a large reduction in inductive reactance is evidenced. Further splitting of the area of conductor cross section results in only lesser reduction of the inductive reactance.

Capacitive susceptance on the other hand increases with number of conductors. Fig. (3.2) illustrates the fact that the increase in capacitive reactance is nonuniform being greater for increased intra-conductor separation. However the increase in capacitive susceptance is uniform with increase in number of conductors above 2.

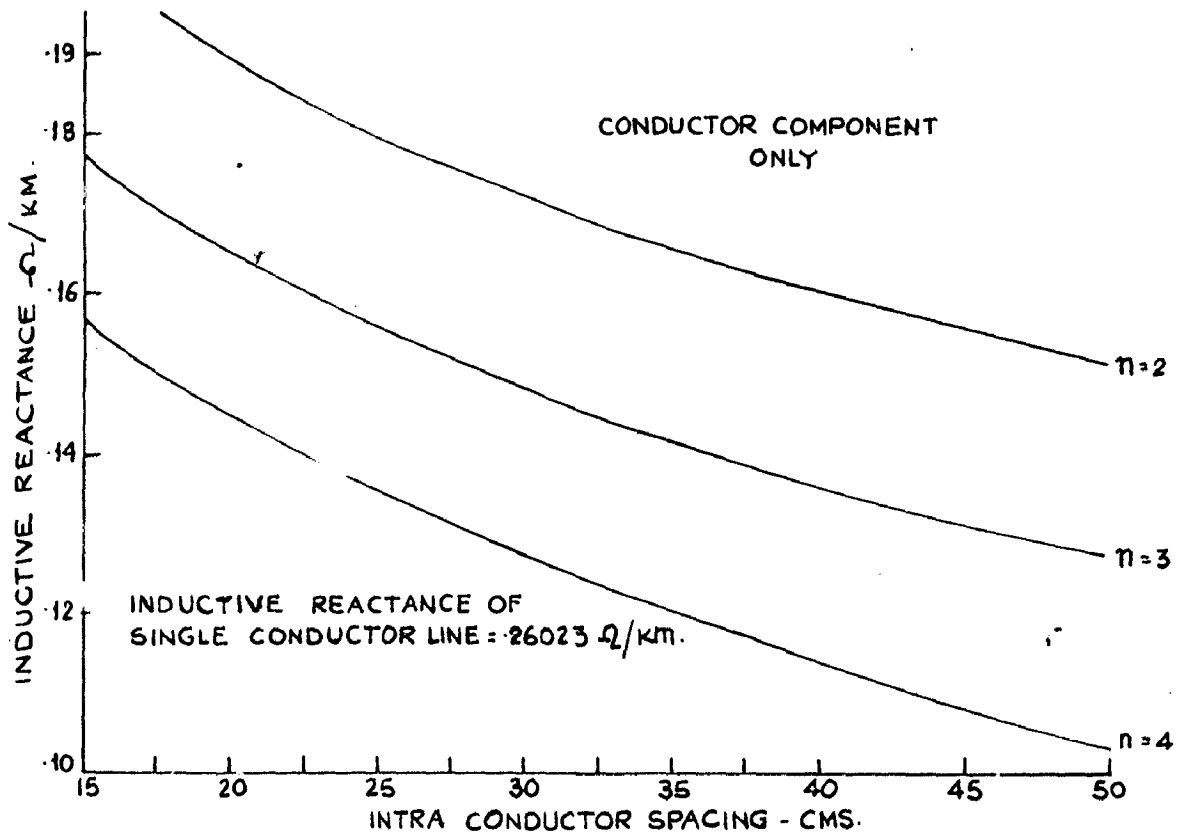


FIG. 3.1 INDUCTIVE REACTANCE OF BUNDLE CONDUCTORS

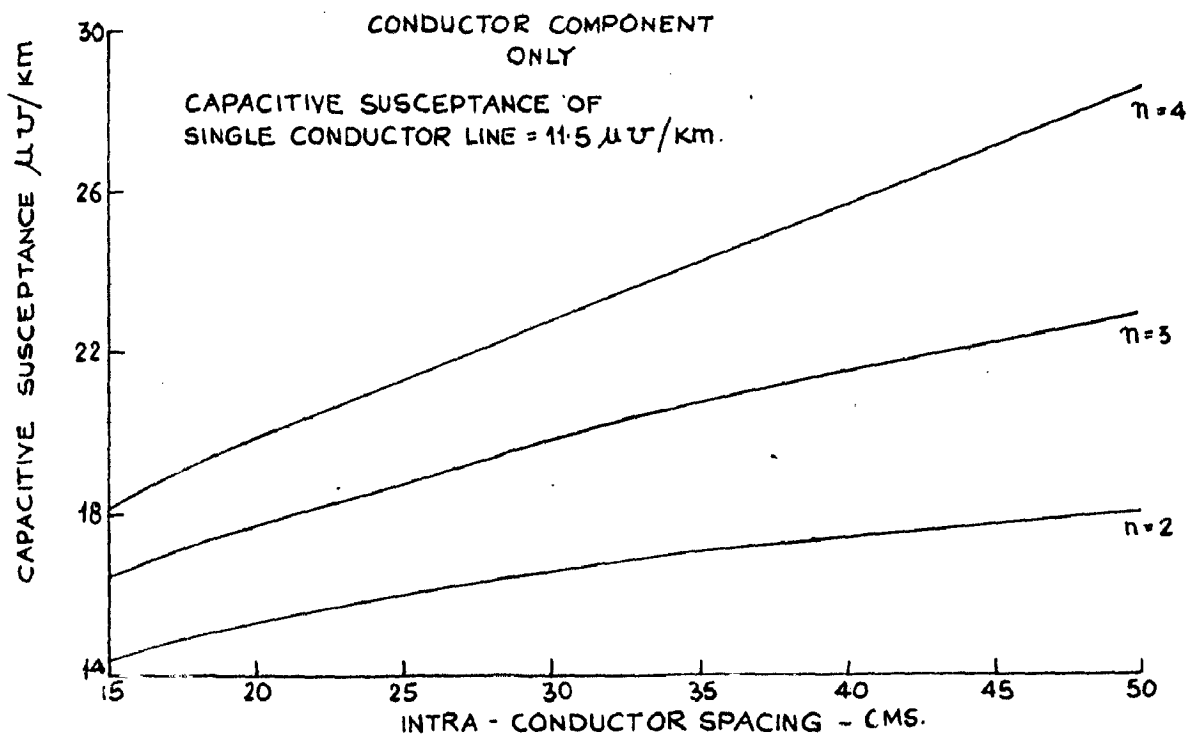


FIG. 3.2 CAPACITIVE SUSCEPTANCE OF BUNDLE CONDUCTORS

3.6. Tables for Quick Estimation of Reactances:

Tables 3.2 to 3.4 list the conductor components and separation components of inductive and capacitive reactances for the double circuit, single circuit- horizontal & triangular, lines. These tables give the values of the reactances at close intervals and cover a voltage range of 66 -600KV.⁽¹¹⁰⁾ For single circuit lines the sum of the conductor and separation components, as listed, gives the value of the required reactance. But, for a double circuit line only half the conductor component is to be added to the listed separation component, to obtain the reactance-inductive or capacitive.⁽¹¹⁰⁾ These tables will be of great use in quick estimation of the pertinent parameters and thus facilitate the selection of the most suitable configuration in the design of EHV lines.

MENT) IN OHMS PER PHASE PER KILOMETER AT 50 HZ

NUMBER OF CONDUCTORS PER PHASE

3

4

INTRA-CONDUCTOR SPACING IN CENTIMETERS

	25	30	35	40	45	30	35	40	45
65	14431	13668	13022	12463	11970	11597	10871	10242	0968
14	14480	13716	13071	12512	12019	11634	10908	10279	0972
67	14533	13769	13124	12565	12072	11673	10947	10318	0976
98	14563	13800	13155	12596	12102	11696	10970	10341	0978
86	14652	13888	13243	12684	12191	11763	11037	10408	0985
48	14714	13951	13305	12746	12253	11809	11083	10454	0990
17	14782	14019	13374	12815	12322	11861	11135	10506	0995
88	14853	14090	13445	12886	12393	11914	11188	10559	1000
61	14927	14164	13518	12959	12466	11969	11243	10614	1005
48	15013	14250	13605	13046	12553	12034	11308	10679	1012
11	15077	14313	13668	13109	12616	12081	11355	10726	1017
38	15104	14340	13695	13136	12643	12102	11376	10747	1019
38	15204	14440	13795	13236	12743	12177	11450	10822	1026
98	15164	14401	13755	13196	12703	12147	11421	10792	1023
00	15066	14303	13657	13098	12605	12073	11347	10718	1016
49	15315	14551	13906	13347	12854	12260	11534	10905	1035
13	15279	14516	13870	13311	12818	12233	11507	10878	1032
15	15181	14418	13772	13213	12720	12160	11434	10805	1025
22	15388	14624	13979	13420	12927	12315	11589	10960	1040
55	15421	14658	14012	13453	12960	12340	11614	10985	1043
34	15400	14637	13992	13432	12939	12324	11598	10969	1041
37	15303	14540	13894	13335	12842	12251	11525	10896	1034
24	15490	14726	14081	13522	13029	12391	11665	11036	1048
85	15451	14688	14042	13483	12990	12362	11636	11007	1045
77	15542	14779	14134	13575	13082	12431	11705	11076	1052
79	15444	14681	14036	13477	12984	12357	11631	11002	1044
90	15556	14793	14147	13588	13095	12441	11715	11086	1053
36	15702	14939	14293	13734	13241	12550	11824	11196	1064
38	15603	14840	14195	13636	13143	12476	11750	11122	1056
25	15891	15128	14482	13923	13430	12692	11966	11337	1078
25	15791	15027	14382	13823	13330	12617	11891	11262	1070
98	16064	15300	14655	14096	13603	12822	12096	11467	1091
06	15971	15208	14563	14004	13511	12752	12026	11397	1084
22	16187	15424	14779	14220	13727	12914	12188	11559	1100
24	16090	15326	14681	14122	13629	12841	12115	11486	1093
43	16309	15546	14901	14341	13848	13006	12280	11650	1109
60	18725	17962	17317	16758	16265	14818	14092	13463	1290
96	18361	17598	16953	16394	15900	14545	13819	13190	1263
34	19000	18237	17592	17033	16539	15024	14298	13669	1311
75	19340	18577	17932	17373	16880	15279	14553	13924	1330
56	19622	18859	18213	17654	17161	15490	14764	14135	1350

TABLE 3.2 X_a INDUCTIVE REACT

AWG	DIA # CONDR CMS	GMR CMS	1 CONDR	NUMBER OF CONDUCTORS PER				
				2			3	
				INTRA-CONDUCTOR			SPACING IN	
			15	20	25	30	35	
780000	4.069	1.622	25882	18898	17994	17294	16721	162
590000	3.924	1.585	26028	18971	18067	17367	16794	163
510500	3.825	1.545	26187	19050	18147	17446	16874	163
431000	3.721	1.523	26278	19096	18193	17492	16920	164
351000	3.617	1.460	26543	19229	18325	17625	17052	165
272000	3.510	1.417	26730	19322	18418	17718	17145	166
192500	3.399	1.372	26936	19427	18521	17821	17248	167
113000	3.284	1.326	27149	19531	18628	17927	17355	168
033500	3.165	1.280	27369	19641	18738	18037	17465	169
954000	3.038	1.228	27628	19771	18868	18167	17595	171
900000	2.952	1.192	27818	19866	18963	18262	17690	172
874500	2.911	1.177	27899	19906	19003	18302	17730	172
795000	2.776	1.122	28199	20056	19153	18452	17880	173
795000	2.814	1.143	28081	19997	19094	18393	17821	173
795000	2.896	1.198	27786	19850	18947	18246	17674	171
715500	2.631	1.064	28532	20223	19320	18619	18046	175
715500	2.670	1.082	28425	20169	19266	18565	17993	175
715500	2.748	1.134	28131	20022	19119	18418	17846	173
666600	2.540	1.027	28752	20333	19429	18729	18156	176
636000	2.482	1.011	28852	20383	19479	18779	18206	177
636000	2.538	1.021	28789	20351	19448	18747	18175	176
636000	2.588	1.070	28496	20204	19301	18601	18028	175
605000	2.421	0.978	29057	20485	19582	18881	18309	178
605000	2.454	0.997	28941	20247	19523	18823	18251	177
556500	2.355	0.954	29216	20565	19661	18961	18388	179
556500	2.421	1.000	28922	20418	19514	18814	18241	177
500000	2.296	0.948	29256	20585	19681	18981	18408	179
477000	2.179	0.884	29695	20804	19900	19200	18628	181
477000	2.243	0.927	29399	20656	19752	19052	18480	179
397500	1.989	0.808	30261	21087	20184	19483	18911	184
397500	2.047	0.847	29960	20937	20034	19333	18761	182
336400	1.831	0.744	30779	21347	20443	19743	19170	186
336400	1.882	0.777	30503	21208	20305	19604	19032	185
300000	1.727	0.701	31151	21532	20629	19928	19356	188
300000	1.778	0.735	30857	21385	20482	19781	19209	187
266800	1.631	0.661	31516	21715	20811	20111	19538	190
266800	1.608	0.209	38765	25339	24436	23735	23163	226
4/0	1.430	0.248	37672	24792	23890	23189	22617	221
3/0	1.275	0.183	39589	25751	24848	24147	23575	230
2/0	1.135	0.156	40610	26261	25358	24658	24085	226
1/0	1.010	0.136	41454	26684	25781	25080	24507	240

T) IN MEGOHMS PER PHASE PER KILOMETER AT 50HZ

NUMBER OF CONDUCTORS PER PHASE

3	INTRA-CONDUCTOR SPACING IN CENTIMETERS										
	30	35	40	45	30	35	40	45	50	55	60
47	04420	04223	04049	03959	03704	03482	03287	03112	02954	02810	
74	04446	04250	04076	03980	03724	03502	03307	03132	02974	02830	
93	04465	04268	04095	03994	03738	03516	03321	03146	02988	02844	
113	04486	04289	04115	04009	03753	03532	03336	03162	03003	02859	
134	04507	04310	04136	04025	03769	03547	03352	03177	03019	02875	
156	04529	04332	04158	04041	03785	03564	03369	03194	03036	02891	
180	04553	04356	04182	04059	03803	03582	03386	03212	03054	02909	
205	04578	04381	04207	04078	03822	03601	03405	03231	03072	02928	
232	04605	04408	04234	04098	03843	03621	03426	03251	03093	02949	
263	04635	04438	04265	04121	03865	03644	03448	03274	03116	02971	
284	04656	04460	04286	04137	03881	03660	03464	03290	03132	02987	
314	04667	04470	04296	04145	03889	03667	03472	03297	03139	02995	
329	04702	04505	04331	04171	03915	03694	03498	03324	03165	03021	
319	04692	04495	04321	04163	03908	03686	03491	03316	03158	03014	
398	04671	04474	04300	04148	03892	03670	03475	03300	03142	02998	
468	04741	04544	04371	04201	03945	03723	03528	03353	03195	03051	
458	04731	04534	04360	04193	03937	03715	03520	03345	03187	03043	
436	04709	04512	04339	04177	03921	03699	03504	03329	03171	03027	
494	04767	04570	04397	04220	03964	03743	03548	03373	03215	03070	
512	04785	04587	04414	04233	03977	03756	03560	03386	03227	03083	
595	04768	04571	04397	04221	03965	03743	03548	03373	03215	03071	
581	04753	04556	04383	04210	03954	03732	03537	03362	03204	03060	
630	04803	04606	04432	04247	03991	03769	03574	03399	03241	03097	
620	04793	04596	04422	04239	03983	03762	03567	03392	03234	03089	
650	04823	04626	04453	04262	04006	03785	03589	03415	03256	03112	
630	04803	04606	04432	04247	03991	03769	03574	03399	03241	03097	
669	04842	04645	04471	04276	04020	03799	03603	03428	03270	03126	
607	04880	04683	04510	04305	04049	03828	03632	03457	03299	03155	
686	04859	04662	04488	04289	04033	03812	03616	03441	03283	03139	
675	04948	04751	04577	04355	04100	03878	03683	03508	03350	03205	
54	04926	04729	04556	04339	04084	03862	03667	03492	03334	03189	
36	05008	04811	04638	04401	04145	03924	03728	03554	03395	03251	
16	04988	04791	04618	034386	04130	03909	03713	03538	03380	03236	
79	05052	04855	04681	04433	04178	03956	03761	03586	03428	03283	
57	05030	04833	04660	04417	04162	03940	03745	03570	03412	03267	
21	05094	04897	04723	04465	04209	03988	03793	03618	03460	03315	
32	05104	04907	04734	04473	04217	03996	03800	03626	03467	03323	
18	05191	04994	04820	04538	04282	04061	03865	03690	03532	03388	
03	05275	05078	04905	04601	04345	04124	03929	03754	03596	03451	
88	05361	05164	04990	04665	04410	04188	03993	03818	03660	03515	
74	05446	05250	05076	04730	04474	04252	04057	03882	03724	03580	

TABLE-3.3 X_a CAPACITIVE REACTANCE (CONDUCTOR

NUMBER OF CONDUCTORS PER PHASE

AWG	CONDR DIA CMS	1 CONDR	2 INTRA CONDUCTOR SPACING IN CENTIMETERS								
			15	20	25	30	35	40	45	15	2
780000	4.069	08615	06406	06087	05841	05639	05469	05321	05191	05669	052
590000	3.924	08695	06446	06127	05881	05679	05509	05361	05231	05696	052
510500	3.825	08752	06474	06156	05909	05707	05537	05389	05259	05715	052
431000	3.721	08813	06504	06186	05940	05738	05567	05420	05289	05735	052
351000	3.617	08876	06536	06218	05971	05769	05599	05451	05321	05756	052
272000	3.510	08942	06569	06251	06004	05802	05632	05484	05354	05778	052
192500	3.399	09012	06605	06287	06040	05838	05668	05520	05390	05802	052
113000	3.284	09089	06643	06324	06078	05876	05706	05558	05428	05827	054
033500	3.165	09171	06684	06365	06119	05917	05747	05599	05469	05854	054
954000	3.308	09261	06729	06411	06164	05962	05792	05644	05514	05885	054
900000	2.952	09325	06761	06443	06196	05994	05824	05676	05545	05906	054
874500	2.911	09356	06776	06458	06211	06010	05839	05691	05561	05916	054
795000	2.776	09461	06828	06510	06264	06062	05891	05744	05613	05951	055
795000	2.814	09431	06813	06495	06248	06047	05876	05729	05598	05941	055
795000	2.896	09368	06782	06464	06217	06015	05845	05697	05567	05920	054
715500	2.631	09580	06888	06570	06323	06121	05951	05803	05673	05991	055
715500	2.670	09547	06872	06554	06307	06105	05935	05787	05657	05980	055
715500	2.748	09483	06840	06521	06275	06073	05903	05755	05625	05958	055
666600	2.540	09657	06927	06609	06362	06160	05990	05842	05712	06017	055
636000	2.482	09709	06953	06634	06388	06186	06015	05868	05738	06034	056
636000	2.538	09660	06928	06610	06363	06161	05991	05843	05713	06017	055
636000	2.588	09616	06906	06588	06341	06139	05969	05821	05691	06003	055
605000	2.421	09764	06980	06662	06415	06213	06043	05895	05765	06052	056
605000	2.454	09734	06965	06647	06400	06198	06028	05880	05750	06042	056
556500	2.355	09825	07011	06692	06446	06244	06074	05926	05796	06073	056
556500	2.421	09764	06980	06662	06415	06213	06043	05895	05765	06052	056
500000	2.296	09881	07038	06720	06473	06272	06101	05954	05823	06091	056
477000	2.179	09996	07096	06778	06531	06330	06159	06011	05881	06130	057
477000	2.243	09933	07064	06746	06499	06298	06127	05980	05849	06108	056
397500	1.989	10198	07197	06879	06632	06431	06260	06113	05982	06197	057
397500	2.047	10134	07165	06847	06600	06399	06228	06081	05950	06176	057
336400	1.831	10381	07289	06970	06724	06522	06352	06204	06074	06258	058
336400	1.882	10320	07258	06940	06693	06492	06321	06174	06043	06238	058
300000	1.727	10510	07353	07035	06788	06587	06416	06269	06138	06301	058
300000	1.778	10446	07321	07003	06756	06555	06384	06237	06106	06280	058
266800	1.631	10638	07417	07099	06852	06650	06480	06332	06202	06343	059
266800	1.608	10669	07433	07114	06868	06666	06495	06348	06218	06354	059
4/0	1.430	10928	07562	07244	06997	06796	06625	06427	06347	06440	060
3/0	1.275	11182	07689	07371	07124	06922	06752	06604	06474	06525	061
2/0	1.135	11438	07817	07499	07252	07051	06880	06733	06602	06610	061
1/0	1.010	11695	07946	07627	07381	07179	07009	06861	06731	06696	062

TABLE 3.4 SEPERATION COMPONENTS X_d AND X'_d FOR DIFFERENT ARRANGEMENTS.
 X_d IN OHMS PER PHASE PER KM. X'_d IN MEGOHMS PER PHASE PER KM. AT 50 HZ
D DOUBLE CIRCUIT SINGLE CKT. HORIZONTAL SING. CKT. TRIANGULAR
MTS. X_d X'_d X_d X'_d X_d X'_d

3.00	.03868	.01363	.08350	.02942	.06900	.02430
3.25	.04119	.01451	.018853	.03119	.07402	.02608
3.50	.04352	.01553	.09318	.03283	.07867	.02772
3.75	.04568	.01609	.09751	.03435	.08301	.02924
4.00	.04771	.01681	.10157	.03578	.08706	.03067
4.25	.04961	.01748	.10538	.03712	.09087	.03201
4.50	.05141	.01811	.010896	.03839	.03485	.03328
4.75	.05310	.01871	.11236	.03958	.09785	.03447
5.00	.05472	.01928	.11558	.04072	.10107	.03561
5.25	.05625	.01982	.11865	.04180	.10414	.03669
5.50	.05771	.02033	.12157	.04283	.10706	.03771
5.75	.05910	.02082	.12436	.04381	.10985	.03870
6.00	.06044	.02130	.12703	.04475	.11252	.03964
6.25	.06172	.02174	.12960	.04566	.11508	.04054
6.50	.06295	.02218	.13206	.04652	.11755	.04141
6.75	.06414	.02260	.13643	.04736	.11992	.04225
7.00	.06528	.02300	.13671	.04816	.12220	.04305
7.25	.06638	.02339	.13891	.04894	.12441	.04383
7.50	.06745	.02376	.14104	.04969	.12653	.04458
7.75	.06848	.02412	.14310	.05041	.12859	.04530
8.00	.06947	.02447	.14510	.05112	.13059	.04600
8.25	.07044	.02481	.14703	.05180	.13252	.04668
8.50	.07138	.02515	.14890	.05246	.13439	.04735
8.75	.07229	.02547	.15072	.05310	.13621	.04799
9.00	.07317	.02578	.15249	.05372	.13798	.04861
9.25	.07403	.02608	.15421	.05433	.13971	.04922
9.50	.07487	.02637	.15588	.05492	.14138	.04980
9.75	.07570	.02666	.13752	.05549	.14301	.05038
10.00	.07648	.02694	.15911	.05605	.14460	.05094
10.25	.07725	.02722	.16066	.05680	.14615	.05150
10.50	.07801	.02750	.16217	.05713	.14770	.05202
10.75	.07875	.02774	.16365	.05765	.14914	.05254
11.00	.07950	.02799	.16509	.05816	.15058	.05305
11.25	.08012	.02825	.16651	.05866	.15200	.05355
11.50	.08087	.02849	.16790	.05914	.15338	.05403
11.75	.08154	.02875	.16924	.05962	.15473	.05451
12.00	.08220	.02896	.17056	.06009	.15605	.05497
12.25	.08285	.02919	.17185	.06054	.15734	.05543
12.50	.08349	.02941	.17312	.06100	.15861	.05588
12.75	.08411	.02963	.17437	.06143	.15986	.05632
13.00	.08472	.02965	.17558	.06186	.16108	.05674
13.25	.08532	.03006	.17678	.06228	.16227	.05717
13.50	.08590	.03026	.17796	.06269	.16345	.05758
13.75	.08648	.03047	.17911	.06310	.16460	.05799
14.00	.08704	.03066	.18024	.06350	.16573	.05838
12.25	.08760	.03086	.18135	.06389	.16684	.05877
14.50	.08815	.03095	.18244	.06427	.16795	.05916
14.75	.08868	.03124	.18352	.06465	.16901	.05954
15.00	.08921	.03143	.18458	.06502	.17006	.05991

CHAPTER 2

CORONA ON BUNDLE CONDUCTORS:

The term 'corona' is derived from French word 'coronae', which means crown referring to the luminous portion around the conductor. Corona or partial break-down of air can be visualised by considering a corresponding virtual increase in conductor diameter.

4.1. Corona Phenomenon:

There always exists a small quantity of ionisation due to various natural radiations viz. cosmic rays etc. The free electrons present due to natural ionisation however collide with neutral molecules but cannot cause further ionisation. However, if the conductor potential is increased so that greater amounts of charges are accumulated on the conductor, these electrons acquire velocity and succeed in separating electrons from the neutral molecules. These newly created electrons can themselves cause further ionisation and for each electron, an electron avalanche is produced.

If the applied potential is positive, the positive ions formed move outward, at a low velocity into ever decreasing potential gradient regions forming positive space charge all around the conductor group. The charge density however depends on the gradient and is nonuniform for bundle conductor lines.

If the applied potential is negative, the electrons being repelled from conductor group move out faster and get attached to the neutral molecules which obviously move outward at a low velocity forming a negative space charge similar to the case of the positive potential.

4.2. Theory of A.C. Corona:

If the applied potential is alternating, the phenomenon in a half cycle will affect that in the other half cycle.

Corona starts on negative half-cycle, this is evidenced by the large number of experiments performed over decades.⁽²⁰⁾ The main feature of negative corona is, it is confined, normally, to the regions of high-gradients caused by mechanical damage, dust collection, precipitation and contamination. With the negative corona at a single point, the discharge currents consist of a large number of short pulses concentrated at the top of the applied voltage wave. In the region nearer to the negative corona inception voltage, a few pulses of current are present, but they increase fast with increase in applied voltage. From experimental evidences it is observed that the instantaneous inception voltage of negative corona and the amplitude of the current pulses remain practically constant over a wide range of voltages.⁽²⁰⁾ The negative corona is bluish in colour and produces a hissing noise of relatively high frequency.

Corona inception on positive half-cycle is dependent on many factors. On clean metal surfaces the corona inception voltage may be as much as one and half times that of the positive corona, whereas with conductors on which some mechanical damage or contamination is present the difference is levelled out. Even though positive corona in general appears at the same area of the preceding point of negative corona, the point of occurrence may not be same. Positive corona is stabler on damaged or contaminated metal surfaces, on the other hand it is intermittent over a wide range of voltages on clean surfaces. With positive corona at a single point, there exists only a current pulse per half-cycle of

magnitude as much as 10^3 times that of the negative corona current pulse. The positive corona is similar in appearance to that of positive streamer of a lightning discharge, and in a similar manner it can jump upto a few cms. from the corona point and form a tree like structure. The colour of positive corona is reddish-orange and gives a crackling sound of low frequency. With a little experience one can easily distinguish between positive and negative coronas from these differences in sound and colour. The discharges due to positive corona are of a few nanosecond duration.

When alternating potential is applied, the ionisation process begins at the negative half-cycle with the help of the free electrons present due to natural ionisation. As stated earlier with an increase in the potential gradient, the electron avalanches are formed which eventually appear as the pulses of current described hitherto. Due to the presence of electric field, the positive ions are attracted toward the conductor (in the negative half-cycle) and electrons are repelled from it since they carry negative charge. This charge movement occurs both axially and radially. Axial movement is due to charge concentrations at particular spots. Due to the inherent difference in masses of positive ions and negative electrons, the latter move faster away from the conductor, whereas the former move relatively slow in a half cycle. At potential zero or at some particular distance away from the conductor where the electric field is weak, the electrons can attach themselves to electro positive oxygen atoms and become relatively immobile. The attachment can also result in regions of high-gradient between two collisions when the electron velocities are low. This type of

release the electrons thus attached.

Towards the end of the negative half-cycle two space charges are created. A positive space charge near the conductor and a negative space charge away from the conductor. For a case where the corona is existing at a particular point only, the two space charges can be visualised as cones, the apex of positive space-charge cone pointing away from the conductor and that of the negative space charge towards the conductor. The height of the positive space charge cone of course is relatively smaller. There exists a difference in charge concentrations in both cases.

Now, with the start of the positive half-cycle, the positive space charge starts moving slowly away from the conductor, and the movement of negative space charge is quite fast and opposite in direction. The negative space charge eventually reaches the conductor and thus the gradient increases at the conductor giving rise to a spark discharge. With the emission of this spark discharge both the space charges tend to be neutralised and the process repeats itself in the next cycle. This feature of a spark discharge in the positive half cycle elucidates the nature and instability of positive corona. In fact, it takes quite a few cycles for the positive corona to become stable and give regular spark discharges. (20)

4.3. Corona in Foul Weather:

Corona phenomenon on transmission lines in foul weather is treated in detail in the references. (79,80) In our country only the losses due to rain assume importance as the regions of snow are relatively less. The effect of weather is discussed in detail in the paragraphs titled "Corona loss results from test projects"

4.4. Corona Initiation Voltage:

When the surface gradient exceeds a critical value the corona is said to have formed on the conductor. The voltage at which the air breaks down allowing formation of corona is known as "disruptive critical voltage". Peak's formula for visual critical voltage is-

$$V_c = 21.1 M_s r \left(1 + \frac{0.301}{\sqrt{r}}\right) \text{ KV}_{\text{rms}} \text{ to neutral} \quad (3)$$

where,
 M_s surface factor
 r radius in cm.

(disruptive critical voltage is less than visual critical voltage by a factor of about 0.9).

In practice, the critical voltage of a conductor at which corona starts may be 50 to 85% of this value because of surface imperfections and environmental conditions experienced in the field. These surface and environmental conditions are candidly summarised mathematically by the use of the factor ' M_s '. Particles caught between strands or nicks and abrasions can become local points of high surface voltage gradient and cause localised breakdown of air surrounding them. Stranding itself can reduce critical voltage on a smooth tube by as much as 10 to 16%, depending upon the ratio of strand diameter to outside conductor diameter.

However, on an actual transmission system the critical corona starting voltage is dependent upon the line geometry. If $\frac{2h}{D}$ is large, the critical voltage is given by^(44,45)

$$V_{c1} = \frac{10.55M_s \text{Log}_e \left| \frac{\sqrt{(d_{11}', d_{12}', \dots, d_{1n}') (d_{11}'', d_{12}'', \dots, d_{1n}'')}}{r(m_{12}, \dots, m_{1n})} \right|}{\sqrt{\left| \frac{1}{m_{1n}} \cos \theta_{1n} \right|^2 + \left| \frac{1}{m_{1n}} \sin \theta_{1n} \right|^2} + \frac{1}{2r}} \text{KV}_{\text{rms to neutral}} \quad \dots \quad (4)$$

The above equation gives the critical voltage on a conductor 1 of phase I, where conductor 1 can be any conductor and phase I can be any phase of the three phase line.

Equation (3) and (4) give values of critical voltage at mean sea level and normal temperature and pressure. However the variations in these quantities can be accounted for by defining a relative air density factor . And the variation of critical voltage is proportional to two-thirds power of . The conductors while being strung are given due care to see that the mechanical damages are minimum. A newly strung line is however vulnerable to low corona starting voltage and higher losses. It takes a few weeks for the corona losses to stabilise. Rain or snow can enhance this process of "ageing" by cleaning the conductors virtually.

Equation (4) assumes that $\left(\frac{2h}{D}\right)$ is large. In actual EHV lines however, the ratio will be around (2.0 ± 0.2) . Thus for EHV lines the above equation is modified and is given as-

$$V_{c1} = \frac{10.55M_s \text{Log}_e \left| \frac{(2h)^n \sqrt{(a_{11}', \dots, a_{1n}') (a_{11}'', \dots, a_{1n}'')}}{r(m_{12}, \dots, m_{1n})} \right|}{\sqrt{\left| \frac{1}{m_{1n}} \cos \theta_{1n} \right|^2 + \left| \frac{1}{m_{1n}} \sin \theta_{1n} \right|^2} + \frac{1}{2r}} \text{KV}_{\text{rms to neutral}} \quad \dots \quad (5)$$

where, $a_{11}' = \frac{d_{11}'}{D_{11}'}$ etc.,

4.5. Effects of Corona:

As noted already corona can be visualised by a corresponding virtual increase in conductor diameter. This fact can be further developed to study the actual effects of corona. A conductor under corona has space charges associated with it. AC transmission line conductor has got surrounding it two space charges which move to and from the conductor in each half cycle. It is this space charge that causes the virtual increase in the conductor diameter (γ times the actual conductor diameter). This however leads to an increase in the charge on the conductor. Finally the gradient increases on the conductor in corona, at all points. Infact, the space charge is surrounding the conductor and is not residing on it, hence, only the gradient in the vicinity of the conductor should increase. The increase in voltage gradient, in the vicinity of conductor, results in the increase in intensity and depth of corona bringing in the additional losses.

Associated with increase in charge is increase in electrostatic flux lines around the conductor. This increase in electrostatic flux should be lower for higher number of conductors. A large difference/increase can be expected when the number of conductors are increased from 1 to 2 per phase. It remains to develop a mathematical/basis for these changes and thereby compute the actual gradient on conductor in corona, since gradient on conductor in corona is definitely different from the one calculated by any of the three methods given in Chapter 2. In the case of AC lines the space charge changes in every half cycle, so, the gradient on conductor in corona should change depending upon the intensity of corona. This indicates a possible extension of the corona phenomenon for further study.

4.6. Corona loss Calculations:

Mathematical determination of corona loss is possible if it can be assumed that the losses are due to a fictitious resistance of the corona envelope surrounding the conductor. Then the loss is the product of corona current, and the resistance of the envelope squared. In single conductor lines the corona forms uniformly around the conductor, but on bundle conductor lines only a portion in which the gradient is in excess of or equal to critical value is under corona. This region is around the maximum surface gradient point, opposite and away from the bundle centre. A loss equation has been derived on the above lines, (38)

$$P = Kfr^2 n \left(g_{e1}^2 \text{Log}_e \frac{g_{e1}}{g_0} + 2 g_{e2}^2 \text{Log}_e \frac{g_{e2}}{g_0} \right) \quad (6)$$

where,

k empirical constant (determined from experiments, varies with the type of weather).

$$f = \frac{\alpha}{2\pi}$$

α = angle of corona

$$= \pi \sin^{-1} \frac{g_0 - g_{av}}{g_{av} \frac{(n-1)r}{m} \sin \frac{\pi}{n}} \quad \text{radians}$$

g_{av} average surface gradient (at $\theta = 0$), KV_{rms}/cm .

However, during rain corona angle extends to a region covering the bottom portion of conductors and the angle increase depends upon the number of conductors. Corona angle is a function of rain intensity with heavy rain the entire conductor will be in corona and thus a saturation of corona losses results in.

4.7. Bundle Conductor Efficiency Coefficients:

The corona initiation voltage on bundle conductor is higher

efficiency coefficient can be defined as-

$$\eta = \frac{V_{cn}}{V_{cl}} \quad \dots \quad \dots \quad (7)$$

where, V_{cn} critical corona voltage on bundle conductor line

V_{cl} critical corona voltage on single conductor line.

⁽⁹⁹⁾ Tichodeev first derived these coefficients for the case of DC transmission line. The proof of these coefficients is based on the assumption that the field due to the conductors of the same phase is uniform in the region of the conductor and that the effect of field due to other conductors is negligible.⁽³³⁾ Crary developed an equation for the gradient at any conductor of any phase as⁽⁴⁵⁾

$$E_{m1} = 4Q1 / \left(\left(\sum \frac{1}{m_{1n}} \cos \theta_{1n} \right)^2 + \left(\sum \frac{1}{m_{1n}} \sin \theta_{1n} \right)^2 + \frac{1}{d} \right) \quad (8)$$

where, 1 is any conductor in any phase.

Designating the phases on a tower (single circuit line) as I, II and III and that $1, 2, \dots, n; 1', 2', \dots, n'; 1'', 2'', \dots, n''$ as the n conductors in each phase respectively, we have,

$$V_1 = P_{11}Q_1 + P_{12}Q_2 + \dots + P_{1n}Q_n + P_{11'}Q_{1'} + P_{12'}Q_{2'} + \dots + P_{1n'}Q_{n'} + P_{11''}Q_{1''} + P_{12''}Q_{2''} + \dots + P_{1n''}Q_{n''} \quad (9)$$

From the usual maxwell's equation. P's are the respective potential coefficients. When the charge on the reference conductor is Q (i.e. the total charge on that phase is nQ) the charges on respective conductors on other phases is assumed to be $-\frac{Q}{2}$ (charge on respective other phases $-\frac{nQ}{2}$). Then we have-

$$V_1 = Q \left[P_{11} + P_{12} + \dots + P_{1n} - \frac{1}{2} (P_{11'} + P_{12'} + \dots + P_{1n'} + P_{11''} + P_{12''} + \dots + P_{1n''}) \right] Q$$

Crary in his derivation of the critical voltage used the assumption that $\frac{2h}{D}$ is large but in EHV systems it is advisable to reduce the height and phase separations for the reasons of economy and the latter especially for the reasons of increasing the transmission line capacity (Chapter 1). So the derivation should take into account the phase separation and height into consideration and usually they are almost equal.

Then we have-

$$P_{1i} = 2 \log_e \frac{4h}{d} ; P_{1j} = 2 \log_e \frac{D_{1j}}{d_{1j}} \quad (11)$$

where,

i & j are any two conductors of the system.

However, the intraconductor separation is small compared to the height and it is evident that $\frac{2h}{m_{1n}}$ is large-

$$\text{Therefore } P_{1n} = 2 \log_e \frac{2h}{m_{1n}} \quad \dots \quad (12)$$

By substituting the value of Q from (8) in (10) we get the equation for the critical voltage in terms of gradients. The derivation for the case of a duplex system (horizontal arrangement), single horizontal circuit is illustrated. The system configuration is as shown in Fig.(4.3).

$$E_2 = 4Q \left(-\frac{1}{m} + \frac{1}{d} \right) \quad \dots \quad (13)$$

where the suffix 2 denotes that there are two conductors in each phase, 'm' intra conductor spacing.

Denoting the conductors as 1,2 etc., as shown for the conductor 1, considering a horizontal line through the conductor 1 as x axis and a line perpendicular to it as Y axis,

$$V_{c2} = Q \left[2 \log_e \frac{4h}{d} + 2 \log_e \frac{2h}{m} - \frac{1}{2} \left(\log_e \frac{4h^2 + D^2}{D^2} + \log_e \frac{4h^2 + (D+m)^2}{(D+m)^2} + \dots \right) \right]$$

$$V_{c2} = \frac{E_2}{2\left(\frac{h}{m} + \frac{1}{d}\right)} \text{Log}_e \left| \frac{4 \sqrt{(1+ac)}}{bc \sqrt{(1+a^2)(1+0.25a^2)}} \right| \quad (15)$$

where, $a = \frac{D}{h}$; $b = \frac{d}{D}$ and $c = \frac{m}{D}$

and critical voltage for a single conductor horizontal circuit line is-

$$V_{c1} = \frac{E_1 d}{4} \text{Log}_e \frac{8}{b^2 \sqrt{(1+a^2)(1+0.25a^2)}} \quad (16)$$

$$\therefore \eta = \frac{2E_2 \text{Log}_e \left| \frac{4 \sqrt{(1+ac)}}{bc \sqrt{(1+a^2)(1+0.25a^2)}} \right|}{E_1 \left(1 + \frac{d}{m}\right) \text{Log}_e \left| \frac{8}{b^2 \sqrt{(1+a^2)(1+0.25a^2)}} \right|} \quad (17)$$

Bundle conductor efficiency coefficients for various conductor arrangements are given in Figures (4.2 to 4.4) Fig.(4.1) shows the critical voltages for three possible arrangements of single circuit simplex lines. The arrangement of the line and various notations used in the formula are as shown in the diagram against each formula.

4.8. Methods of Corona Loss Measurements:

Corona losses assume importance in the design of transmission lines, since a severe unanticipated loss would mean a restriction on reserve capacity available. Hence it has been given due importance in all the tests conducted over EHV transmission lines. The measurement of corona losses has been reported as far back as 1878 by Dr. Scott and subsequently many have reported on the techniques and results of measurement of corona losses. A few of the references are. (2,4,11,23,38,41,64,65,68,88,90,91)

Considering the methods used for loss determination, a broad

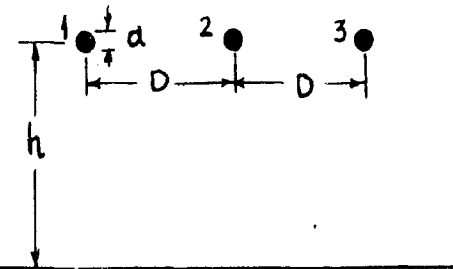
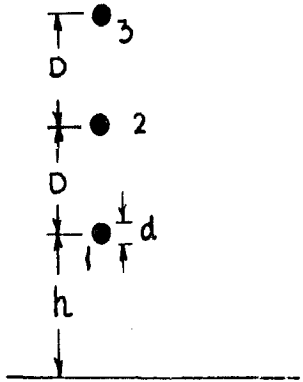
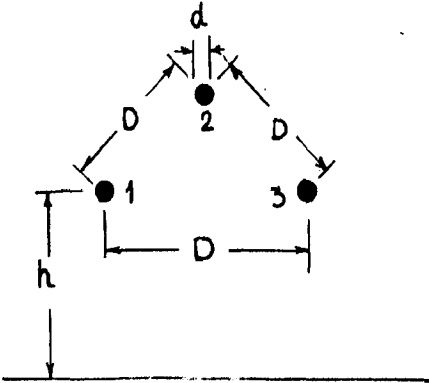
ARRANGEMENT	CRITICAL CORONA VOLTAGE ON CONDUCTOR 1
	$V_{c1} = \frac{g_1 \cdot d}{4} \ln \frac{8}{b^2 \cdot \sqrt{(1+a^2)(1+0.25a^2)}}$
	$V_{c1} = \frac{g_1 \cdot d}{4} \ln \frac{8}{b^2 (1+a)(1+0.5a)}$
	$V_{c1} = \frac{g_1 \cdot d}{4} \ln \frac{4}{b^2 \sqrt{(1+0.25a^2)(1+0.086a+0.25a^2)}}$

FIG. 4.1 SINGLE CIRCUIT LINE AND CRITICAL VOLTAGE

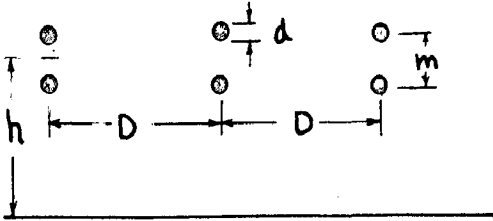
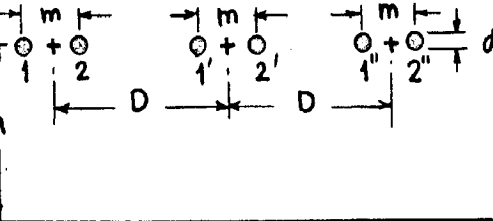
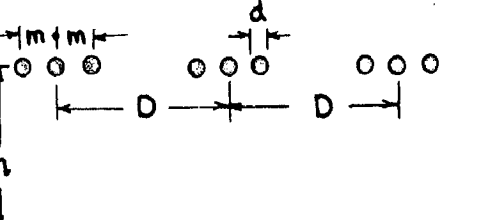
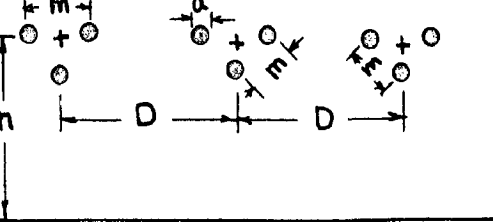
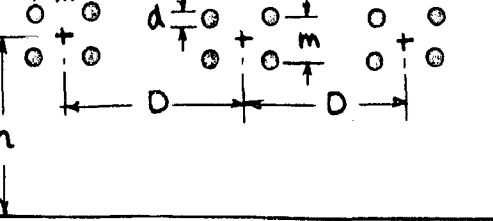
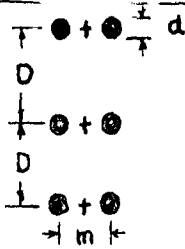
ARRANGEMENT	BUNDLE EFFICIENCY COEFFICIENTS
	$\eta = \frac{g_2}{g_1 \left(1 + \frac{d}{m}\right)} \frac{\text{Ln} \left\{ \frac{16 \sqrt{(1+c^2)(1+0.25c^2)}}{b^2 c^2 (1+a^2)(1+0.25a^2)} \right\}}{\text{Ln} \left\{ \frac{8}{b^2 \sqrt{(1+a^2)(1+0.25a^2)}} \right\}}$
	$\eta = \frac{2g_2}{g_1 \left(1 + \frac{d}{m}\right)} \frac{\text{Ln} \left\{ \frac{4 \sqrt{1+c}}{bc \sqrt{(1+a^2)(1+0.25a^2)}} \right\}}{\text{Ln} \left\{ \frac{8}{b^2 \sqrt{(1+a^2)(1+0.25a^2)}} \right\}}$
	$\eta = \frac{g_3}{g_1 \left(1 + \frac{3d}{2m}\right)} \frac{\text{Ln} \left\{ \frac{8(1+2c)(1+c)^2(1+0.5c)}{b^2 c^2 (1+a^2)(1+0.25a^2)(1+0.5a^2)} \right\}}{\text{Ln} \left\{ \frac{8}{b^2 \sqrt{(1+a^2)(1+0.25a^2)}} \right\}}$
	$\eta = \frac{g_3}{g_1 \left(1 + \frac{2d}{m}\right)} \frac{\text{Ln} \left\{ \frac{32(1+c)(1+0.5c)}{b^2 c^4 \sqrt{(1+a^2)^3(1+0.25a^2)^3}} \right\}}{\text{Ln} \left\{ \frac{8}{b^2 \sqrt{(1+a^2)(1+0.25a^2)}} \right\}}$
	$\eta = \frac{2g_4}{g_1 \left(1 + \frac{0.241d}{m}\right)} \frac{\text{Ln} \left\{ \frac{\sqrt{2(1+ac)(1+0.5ac)(1+c)(1+0.5c)}}{bc^3 (1+a^2)(1+0.25a^2)} \right\}}{\text{Ln} \left\{ \frac{8}{b^2 \sqrt{(1+a^2)(1+0.25a^2)}} \right\}}$

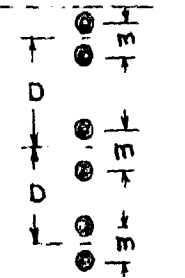
FIG.4.2 HORIZONTAL SINGLE CIRCUIT

ARRANGEMENT

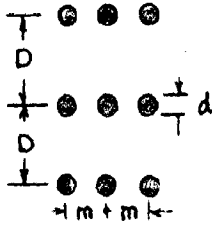
BUNDLE EFFICIENCY COEFFICIENTS



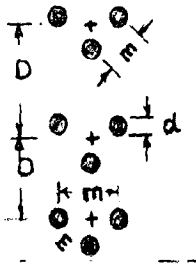
$$\eta = \frac{g_2}{g_1(1+\frac{d}{m})} \frac{\text{Ln} \left\{ \frac{1b \sqrt{(1+c^2)} (1+0.25c^2)}{b^2 c^2 (1+a)(1+0.5a)} \right\}}{\text{Ln} \left\{ \frac{8}{b^2 (1+a)(1+0.5a)} \right\}}$$



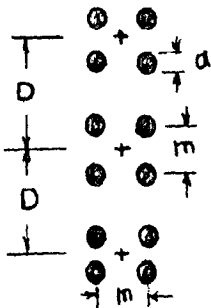
$$\eta = \frac{2g_2}{g_1(1+\frac{d}{m})} \frac{\text{Ln} \left\{ \frac{4 \sqrt{(1+c)(1+0.5c)}}{bc (1+a)(1+0.5a)} \right\}}{\text{Ln} \left\{ \frac{8}{b^2 (1+a)(1+0.5a)} \right\}}$$



$$\eta = \frac{g_3}{g_1(1+\frac{3d}{2m})} \frac{\text{Ln} \left\{ \frac{8(1+c^2) \sqrt{(1+4c^2)} (1+0.25c^2)}{b^2 c^2 (1+a)^2 (1+0.5a)^3 \sqrt{a^2 c^2 + 1+0.5a^2}} \right\}}{\text{Ln} \left\{ \frac{8}{b^2 (1+a)(1+0.5a)} \right\}}$$



$$\eta = \frac{2g_3}{g_1(1+\frac{2d}{m})} \frac{\text{Ln} \left\{ \frac{4(1+c)\sqrt{(2+c)}}{bc^2 \sqrt{(1+0.5a)(1+0.5a+0.86ac)(1+a+0.86ac)}} \right\}}{\text{Ln} \left\{ \frac{8}{b^2 (1+a)(1+0.5a)} \right\}}$$



$$\eta = \frac{2g_2}{g_1(1+\frac{4d}{m})} \frac{\text{Ln} \left\{ \frac{4(1+ac)(1+0.5ac)(1+c)(1+0.5c)}{bc^3 (1+a)^2 (1+0.5a)^2} \right\}}{\text{Ln} \left\{ \frac{8}{b^2 (1+a)(1+0.5a)} \right\}}$$

FIG. 43 VERTICAL SINGLE CIRCUIT

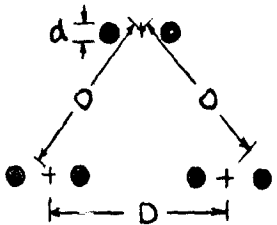
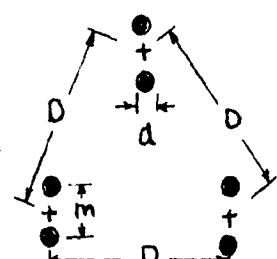
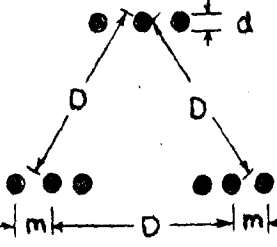
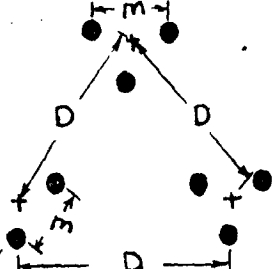
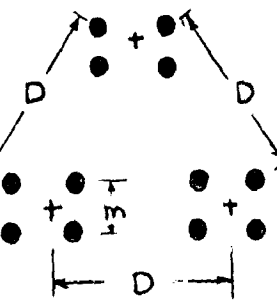
ARRANGEMENT	BUNDLE EFFICIENCY COEFFICIENTS
	$\eta = \frac{g_2}{g_1(1+\frac{d}{m})} \frac{\text{Ln} \left\{ \frac{4(1+c)^2}{b^2 c^2 (1+0.25a^2)(1+0.086a+0.25a^2)} \right\}}{\text{Ln} \left\{ \frac{4}{b^2 \sqrt{(1+0.25a^2)(1+0.086a+0.25a^2)}} \right\}}$
	$\eta = \frac{g_2}{g_1(1+\frac{d}{m})} \frac{\text{Ln} \left\{ \frac{4(1+c)\sqrt{1+c^2}}{b^2 c^2 (1+0.25a^2)(1+0.086a+0.25a^2)} \right\}}{\text{Ln} \left\{ \frac{4}{b^2 \sqrt{(1+0.25a^2)(1+0.086a+0.25a^2)}} \right\}}$
	$\eta = \frac{g_3}{g_1(1+\frac{3d}{2m})} \frac{\text{Ln} \left\{ \frac{(1+c)(1+2c)\sqrt{(1+c^2)(1+4c^2)}}{b^2 c^4 (1+0.25a^2)\sqrt{(1+a^2+5c^2)(1+0.086a+0.25a^2+2(1+c^2))}} \right\}}{\text{Ln} \left\{ \frac{4}{b^2 \sqrt{(1+0.25a^2)(1+0.086a+0.25a^2)}} \right\}}$
	$\eta = \frac{g_3}{g_1(1+\frac{3d}{m})} \frac{\text{Ln} \left\{ \frac{4(1+c)^2}{b^2 c^4 \sqrt{(1+0.25a^2)^3(1+0.086a+0.25a^2)^3}} \right\}}{\text{Ln} \left\{ \frac{4}{b^2 \sqrt{(1+0.25a^2)(1+0.086a+0.25a^2)}} \right\}}$
	$\eta = \frac{2g_4}{g_1(1+\frac{2.41d}{m})} \frac{\text{Ln} \left\{ \frac{(1+ac)(1+0.5ac)(1+c)\sqrt{2(1+c)}}{bc^3(1+0.25a^2)\sqrt{(1+0.25a^2)(1+0.086a+0.25a^2)}} \right\}}{\text{Ln} \left\{ \frac{4}{b^2 \sqrt{(1+0.25a^2)(1+0.086a+0.25a^2)}} \right\}}$

FIG. 4.4 TRIANGULAR SINGLE CIRCUIT

classification can be done as follows:

(i) direct methods (ii) wattmeter method (iii) Bridge method and (iv) Antenna method.

Direct method consists in measuring input to the transformers and transformer loss at both ends. The difference of the two gives the corona loss of the transmission line. This method is usually employed on lines in operation to obtain an approximate value of the losses. This method avoids the use of any sophisticated measuring circuits. (50)

Wattmeters specially constructed can be used for loss measurement either on test lines or on actual lines. Stringent accuracy restrictions on wattmeters due to relatively large errors with small changes in powerfactor, can be reduced by operating the meters at ground potential. (107,38) This also reduces the vital compensation necessary to counter the large errors. However a method of measurement in which a wattmeter located at high potential taken from an extension of HV winding has been reported. (4) This while avoiding the necessity to subtract transform loss requires compensation for power factor errors and so is inferior to that reported in the reference. (35)

The Schering bridge can be used for corona loss measurement. (64) This however requires an antenna as a pick up of charge on the conductor. A self compensating three phase bridge has been constructed which can be used to measure losses over a wide range with good accuracy. (41) The voltage and line current are measured with the help of a precision high accuracy SF_6 capacitor and frequency modulated transducer. The latter method has produced satisfactory results over the many years of testing. (41,88) Evidently the latter measuring system is costlier.

A system of antennae located directly below the line conductors with two shielding antennae along with the necessary electronic equipment can be used to measure losses with equal facility on test lines as well as on actual lines. ⁽¹¹⁾ A method combining the bridge and antenna is indicated above.

In addition to loss measurements it is necessary to record the weather conditions prevailing to classify the loss and thereby study the effect of weather on losses. Effects such as altitude change cannot be easily obtained in practice. However after taking into account some assumptions regarding the prevailing conditions a good correlation can be obtained of the results from such projects. ^(4,97)

4.9. Corona Loss Results from Test Projects:

4.9.4. Factors that Influence:

When a line either on test project or in actual system is energised the losses fluctuate greatly due to the so called weathering phenomena. So a reliable data can only be obtained after a continuous energisation of the line for some time.

It is very difficult to correlate the results from the test projects unless some allowances and approximations within certain limits are made due to inherent methods of loss measurement, prevailing weather and line conditions. However

In the testing unloaded EHV lines early observers noted that morning dew, light rain, and fog will appreciably increase corona losses as well as RI levels of the conductors. ^(2a) Since, in such test projects, the conductors carried only their changing current, the surface temperature could be less than the surrounding air and moisture would condense on the surface. Limited tests with

that the corona losses and RI would appreciably reduce. Some of the recent test projects have employed the techniques of heating the conductor. (88)

4.9.2. Hourly Loss Variations:

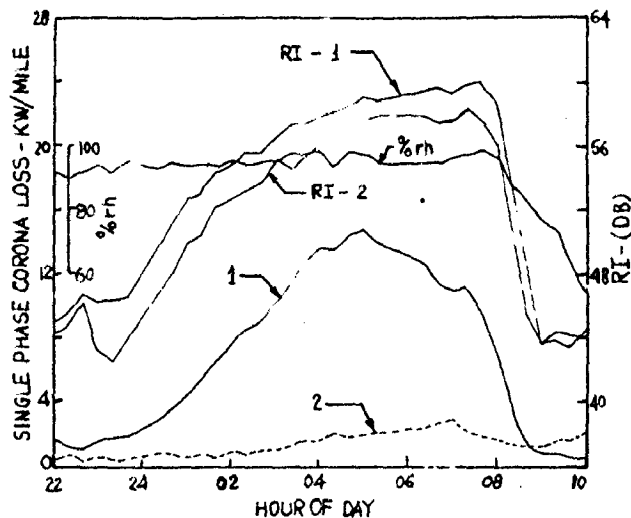
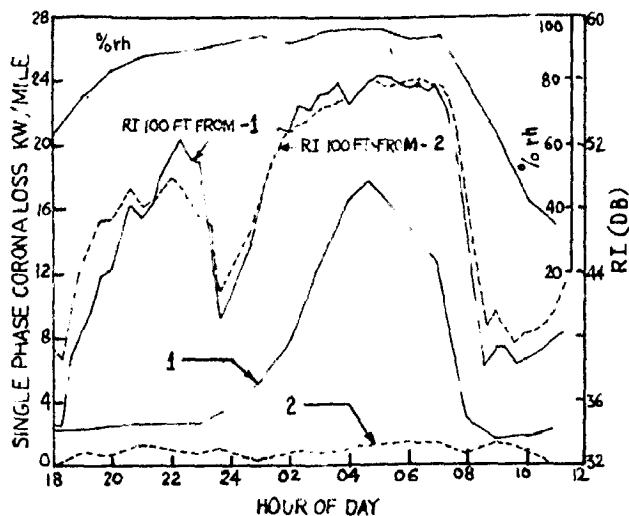
Since corona losses are dependent on numerous factors one can expect fairly high variations in losses. Fig.(4.5) shows loss variations under weather conditions such as dew, fog, frost, snow and rain. In our country snow losses will not be of great importance as any transmission system would rarely pass through the mountaineous terrain where snow fall is severe. Snow is found to be causing much mechanical damage due to twisting of subconductors, so the absence of snow fall is clearly a green signal for the adoption of bundle conductor transmission systems.

i) Dew: In absence of rain dew is often the cause of increased losses on the line at low load. Fig.4.5(A) shows the effect of dew. On actual transmission line conductors operating at considerable load the losses are not increased by the presence of dew. This is so because moisture cannot deposit on the conductor due to its inherent increased ambient level.

ii) Fog: Similar explanation holds good for Fog also. Whereas the losses on an unheated line increase tremendously, the losses on heated or line in practice remain substantially constant ruling out the effect of the two frequently occurring weather variables.

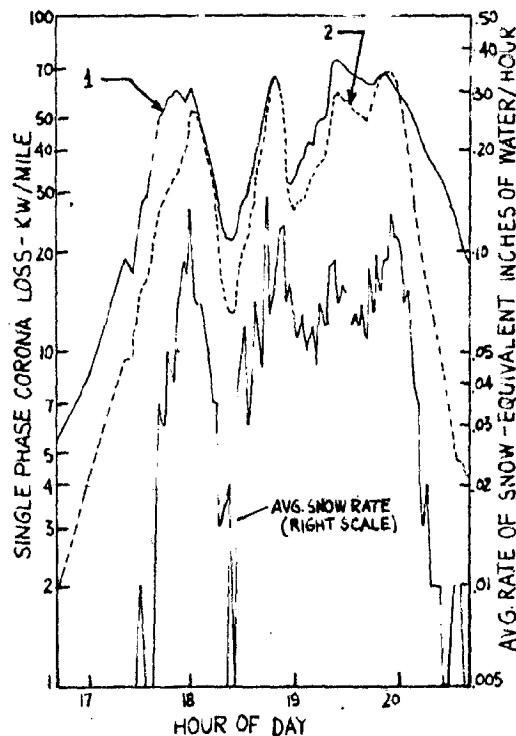
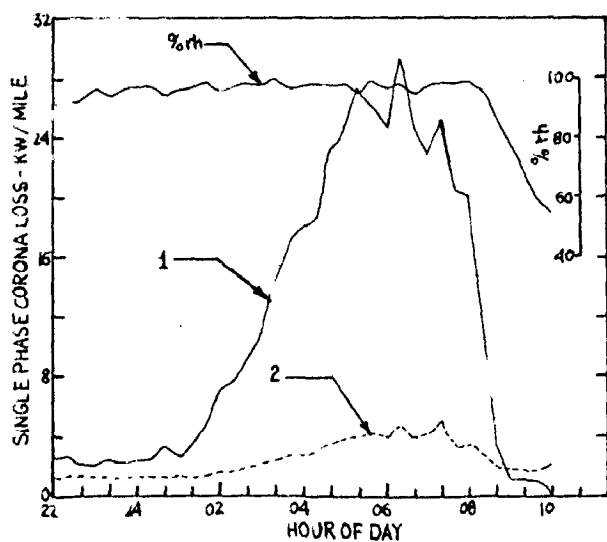
iii) Frost: Frost causes a slight increase in losses on heated line and considerable amount on unheated line. This shows that load current of relatively small magnitude is enough to stop the deposition of frost on conductors.

iv) Rain: Rain is an important aspect to be considered in the



DEW 2X1.465"; D=38.5'; 500KV; 550A FOG 2X1.465"; D=38.5'; 500KV; 550A

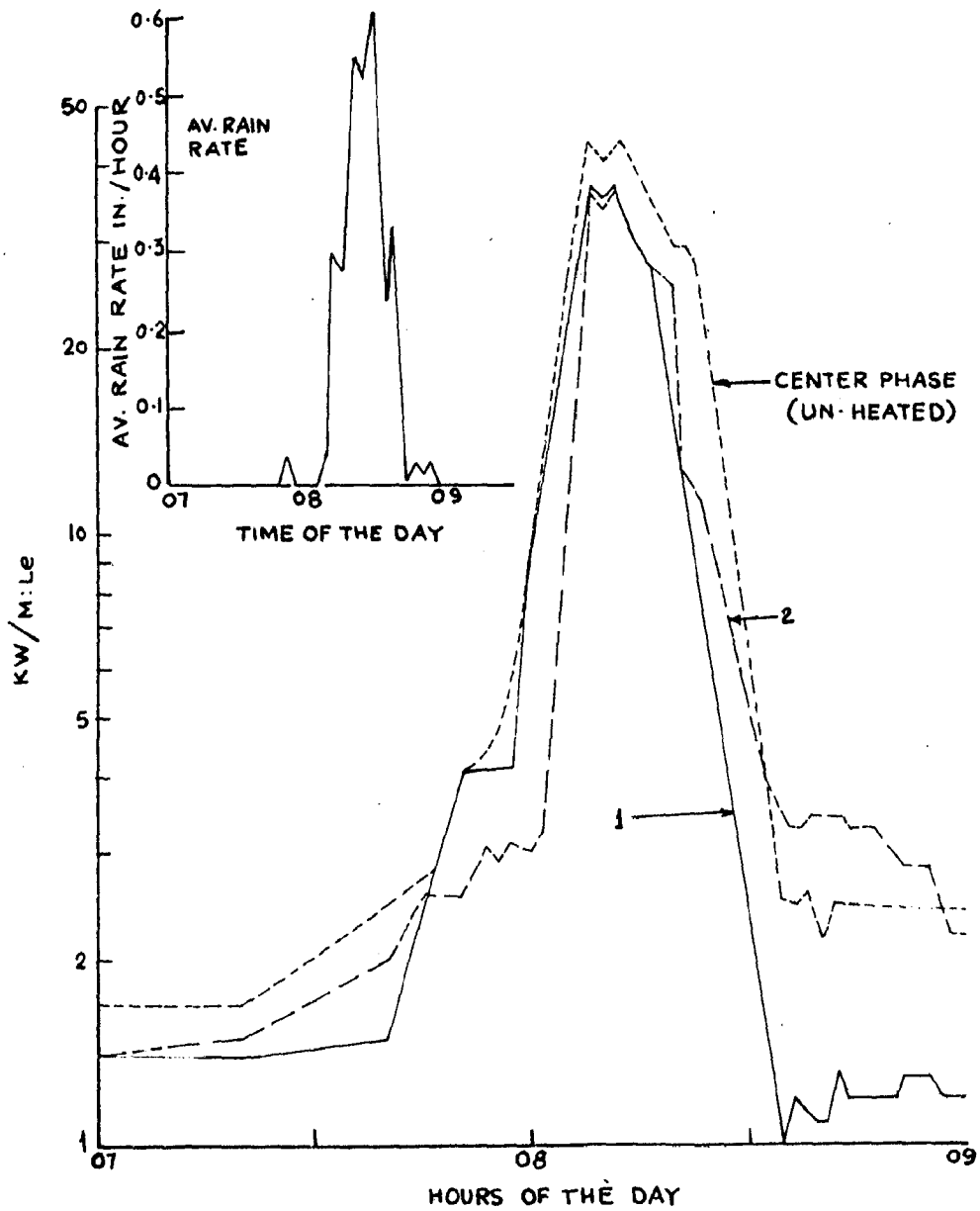
- 1 - UNHEATED PHASE CURVES
- 2 - HEATED PHASE, CIRCULATING CURRENT AS INDICATED IN AMPERES



FROST 2X1.465"; D=38.5'; 550KV; 193A

SNOW 2X1.465"; D=38.5'; 500KV; 550A

FIG. 4.5A HOURLY VARIATIONS OF CORONA LOSSES ON HEATED AND UNHEATED CONDUCTORS (PROJECT EHV)



RAIN $2 \times 1.465''$; $D = 38.5'$; 500KV; 550 A

1. UNHEATED PHASE CURVE

2. HEATED PHASE, CIRCULATING CURRENT AS INDICATED ABOVE IN AMPERES.

FIG. 4.5B HOURLY VARIATIONS OF CORONA LOSSES ON HEATED AND UNHEATED CONDUCTORS (PROJECT EHV)

every where on earth. Drops of rain as they fall on the conductors collect at the bottom of the conductors in the form of small globules thus catalising the formation of corona. Corona under rain conditions forms uniformly throughout the length of the line. This obviously leads to a tremendous increase in corona losses almost about a hundred times the normal fair weather loss. The number & hours of rain in a year can be fairly estimated with the weather data available for the terrain under investigation. This leads to a good and approximate estimation of losses due to rain. Fig.(4.5-B) shows the variation of losses. On left hand top of it is a curve showing the average rain rate. The loss curves follow the shape of the intensity of rain curve. The loss is almost same for all load conditions. Losses on center phase are also shown. Losses are more on center phase by nearly the same proportion as the gradients.

Fig.(4.6) shows the probable decrease in losses after rain as the conductor dries up. The test was conducted with an artificial rain spray of constant value. However, the time constant of drying is dependent on the high wind following the rain, or high ambient or conductor temperatures.⁽⁸⁸⁾ The corona loss varies as-

$$P = P_0 e^{-\frac{t}{\tau}}$$

where,

τ = time constant of drying

and P_0 = loss before rain stops (initial value).

v) Snow: Generally, the precipitation measurements - may be due to snow or rain- are difficult due to many side effects such as wind. Moreover the precipitation rate measured at a particular

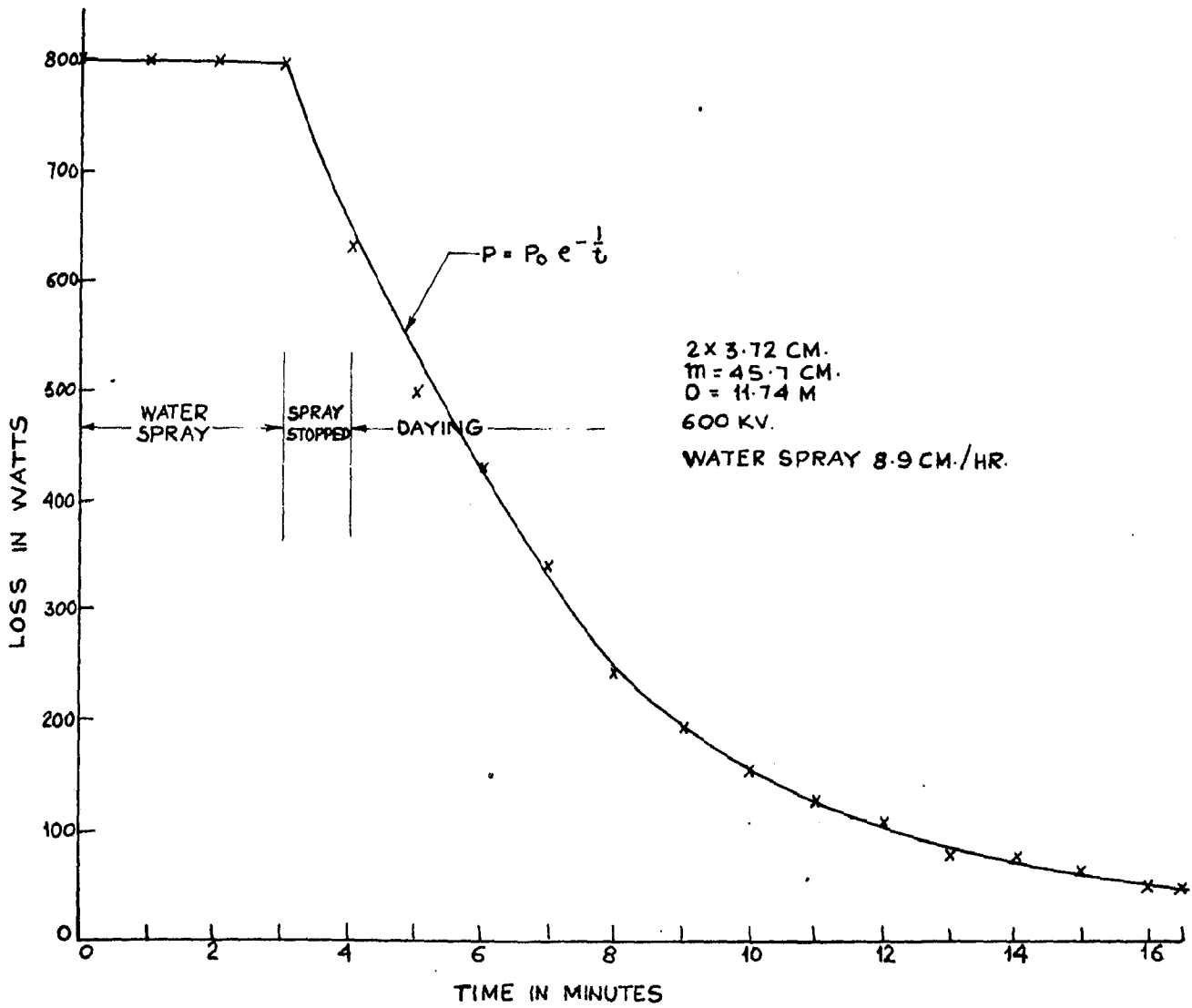


FIG. 4.6 LOSS VARIATION AFTER RAIN (PROJECT EHV)

due to the same reason. Thus only a rough estimate can be made when these effects are neglected. Measurement of snow fall rate is more vulnerable to errors depending on whether it is sticky, or wet or dry. Snow will increase the losses. The increase in losses due to wet snow is more than due to dry snow. The load current plays an important role at the beginning and end of the snow storm as evidenced by Fig.(4.5-A). The settled snow melts and falls off if the conductor temperature is higher. However if the rate of snow fall is greater than the rate of snow removal the losses are not affected by the load current, they increase steadily with the rate of snow fall. It is evident from the figure that at the peak of snow fall rate, the losses on a loaded line will be higher than the line at low load. This is because as the ice melts and forms water globules at the bottom of the conductor more space is cleared for the fresh snow to fall on the conductor. This in the author's opinion leads to increased corona losses.

It can be noted that the corona losses follow the shapes of the curves showing rates of rain or snow fall elucidating the direct effect of these two weather variables on the corona losses.

4.9.3. Losses and System Variables:

Study of the effect of the system variables on losses are as important as the study of hourly loss variations. A significant system variable is voltage. With the increase in voltage the losses increase greatly under all weather conditions. Fig.(4.7) shows comparative loss values under all of the weather conditions and their variance with voltage, as a triplex line. ⁽¹⁹⁾ Losses increase with the intensity of rain, and after some value of rain intensity ^{is reached} the losses almost tend to saturate. The author feels

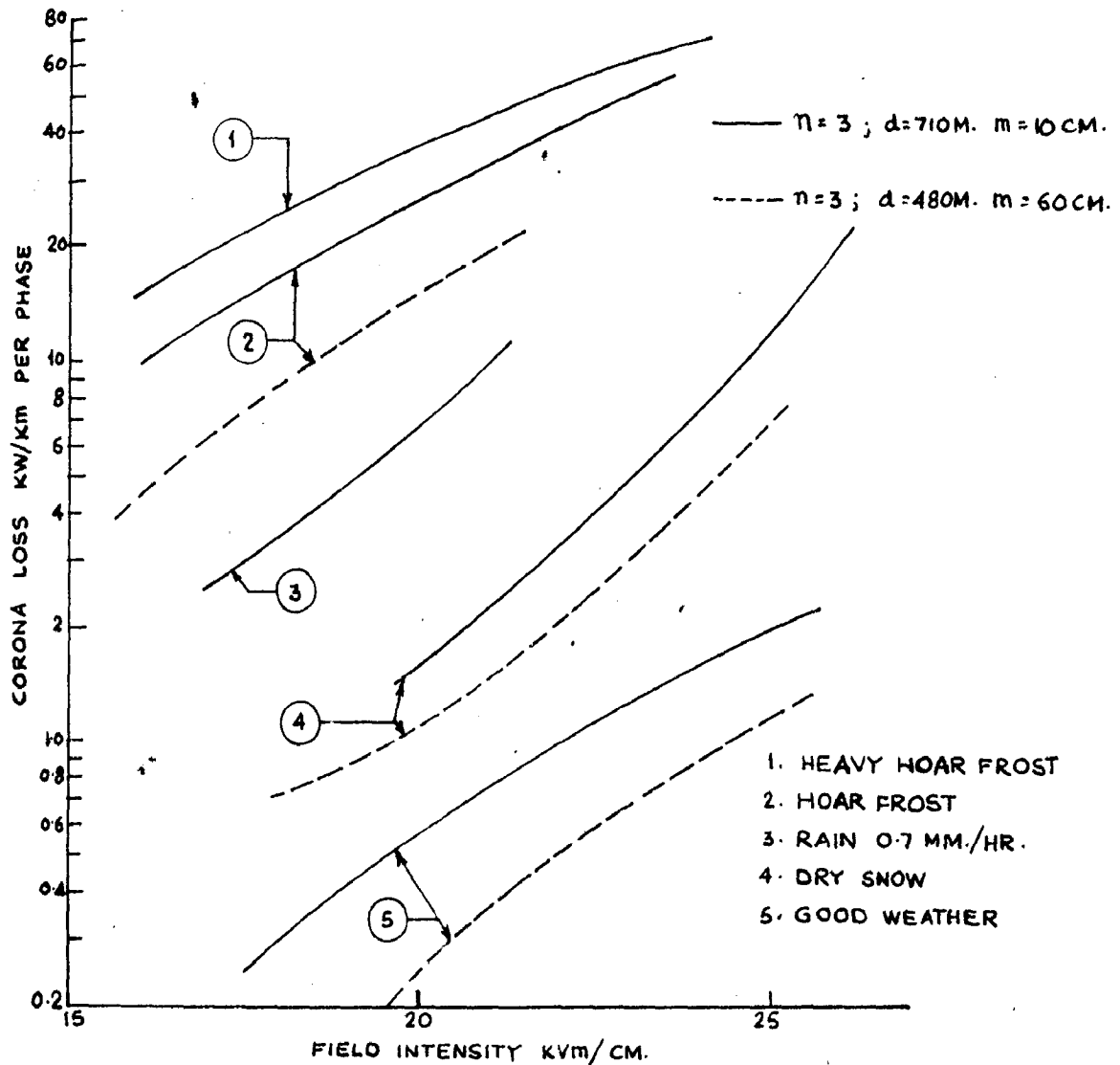
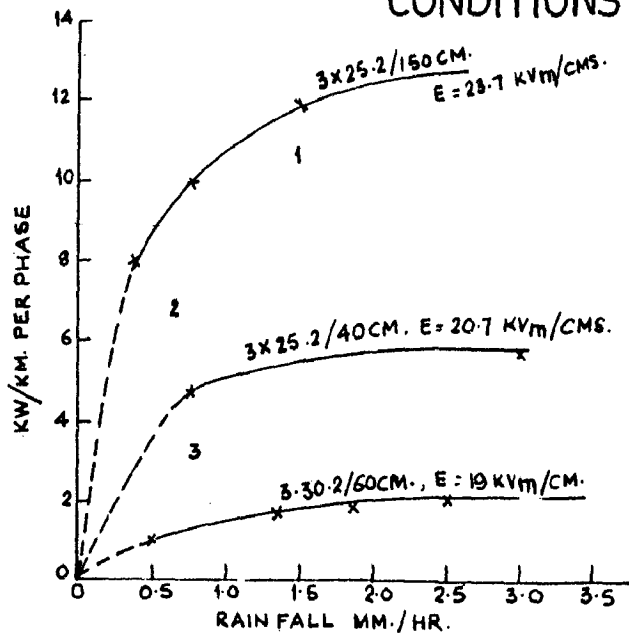


FIG.4.7 CORONA LOSSES DURING DIFFERENT WEATHER CONDITIONS



1. $\eta = 3$; $d = 25.2MM$; $m = 150CM$; $g = 23.7 KV/M/CM$.
2. $\eta = 3$; $d = 25.2MM$; $m = 40CM$; $g = 20.7 KV/M/CM$.
3. $\eta = 3$; $d = 30.2MM$; $m = 60CM$; $g = 19.0 KV/M/CM$.

FIG.4.8 EFFECT OF RAIN FALL

that the reason for this is, after a certain intensity of rain is reached the entire circumference of conductor is in corona and water drops falling on the conductor have very little effect afterwards. The experimental results in evidence of this are shown in Fig.(4.8). Lastly the losses predicted (average annual losses) for duplex, triplex and quadruplex systems are shown in Fig.(4.9).

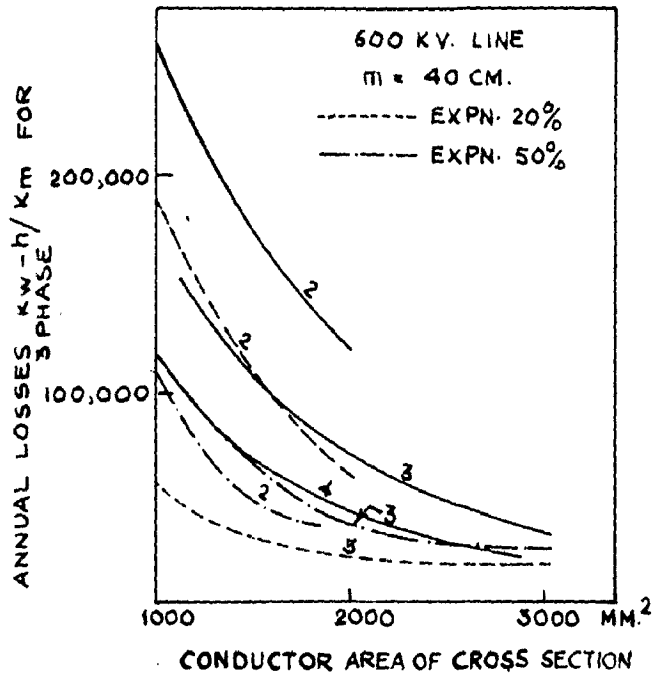


FIG. 4.9 ANNUAL CORONA LOSSES

CHAPTER 5.

RADIO INTERFERENCE FROM BUNDLE CONDUCTOR LINES:

5.1. Introduction:

Radio interference (RI) from EHV transmission line is being studied since the inception of the transmission at EHV. Radio and Television interference is not a major problem on transmission lines upto about 220KV. Bundle conductors are used at 220KV and above and the studies relating to the RI phenomena on EHV transmission lines are important. RI level on bundle conductor line is less than that on single conductor line. One obvious explanation is as follows. Gradient is non-uniform around the bundle, being maximum on each conductor at a point opposite and away from the bundle center. So, when the operating gradient is limited corona forms on lesser surface area than on single conductor lines. Thus high frequency electro-magnetic wave emissions are comparatively less. This obviously is a major advantage. However, on EHV lines the noise levels are quite high, thus the limitation of operating RI level forms an important design consideration. Curves representing typical practices in various countries have been presented.

5.2. Noise Generation and Propagation:

Interference from power lines is due to the high frequency currents generated by a partial or complete break-down of an insulation medium, such as conductor corona, or across corrosion products in hardware or in small metal-to-metal gaps due to deficiencies in design or in construction of lines or apparatus. The presence of some corona, however does not mean an interference problem, and a certain amount of conductor corona can be justified economically in EHV systems.

Corona discharges occur in the region of negative and positive peaks of conductor voltage when the gradient exceeds the critical value. The impulsive noise produced by positive corona is much higher than the negative corona and the latter can be ignored in evaluation of noise generation, excepting at extremely high voltages. (89) Corona sources are randomly distributed along the conductor, and each source produces a train of irregular noise pulses of varying height, shape, and separation in time.

The random nature in space, time and pulse height of the corona noise led to the consideration of power density spectra. Because of the randomness, the noise level is proportional to the square root of the number of sources, or the noise is power additive and that the sources are uncorrelated. (14)

RMS noise meters have been developed. These are most adaptable in correlating the fundamental theoretical study of Adams with the experimental data on noise generation and propagation. (30) The most commonly used noise meter, however, is equipped with a quasi peak detector. Specifications for such a meter are based on tests of nuisance value of the noise within the audible band.

Noise impulses, produced on one phase will induce current impulses in the adjacent conductors. This induced noise can be calculated from the electrostatic line equations, considering the adjacent conductors to be at ground potential. Conductor corona and hardware discharge involve a limited charge. The equivalent noise generator is thus considered to be constant current generator with high internal impedance. (27) The noise current flowing in the conductor is directly related to the amount of noise generation and can be referred to single or uniformly distributed sources per unit length of conductor. Further, the value of noise current at

power corresponds to a limited bandwidth, such as that of AM broadcast bandwidth.

Since conductor noise is random and repetitive in nature, some assumptions are to be made before any analytical method can be adopted. Modern analysis of corona pulse propagation is due to Adams. (14,27,17) His method demonstrates the effects of power line parameters on the natural mode components or eigen vectors, calculated from the conductor system matrix. He directly applies natural modes to the electromagnetic field at ground level at right angles to the transmission line. Various recent workers refer to his work on many aspects of corona noise generation, propagation and the field strength of RI. (41,46)

5.3. Adam's Theory and Analytical Determination of RI:

The corona avalanche's give rise to currents which flow in the space near the conductor. However the motion of charged particles in a plane perpendicular to the line predominates over such current and this also causes currents to flow in ground as well as in the conductor. These currents are transient in nature and propagate along the line in accordance with the electromagnetic theory (Maxwell's equations). Since these currents and the electromagnetic field associated can be propagated over great distances before they are completely attenuated, corona on one section of the line can cause disturbance in a receiver far away from it.

In case of bundle conductors, the line cross-section can be divided into Pi shaped volumes with an inner and outer circles selected suitably depending on the line. The total corona current is obtained from the summation of the elemental currents over a length l . The equivalent circuit for a line section of length l is shown in Fig. (5.1).

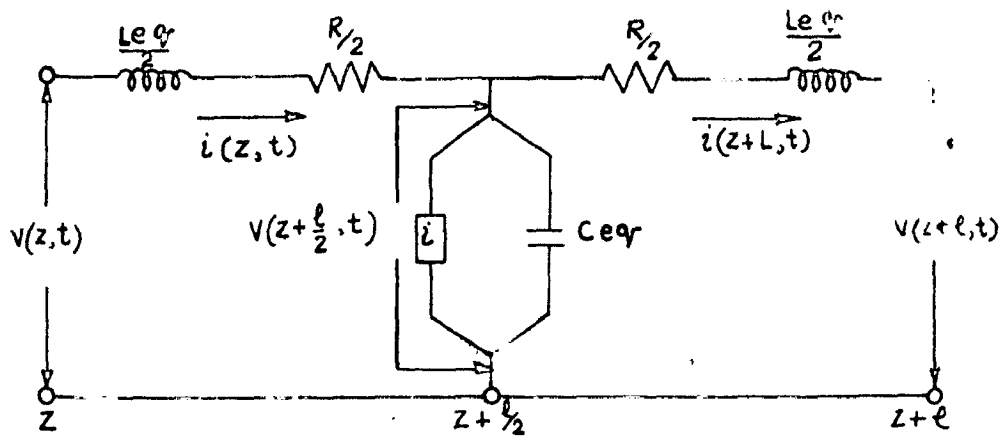


FIG. 5.1 EQUIVALENT CIRCUIT

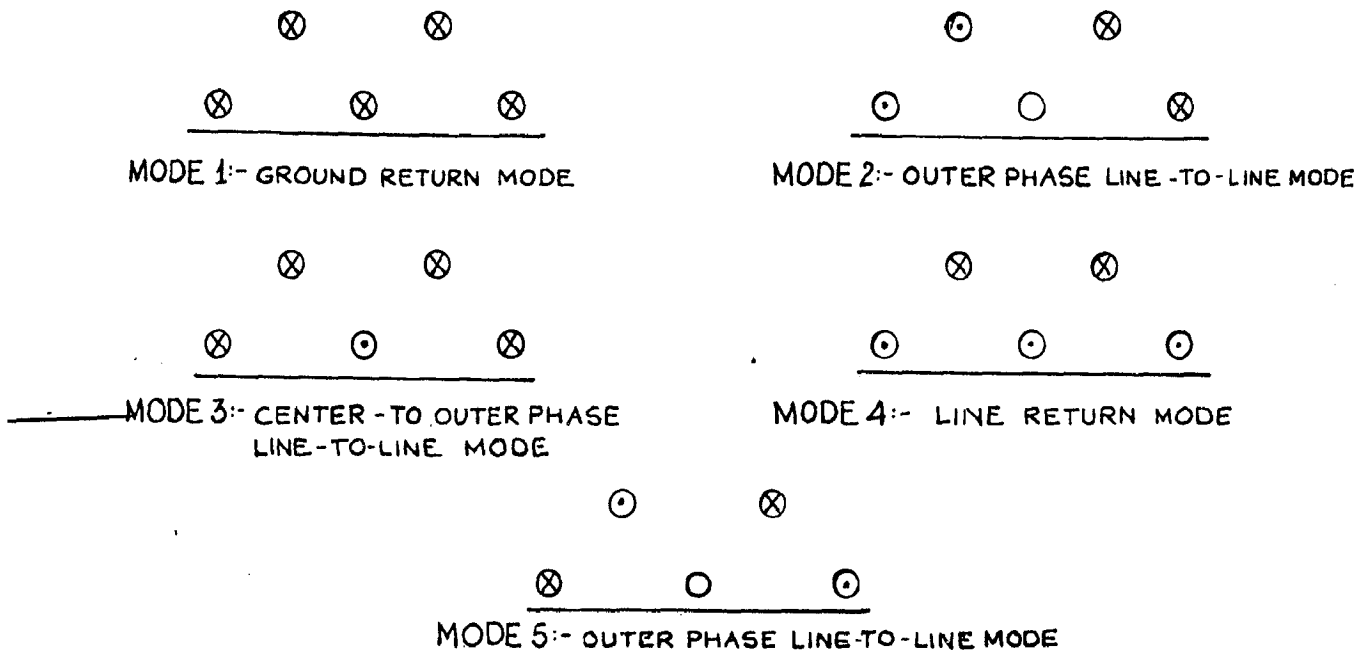
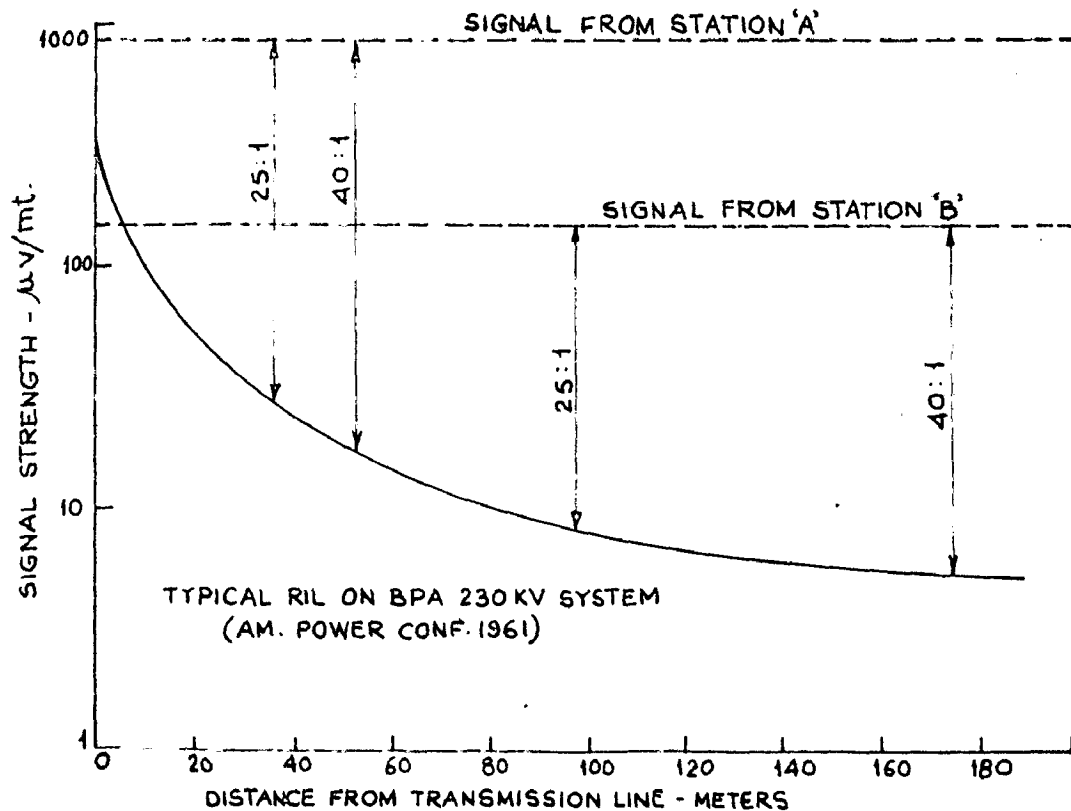


FIG. 5.2 THE FIVE MODES & 3 PHASE LINE WITH TWO G.WIRES



An empirical expression for spectral density of noise current density for a single conductor is given as⁽¹⁴⁾

$$SD(J) = 10 (g-g_0)/\beta \quad \text{Amp.}^2 \text{ sec./m}^2 \quad \dots (1)$$

The above expression considers only change in generation due to the difference between actual surface gradient(g) and critical gradient (g_0) for a particular conductor and air density, and is based on the observed changes in noise level with voltage on transmission lines. The expression is suitably modified for bundle conductor lines as stated in the previous paragraph wrt corona current.

The corona impulses are assumed to propagate in a number of modes equivalent to the number of conductors (each bundle of a phase is assumed to be a single conductor for such consideration). In each mode the transmission line represented by connecting the equivalent circuits of various sections together. The current from each generator divides and flows in the two opposite directions. In transit the currents and corresponding line to ground voltages are attenuated. This attenuation is different for different frequencies and for different modes. For a long line on which the sections are all identical, the spectral density of the total current at any section for any particular mode is given as-

$$SD (I_p)_{\text{total}} = \beta SD(I) \quad \dots \quad \dots (2)$$

where

$$\beta = \frac{1}{2} (e^{-\alpha l} + e^{-2\alpha l} + e^{-3\alpha l} + \dots); \text{ propagation constant}$$

At any point on the line the total current is obtained from the summation of all the mode currents. However, the line to ground mode is predominant as regards the interference near the ground. The modes for a 3-phase line with two ground wires are as shown in fig.

In terms of modal analysis the relation between spectral densities of current and current density for m^{th} mode is given by-

$$SD\{I^{(m)}\} = \frac{SD\{J^{(m)}\}}{\alpha^{(m)}} \dots \quad (4)$$

complete analysis of the resolution of noise quantities on each phase has been presented in the reference. (59)

The disturbing field at any point is influenced to a great extent by the noise sources at remote points. To account for this a field factor can be defined and for a single circuit line it is given by-

$$\gamma^{(m)} = 10.767 \{nA_1^{(m)} \frac{2h_A}{x_A^2 + h_A^2} + nB_1^{(m)} \frac{2h_B}{x_B^2 + h_B^2} + nC_1^{(m)} \frac{2h_C}{x_C^2 + h_C^2}\} \dots \quad (5)$$

To determine the electric field the following expression has been derived. (89)

$$SD\{E^{(m)}\} = \frac{(Z_0)^2 (\gamma^{(m)})^2}{4 \alpha^{(m)}} \{ SD(G_A) (A_1^{(n)})^2 + SD(G_B) (B_1^{(n)})^2 + SD(G_C) (C_1^{(n)})^2 \} \dots \quad (6)$$

$$\text{where, } SD(G) = r \int_0^{2\pi} \left| 1 + 2r \left(\frac{n-1}{n} \right) \cdot \sin \frac{\pi}{n} \cdot \cos \theta \right|^2 \cdot SD(GD) d\theta$$

$$SD(GD) d\theta \text{ Amp}^2 \cdot \text{sec./met.}$$

= generation per unit length.

$$Z_0 = 377 \text{ ohms.}$$

The above discussion outlines in brief the method of calculation from the fundamental theory of Adam's. It has been used in determination of the corona noise levels on project EHV. (41,89). However, this theory gives only rms values of noise levels and all the tests conducted worldwide use only quasi-peak response meters. Hence it is necessary to correlate both before the application of

5.4. Design Factors:

1) SN Ratio: RI is a nuisance factor which the transmission systems have to give due care, largely depending upon the locality through which they pass viz. urban or rural. Thus the absolute value of interference in itself is not wholly significant. RI in one locality may be entirely satisfactory and same at another point may be intolerable. This is due to the fact that radio signal strength is a variable, decreasing with distance, away from the broad-casting station. Table 5.1 shows the various signal to noise ratios adapted for EHV transmission lines.

TABLE 5.1.

Signal to noise ratios for EHV transmission systems:

Type of Reception	SNR		dB
Ideal reception ..	100:1	..	40.0
Reasonable urban reception	40:1	..	32.2*
Reasonable rural reception	25:1	..	28.0*
Satisfactory reception	16:1	..	24.0**
Tolerable reception	10:1	..	20.0*
Limit of acceptability	4:1	..	12.0*

*Ontario hydro research news, Jan. 1959, **Reference 76.

The radiated interference (RI) from a transmission line, however, drops off very rapidly with distance from the line following the pattern shown in Fig.(5.3) Therefore, the distance from the line determines the SNR for a given receiver. For example, if a listener living 60 meters from the transmission line prefers to listen to a radio station "A", he will not be affected by the transmission, (excepting in foul weather with intense rain); where as a listener at a greater distance say 90 meters, who prefers to listen station "B" will find the transmission line noise objectionable. Obviously the selection of a standard interference maximum level to apply throughout the system is arbitrary. Listening tests reveal the

of reception.⁽⁹²⁾ Signal to noise ratio adaptable for a transmission system is decided depending upon the locality and class of reception required. The radio signal in a particular locality is quite uniform for all listeners.

TABLE 5.2

<u>Signal to noise ratios for various Classes of Reception:</u>		
<u>Class of Radio Reception</u>		<u>Signal to Noise Ratio (dB)</u>
Entirely satisfactory	...	32
Very good, back ground unabtrusive		27
Fairly satisfactory, background plainly evident	22
Back ground very evident, but speech easily understand	16

ii) Conductor Selection: In the design of an EHV transmission line for a given voltage a careful selection of a combination of conductor size and bundling for various phase spacings must be made based on experience and judgement of operating conditions and environments to obtain an estimation of the RIV generation. Once a conductor and the geometry of the system is decided upon with the help of the figures in Chapter 1, the adequacy of line performance may then be estimated using some design criteria; for example, comparison of broadcast station signal strength with noise levels at the edge of right of way.

iii) Surface and Environmental Factors: Precipitation, such as rain or snow or dew or fog, can increase the generation of conductor corona 5 to 10 or more times. Even under apparently identical environments of fair weather the RI levels may vary from the average value by about 6 dB.⁽⁴¹⁾ So when selecting a radio noise figure for the performance of a given transmission

obtain a statistical value are used. Statistical data collected over a long time provides the best measure of the RI performance of a transmission line. Gap noise, in contrast may be reduced or completely eliminated in wet weather.

The best basis available for making a judgement of the RI generation to be expected from a conductor system is by a comparison with data from existing lines of similar parameters operating under similar environmental conditions. If necessary, test line data must be used for such evaluation where no such comparable line is existing.

An analytical method for comparison outlined as above has been developed. (57) The differences in field strength at ground level between two lines (A and B) at a distance X from the lines is given by:

$$dB_A - dB_B = 3.5 (V_A \cdot G_A - V_B \cdot G_B) - 30 \log \frac{d_B}{d_A} - 20 \log \frac{h_B \sqrt{(X - D_A)^2 + H_A^2}}{h_A \sqrt{(X - D_B)^2 + H_B^2}}$$

where,

X distance from centre of the line.

Even though the gradient or center phase is higher than an outer phases, With phase spacings of the order of 6 mts., the RI field from the outer phase predominates at the edge of the right of way. Therefore in RI calculations on EHV lines gradient on outer phases is often used.

5.5. RI Formulae:

Results from the various test projects and the operating experience on existing transmission lines has led the workers in this field in various countries to form semi-empirical formulae

predetermination give absolute value of RI, the semiempirical formulae are limited in their use and give only comparative values. Such comparative values on the other hand are useful and often sufficient for a designer who wishes to know whether the line is quieter or not than the line with which it is being compared. Moreover, the simplicity of the formulae is what makes them versatile and useful in selecting a particular solution among many other possible solutions. Table 5.3 shows the formula against the country in which it is practised.

TABLE 5.3.

Semi-Empirical RI Predetermination Formulae

Country	Formula
1. America*	$RI = RI_0 + 4(g - g_0) + 40 \log(d/d_0)$
2. Germany ⁽⁶³⁾	$RI = RI_0 + 4(g - g_0)$
3. Italy* ⁽⁷³⁾	$RI = RE_0 + 4(g - g_0) + 40 \log(d/d_0) + 10 \log(n/n_0) + (\overline{q - q_0}/300)$
4. Japan ^(69,70)	$RI = RI_0 + 3.5(g - g_0) + \Delta E_d$
5. Russia ⁽⁸³⁾	$RI = RI_0 + 2.6(g - g_0) + 10 \log \frac{\sum d}{\sum d_0}$

*Ref. Chapter 1.

The symbols used in Table 5.3 are as follows:

- RI, RI₀ RI electric field (in dB above 1 μ V/m) for the line under investigation and standard line respectively.
- g, g₀ Gradient (in KV/cm) on the surface of conductors. max. in case of (1), (2) (4) and (5); average in case of (3).
- d, d₀ Subconductor diameters.
- n, n₀ number of subconductors
- q, q₀ heights above sea level
- ΔE_d (dB above 1 μ V/m), a correction factor for the diameter (Fig.15 Ref.70).

The Russian formula has essentially been developed for use on triplex and quadruplex systems. Depending upon the existing conditions in a country the formulae can be modified, since a line similar in nature produces different radio noise levels at different places. Such variation can be accomplished by changing the constants used in the formulae. As an extension of this study, a comparative analysis of the above formulae can be made once an EHV line is constructed with bundle conductors, and study their suitability to evolve a formula suitable for the conditions in our country.

5.6. Measurement of RI:

RI can be measured with the help of four types of detectors, quasi-peak, rms and average. Quasi-peak meters are being used extensively on all systems. The peak detector is especially useful in obtaining by visual means the corona pulses on any conductor, since corona pulses necessarily occur at different times on a 3 phase system. The rms detector is advantageous in that the random noise energy can be determined and is capable of correlating the analytical theories developed. ^(30,31) However, of all the four only quasi-peak type of meters are commercially available.

There exist two standards of measurement. ^(92,73) These two standards are different from each other in that the USASI standard specifies the lateral field measurement at ground level and the CISPR specifies the meter location 2 meters above ground and the point of measurement is different from each other. The former is used in American Continent and the latter in the European countries. At present vertical rod and loop antennae are being used following the specifications given in reference. ⁽⁹²⁾

differently on the same line, and the variation can be as much as ± 2.35 dB on the quasi-peak detector. This in comparison with the reading of the meter and range of measurement is suggested to be tolerable. ⁽⁹²⁾ When measuring RI levels on a line simultaneously, the meters should be correlated and accurately calibrated. The "human error" in measuring the meters, ^{is} accounted as ± 2 dB when the same meter was read by 14 operators and (i) 5.5 dB at 0.145 MHz and 0.495 MHz and (ii) only 1.5 dB at 1.04 MHz when the same operator read seven stoddart NM20's. ⁽⁴⁷⁾

5.7. Frequency Spectrum:

The current pulse due to conductor corona, which is the main cause of RI, has a very fast rise time of the order of lengths of microseconds. ⁽⁸⁸⁾ However the frequency spectrum typical of conductor corona on long lines between 0.35 and 3 MHz generally has to form which follows the relation $(\frac{1}{f})$, over and above 4 MHz it follows the relation $(\frac{1}{f^2})$. ⁽⁴⁷⁾ Therefore for the usual EHV line design, the frequency spectrum is such as to fall off so rapidly as not to be the cause of interference in the FM and TV bands. Mostly the conductor corona noise frequency spectrum is measured between 0.2 and 1.6 MHz. ⁽⁵⁷⁾

If a gap type discharge exists on a line, then the frequency spectrum of such line will be entirely different, being flatter than that of conductor corona and extends quite a bit higher in frequency before an appreciable decrease in field strength can be observed. In such a case TV interference can become a problem.

The radiation characteristics of line and towers can affect the frequency spectra measured, causing peaks and valleys corresponding to natural electric lengths of the radiating line

On the frequency spectrum the RI levels at various distances such as 30 and 60 mts. lateral to the line can be superimposed to study the effect of line noise on radio reception at various frequencies at the particular locatin. By suitable adjustment of line geometry, if necessary, the required satisfactory radio reception can be attained. However, in rural areas, where the signal strength is evidently lower it may not be possible to safe guard all the signals in broadcast band.

Extensive experimental investigations on the frequency spectra on a 750 KV test project have been presented in the literature. (90,91)

5.8. Radio Interference and System Variables:

To study the transmission system RI thoroughly it is necessary to consider the effect of the system variables such as voltage, transients and prevailing ^{weather} conditions. For such a study in absence of experimental results the results obtained over a long period on many existing lines and test projects are used.

(i) Voltage: Voltage has a significant effect on RI. RI varies linearly with the voltage in fair weather. Small changes in voltage have very little effect on RI. However, a casual relationship is observed for unintentional small changes of system voltages. Infact, in such a case the RI is observed to go down with the increase in voltage. (89) Table 5.4 illustrates the above points through experimental values. (71) In fair weather an increase of 3 dB of $1 \text{ KV}_{\text{rms}}/\text{cm}$ change in maximum gradient is typical.

ii) Conductor Cross Section: The effect of conductor cross section is evident from the formulae listed in Table 5.3. RI

TABLE 5.4

Effect of Voltage on RI Levels:

Applied voltage (KV)		RI,dB		Standard deviation
470	...	61.0	..	4.4
520	...	71.0	..	5.4
570	...	74.7	..	4.8
625	...	81.5	..	6.8
675	...	84.6	..	3.9
730	...	94.0	..	4.0

dependent upon the number of corona points, one can expect a higher RI level with larger conductor diameter. Hence a single conductor line having uniformly distributed noise sources around and along the conductor will have higher noise level. A bundle conductor line using a number of conductors of same dia. as single conductor line have the same RI level. However, a bundle conductor line uses a smaller conductor diameter, hence an increase in operating voltage can be effectively done without increasing the RI levels along with it. Infact RI levels on 400 KV, $4 \times 240 \text{mm}^2$ ACSR line are same as on 275 KV, $2 \times 240 \text{mm}^2$ line.

iii) Rain: Rain is an important factor in the studies of RI. RI levels increase by ten times the fair weather values. The intensity of rain has the same effect as on the corona losses. RI increases with increase in rain intensity upto some value, above which the RI curve is flat. Fig.(5.4) elucidates the above statement. RI variation with rain fall on hourly basis is shown on Fig.(4.1E) where the relative variation in corona loss is also shown. After the rainfall the conductor will be wet and in this state the RI levels will be higher. An empirical relation between rain intensity and RI is as follows. (7D)

$$81.3I_{\text{rain}}$$

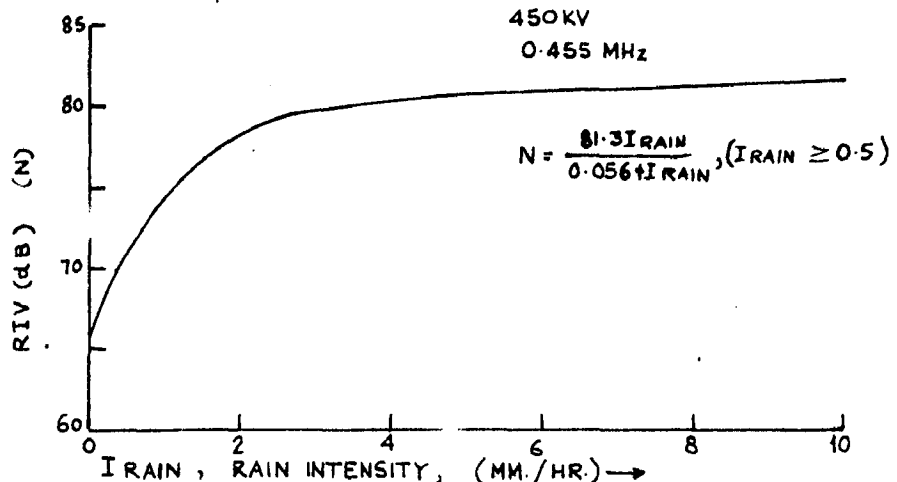


FIG. 5.4 EFFECT OF RAIN INTENSITY

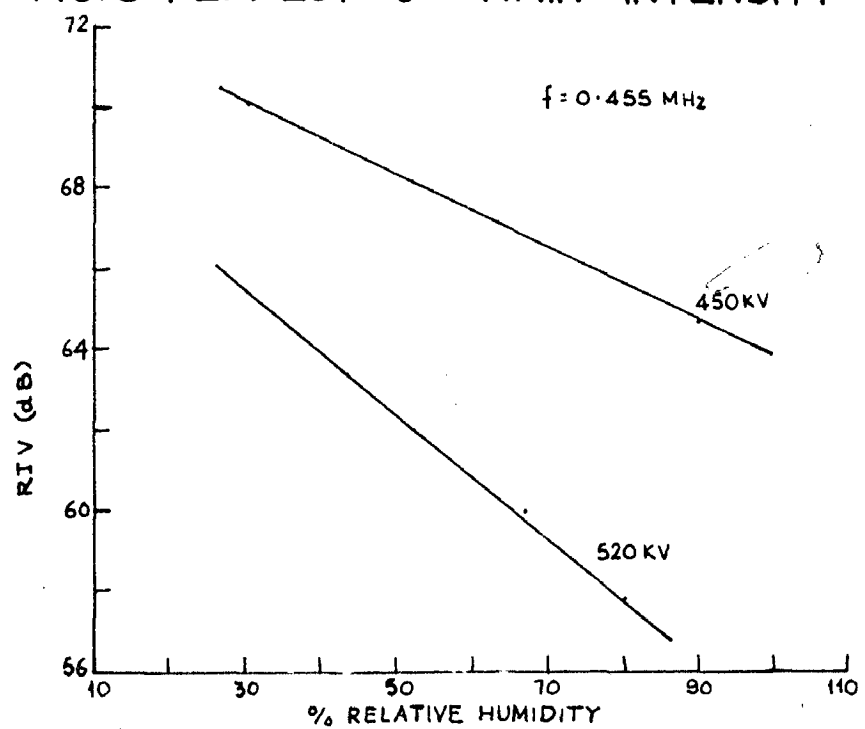


FIG. 5.5 EFFECT OF RELATIVE HUMIDITY

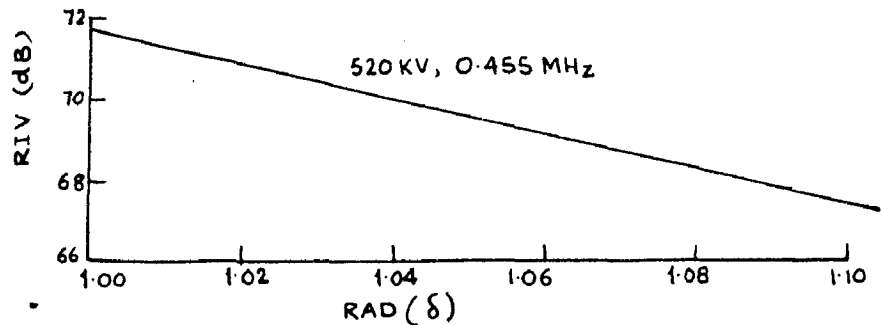


FIG. 5.6 RELATIVE AIR DENSITY FACTOR

(iv) Relative Humidity: Contradictory opinions exist on the effect of relative humidity on radio interference. Japanese reports show that the RI levels decrease with increase in relative humidity. The rate of decrease however is high for higher voltages, Fig.5.5-(70) Knudsen reports a lesser effect than this. (64) Results from project EHV show that RI Level increases by about 0.5 dB per 10% increase in rh, and reduction of the same order below 50% relative humidity. (69)

(v) Relative Air Density: Relative air density when increased above unity will cause a reduction in RI level linearly. The reduction of RI level is as shown by Fig.(5.16). American investigations reveal a lower reduction than the one illustrated.

(vi) Dew, Fog and Frost: The RI as affected by dew, fog and frost are illustrated in Fig.(4.5A and B) respectively. The same figure also illustrates the effect of load current on RI levels under these conditions. Load current has a very little effect in that the RI levels are lower than on loaded lines. Frost increases the RI and when it melts due to load current or due to ambient temperature it further increases the interference level. This is illustrated in Fig.(5.7).

(vii) System Over Voltages: Transients and system over voltages have very little effect upon the RI levels. Over voltages when they exceed two or three times the normal operating voltage may give rise to an impulsive noise. By suitably designing the system however, such noise spurts can be reduced to a good degree.

5.9. The Case of a Distribution Line Crossing The EHV Line:

Radio noise generated on an EHV line is not only radiated but is also conducted. The latter process will be of great

transmission line. There exists a mutual coupling between two such lines and thus radio frequency waves are induced into the latter which propagate in both the directions from the crossing point and can reach receivers quite far off. For a case of a distribution line of equal length on both sides of crossing (for simplicity mutually perpendicular crossing is assumed) and terminated at both ends by its characteristic impedance, the coupling ratio will be given by⁽⁷⁰⁾

$$\frac{V_{rf}}{V_{rf}} = \frac{2}{\omega C_c Z_0}$$

where,

V_{rf} Radio frequency voltage between transmission line and earth.

V_{rf} Radio frequency voltage between distribution line and earth.

$$= RI. \omega \frac{Z_0}{4} C_c h \text{ Log } \left(\frac{2h}{R_c} \right)$$

RE Field intensity under transmission line.

Z_0 Characteristic impedance of distribution line

C_c Coupling capacitance between the two lines.

5.10. Reduction of RI:

While a suitable design can reduce to a great extent the effect of RI, counter-measures should be taken by the individual receivers which are severely affected. For instance the aerial of a receiver can be shielded, which improves its performance. Or the aerial itself can be located away from the disturbing field, thus improving the signal to noise ratio. While these methods may be of good use in rural areas and medium populated areas, the use of an amplifier along with isolating the aerial from the interference field is the solution for densely populated localities.

to the quarter the wave length can be connected to the transmission line conductors. This effectively attenuates the particular frequency noise selected.

CHAPTER 6

UNBALANCES OF UNTRANSPOSED BUNDLE CONDUCTOR LINES:

6.1. Introduction:

The modern trend in power transmission is to avoid transpositions. Transpositions if employed at regular intervals, make the transmission system perfectly balanced but on the other hand they are the major sources of short circuits. Especially with bundle conductor lines transpositions are not only uneconomical but are also cumbersome. So the necessity arises to evaluate to a good approximation the unbalances that exist on such lines. Unbalances are of two types- electrostatic and electromagnetic. These unbalances are mostly because of geometric dissymmetries with respect to each phase and in turn with respect to ground. As a result of these two unbalances circulating currents will flow in transmission lines with solidly grounded neutral. In high impedance or resonant grounded lines the effect is to introduce a voltage between line neutral and ground. However unbalance is not restricted to zero-sequence quantities only. Negative sequence charging currents result from capacitive unbalance and magnetically induced negative sequence currents flow in the lines, transformer and generator windings. The operation in sensitive elements in ground relays may be affected by charging current where as undesirable losses may result in rotating machines. Electrostatic effects occur under all conditions of operation and are essentially independent of load currents. Electromagnetic effects on the otherhand depend on load currents and so are negligible under open circuit conditions.

6.2. Investigation of Unbalances:

unbalances, the other types of arrangements viz., horizontal and vertical have unbalances in increasing order. Raising the centre phase over the outer phases is found to reduce unbalances in high voltage lines, but not in the case of extra high-voltage lines without ground wires. (49) On lines with ground wires raising the center phase upto a certain height lowers the unbalance, but beyond this height the unbalances increase. Ground wires definitely reduce the unbalance. But by suitably lowering the center phase on lines with or without ground wires unbalance can be practically reduced to zero. In certain cases the lowering might be objectionable. A study of the variation of ratio of intra-conductor spacing of center to outer phases reveals that, with the ratio about 2.5 it is possible to reduce the electrostatic unbalance practically to zero. Feasibility of adopting such ratio should be considered along with other factors of line design. There is very little effect of ground wire diameter on electrostatic unbalance.

There exist reports on unbalance computations of simplex lines. (25,42,49) But no extensive reports ^{on bundle condn. lines} have been encountered by the author. However a report dealing with calculation of a particular transmission line exists. (32) The author agrees fully with the opinion expressed in the reference (32) that it is extremely tedious to compile general charts, if not impossible, of unbalances on bundle conductor lines. And often such charts are of academic interest only.

In the present investigation the range of calculations are limited to horizontal single circuit lines only.

6.3. Electrostatic Unbalance to Ground:

6.3.1. Outline of the Method:

The method of calculation of electrostatic unbalance assumes that the voltage drop due to capacitive charging current and load current is zero. This is practically true in the case of extra-high voltage systems. A general solution for determination of electrostatic unbalance to ground is indicated. Digital calculation of unbalance is carried out with the help of IBM 2620.

Electrostatic unbalance to ground factor or simply ground displacement factor d_o is defined as the ratio of the neutral displacement voltage E_o to the phase to neutral voltage E ,

$$d_o = \frac{E_o}{E} \quad \dots \quad \dots \quad (1)$$

The above definition holds good for ungrounded systems. In the case of grounded systems, the neutral displacement voltage adjusts itself as a neutral to ground current and so d_o can also be defined as

$$d_o = \frac{I_u}{I_{GF}} \quad \dots \quad \dots \quad (2)$$

where, I_u unbalance current

$$I_{GF} = \frac{3E}{X'_o}$$

X'_o capacitive zero sequence shunt reactance

Both the definitions essentially lead to the same results.⁽⁴⁹⁾ However, the solution based on the former definition is general in nature and is used in the investigation.

It is a well known fact that a system of charged overhead conductors and the ground can be replaced by an equivalent system composed of the actual conductors and the image conductors, which are suspended in free space and are separated vertically by a

image conductors carry a charge that is equal in magnitude and opposite in sign to that of the actual conductors. In such a case

$$\begin{bmatrix} V_1 \\ V_2 \\ \vdots \\ V_n \end{bmatrix} = \begin{bmatrix} P_{11} & P_{12} & \cdots & P_{1n} \\ P_{21} & P_{22} & \cdots & P_{2n} \\ \vdots & \vdots & \ddots & \vdots \\ P_{n1} & P_{n2} & \cdots & P_{nn} \end{bmatrix} \begin{bmatrix} Q_1 \\ Q_2 \\ \vdots \\ Q_n \end{bmatrix} \quad (3)$$

where,

$$P_{nn} = 2 \log_e \frac{2D_{nn}}{2r_n}$$

$$P_{nm} = 2 \log_e \frac{D_{nm}}{d_{nm}}$$

$$d_{nm} = d_{mn} \quad \text{and} \quad P_{nm} \neq P_{mn} \quad \text{if } n \neq m$$

It is evident that equation (3) holds good under the assumption that the charge is concentrated at the centre of the conductor. This is perfectly true in the case of single conductor lines. However, for bundle conductor lines of practical intra-conductor spacings employed in the existing EHV lines, the above assumption is equally valid and has been analytically proved. (49)

6.3.2. General Solution:

A general solution can be obtained for all the cases with duplex, triplex and quadruplex systems, with conductor disposition as shown in Fig.1.3. If a bundle conductor line is represented as in equation (3), the matrix to be handled will be very big. A short cut however exists. This consists in representing each bundle by an equivalent conductor of same total capacitance of the bundle. The equation for R_c is (Chapter 2)-

$$R_c = r \left(\frac{m}{2r \sin \frac{\pi}{n}} \right)^{\frac{n-1}{n}} \cdot n^{\frac{1}{n}} \quad (6)$$

$$= \left(\frac{m}{2r} \right)^{.5} \quad \text{For } n = 2$$

$$= \left(\frac{m}{r}\right) \cdot 666 \quad \text{For } n=3$$

$$= 2 \cdot 125 \left(\frac{m}{r}\right) \cdot 75 \quad \text{For } n=4$$

Table 5(A, B & C) lists the values of R_0 for all conductors used in practice and the intra-conductor spacings. Thus when each phase is represented by a single conductor carrying the same total charge per phase a large simplification results, since the line essentially would consist of a maximum of 5 conductors for a single circuit and 8 conductors for a double circuit.

6.3.3. Line With no Ground Wires:

For a line without ground wires equation (2) reduces to,

$$\begin{bmatrix} V_a \\ V_b \\ V_c \end{bmatrix} = \begin{bmatrix} P_{aa} & P_{ab} & P_{ac} \\ P_{ba} & P_{bb} & P_{bc} \\ P_{ca} & P_{cb} & P_{cc} \end{bmatrix} \begin{bmatrix} Q_a \\ Q_b \\ Q_c \end{bmatrix} \quad (5)$$

For a horizontal circuit $P_{aa} = P_{bb} = P_{cc}$

$$\text{and } P_{ab} = P_{bc} = P_{ba} = P_{cb}$$

Substituting these into (5) and noting that $V_a + V_b + V_c = 3E_0$ and that $Q_a + Q_b + Q_c = 0$, we get-

$$3E_0 = (P_{ab} - P_{ac}) Q_b \quad \dots \quad (6)$$

and also from the second equation of (5)-

$$E - E_0 = (P_{aa} - P_{ab}) Q_b \quad \dots \quad (7)$$

From (6) and (7)-

$$\frac{E - E_0}{3E_0} = \frac{P_{aa} - P_{ab}}{P_{ab} - P_{ac}}$$

$$\text{or } d_0 = \frac{E_0}{E} = \frac{P_{ab} - P_{ac}}{3P_{aa} - 2P_{ab} - P_{ac}} \quad (8)$$

TABLE 5-A. EQT. RADIUS OF SAME CAPACITANCE PER PHASE DUPLEX-SYSTEM

DIA.CMS	INTRA-CONDUCTOR SPACING						
	15CMS	20CMS	25CMS	30CMS	35CMS	40CMS	45CMS
4.069	5.52432	6.37893	7.13187	7.81257	8.43854	9.02118	9.56840
3.924	5.42515	6.26442	7.00384	7.67232	8.28705	8.85923	9.39664
3.825	5.35624	6.18485	6.91488	7.57487	8.18179	8.74670	9.27728
3.721	5.28283	6.10008	6.82010	7.47104	8.06965	8.62682	9.15012
3.617	5.20838	6.01412	6.72399	7.36576	7.95593	8.50525	9.02118
3.510	5.13099	5.92476	6.62409	7.25632	7.83772	8.37888	8.88714
3.399	5.04865	5.82968	6.51778	7.13987	7.71195	8.24442	8.74452
3.284	4.96303	5.73081	6.40724	7.01878	7.58115	8.10459	8.59622
3.165	4.87199	5.62569	6.28971	6.89004	7.44209	7.95593	8.43854
3.038	4.77324	5.51166	6.16222	6.75038	7.29124	7.79467	8.26749
2.951	4.70490	5.43275	6.07400	6.65374	7.18686	7.68307	8.14913
2.911	4.67240	5.39522	6.03204	6.60777	7.13721	7.62999	8.09283
2.776	4.56307	5.26898	5.89090	6.45316	6.97021	7.45147	7.90348
2.814	4.59428	5.30502	5.93119	6.49729	7.01788	7.50243	7.95752
2.896	4.66015	5.38108	6.01623	6.59045	7.11850	7.60999	8.07162
2.631	4.44250	5.12976	5.73524	6.28264	6.78603	7.25457	7.69463
2.670	4.47454	5.16676	5.77661	6.32796	6.83498	7.30690	7.75014
2.748	4.54006	5.24240	5.86119	6.42061	6.93505	7.41388	7.86361
2.540	4.36463	5.03984	5.63471	6.17252	6.66708	7.12741	7.55976
2.482	4.31415	4.98155	5.56954	6.10112	6.58997	7.04497	7.47232
2.537	4.36245	5.03732	5.63190	6.16943	6.66375	7.12385	7.55598
2.588	4.40590	5.08749	5.68799	6.23088	6.73012	7.19480	7.63124
2.421	4.26083	4.91998	5.50070	6.02572	6.50852	6.95790	7.37997
2.454	4.28979	4.95342	5.53810	6.06668	6.55276	7.00520	7.43013
2.355	4.20230	4.85240	5.42515	5.94295	6.41912	6.86233	7.27860
2.421	4.26083	4.91998	5.50070	6.02572	6.50852	6.95790	7.37997
2.296	4.14984	4.79183	5.35742	5.86877	6.33899	6.77667	7.18774
2.179	4.04288	4.66832	5.21934	5.71750	6.17561	6.60200	7.00248
2.243	4.10136	4.73584	5.29483	5.80020	6.26493	6.69749	7.10376
1.989	3.86214	4.45962	4.98601	5.46190	5.89952	6.30685	6.68943
2.047	3.91846	4.52464	5.05871	5.54153	5.98554	6.39881	6.78697
1.831	3.70608	4.27942	4.78453	5.24119	5.66114	6.05201	6.41912
1.882	3.75713	4.33836	4.85044	5.31339	5.73912	6.13537	6.50755
1.727	3.59917	4.15596	4.64650	5.08999	5.49782	5.87741	6.23394
1.778	3.65171	4.21663	4.71434	5.16430	5.57808	5.96322	6.32495
1.631	3.49716	4.03817	4.51481	4.94573	5.34199	5.71083	6.05725
1.608	3.47256	4.00976	4.48305	4.91094	5.30442	5.67066	6.01464
1.430	3.27493	3.78156	4.22791	4.63145	5.00253	5.34793	5.67234
1.275	3.09243	3.57083	3.99231	4.37335	4.72376	5.04991	5.35624
1.135	2.91811	3.36954	3.76726	4.12683	4.45748	4.76525	5.05431
1.011	2.75353	3.17950	3.55479	3.89407	4.20608	4.49649	4.76925

ABLE 5-B. EQT. RADIUS OF SAME CAPACITANCE PER PHASE TRIPLEX-SYSTEM

DIA.CMS	INTRA-CONDUCTOR SPACING						
	15CMS	20CMS	25CMS	30CMS	35CMS	40CMS	45CMS
4.069	7.70685	9.33617	10.83365	12.23381	13.55790	14.82018	16.03079
3.924	7.61434	9.22410	10.70361	12.08696	13.39516	14.64228	15.83835
3.825	7.54972	9.14582	10.61277	11.98438	13.28148	14.51802	15.70395
3.721	7.48058	9.06206	10.51557	11.87462	13.15984	14.38506	15.56012
3.617	7.41013	8.97672	10.41654	11.76280	13.03591	14.24959	15.41358
3.510	7.33655	8.88758	10.31311	11.64599	12.90647	14.10809	15.26053
3.399	7.25785	8.79224	10.20247	11.52106	12.76801	13.95674	15.09682
3.284	7.17555	8.69254	10.08679	11.39042	12.62323	13.79849	14.92563
3.165	7.08753	8.58592	9.96305	11.25070	12.46839	13.62923	14.74255
3.038	6.99143	8.46950	9.82796	11.09815	12.29933	13.44442	14.54265
2.951	6.92454	8.38846	9.73393	10.99197	12.18165	13.31579	14.40351
2.911	6.89261	8.34978	9.68905	10.94128	12.12548	13.25439	14.33710
2.776	6.78467	8.21902	9.53732	10.76994	11.93559	13.04683	14.11258
2.814	6.81556	8.25645	9.58075	10.81899	11.98994	13.10624	14.17684
2.896	6.88056	8.33519	9.67211	10.92216	12.10428	13.23122	14.31203
2.631	6.66461	8.07359	9.36856	10.57937	11.72439	12.81596	13.86285
2.670	6.69663	8.11237	9.41356	10.63018	11.78071	12.87752	13.92944
2.748	6.76183	8.19136	9.50522	10.73369	11.89542	13.00291	14.06507
2.540	6.58650	7.97896	9.25876	10.45537	11.58698	12.66576	13.70038
2.482	6.53562	7.91732	9.18722	10.37459	11.49746	12.56790	13.59453
2.537	6.58431	7.97630	9.25567	10.45189	11.58312	12.66154	13.69581
2.588	6.62796	8.02918	9.31703	10.52118	11.65991	12.74547	13.78661
2.421	6.48165	7.85195	9.11137	10.28893	11.40253	12.46413	13.48228
2.454	6.51099	7.88749	9.15261	10.33551	11.45414	12.52055	13.54331
2.355	6.42216	7.77988	9.02774	10.19450	11.29787	12.34974	13.35854
2.421	6.48165	7.85195	9.11137	10.28893	11.40253	12.46413	13.48228
2.296	6.36860	7.71500	8.95245	10.10948	11.20365	12.24674	13.24713
2.179	6.25869	7.58185	8.79795	9.93501	11.01030	12.03538	13.01851
2.243	6.31890	7.65479	8.88258	10.03058	11.11621	12.15116	13.14375
1.989	6.07074	7.35416	8.53373	9.63665	10.67965	11.67395	12.62755
2.047	6.12961	7.42548	8.61649	9.73010	10.78321	11.78715	12.75000
1.831	5.90608	7.15469	8.30227	9.37527	10.38998	11.35731	12.28504
1.882	5.96019	7.22024	8.37834	9.46117	10.48517	11.46137	12.39760
1.727	5.79193	7.01641	8.14181	9.19408	10.18917	11.13781	12.04761
1.778	5.84817	7.08454	8.22087	9.28335	10.28810	11.24595	12.16459
1.631	5.68197	6.88320	7.98723	9.01952	9.99572	10.92634	11.81888
1.608	5.65529	6.85088	7.94973	8.97717	9.94879	10.87504	11.76339
1.430	5.43863	6.58842	7.64517	8.63324	9.56764	10.45841	11.31272
1.275	5.23465	6.34131	7.35843	8.30945	9.20880	10.06616	10.88843
1.135	5.03603	6.10071	7.07923	7.99416	8.85939	9.68422	10.47529
1.011	4.84485	5.86910	6.81048	7.69068	8.52306	9.31657	10.07761

ABLE 5-C. EQT. RADIUS OF SAME CAPACITANCE PER PHASE QUADRUPLIX-SYSTEM

DIA.CMS	INTRA-CONDUCTOR SPACING						
	30CMS	35CMS	40CMS	45CMS	50CMS	55CMS	60CMS
4.069	16.69499	18.74115	20.71526	22.62845	24.48910	26.30372	28.07752
3.924	16.54446	18.57218	20.52849	22.42442	24.26829	26.06656	27.82436
3.825	16.43905	18.45385	20.39769	22.28155	24.11367	25.90048	27.64708
3.721	16.32601	18.32695	20.25742	22.12832	23.94785	25.72237	27.45696
3.617	16.21056	18.19736	20.11418	21.97184	23.77851	25.54049	27.26281
3.510	16.08969	18.06167	19.96419	21.80801	23.60120	25.35004	27.05952
3.399	15.96007	17.91616	19.80335	21.63231	23.41106	25.14581	26.84152
3.284	15.82415	17.76358	19.63470	21.44809	23.21169	24.93167	26.61294
3.165	15.67834	17.59990	19.45378	21.25047	22.99782	24.70195	26.36773
3.038	15.51863	17.42062	19.25561	21.03399	22.76355	24.45032	26.09912
2.951	15.40715	17.29547	19.11728	20.88289	22.60001	24.27467	25.91163
2.911	15.35384	17.23562	19.05113	20.81063	22.52181	24.19067	25.82196
2.776	15.17315	17.03278	18.82694	20.56573	22.25678	23.90599	25.51809
2.814	15.22494	17.09093	18.89120	20.63593	22.33275	23.98759	25.60519
2.896	15.33370	17.21301	19.02614	20.78334	22.49228	24.15895	25.78810
2.631	14.97134	16.80624	18.57653	20.29220	21.96075	23.58802	25.17868
2.670	15.02524	16.86674	18.64341	20.36525	22.03981	23.67295	25.26933
2.748	15.13483	16.98977	18.77939	20.51379	22.20057	23.84561	25.45364
2.540	14.83954	16.65830	18.41300	20.11357	21.76743	23.38038	24.95703
2.482	14.75347	16.56167	18.30620	19.99690	21.64118	23.24477	24.81228
2.537	14.83583	16.65413	18.40840	20.10854	21.76199	23.37454	24.95080
2.588	14.90954	16.73687	18.49985	20.20843	21.87010	23.49066	25.07475
2.421	14.66202	16.45901	18.19273	19.87295	21.50703	23.10068	24.65847
2.454	14.71177	16.51486	18.25446	19.94038	21.58000	23.17906	24.74214
2.355	14.56098	16.34559	18.06736	19.73599	21.35881	22.94148	24.48854
2.421	14.66202	16.45901	18.19273	19.87295	21.50703	23.10068	24.65847
2.296	14.46980	16.24324	17.95423	19.61242	21.22507	22.79784	24.33521
2.179	14.28211	16.03255	17.72134	19.35802	20.94975	22.50212	24.01955
2.243	14.38503	16.14808	17.84904	19.49752	21.10072	22.66427	24.19264
1.989	13.95922	15.67008	17.32069	18.92036	20.47611	21.99338	23.47651
2.047	14.06061	15.78391	17.44651	19.05780	20.62485	22.15314	23.64704
1.831	13.67428	15.35022	16.96713	18.53415	20.05815	21.54446	22.99731
1.882	13.76814	15.45558	17.08359	18.66137	20.19583	21.69233	23.15516
1.727	13.47559	15.12718	16.72060	18.26485	19.76671	21.23142	22.66316
1.778	13.57360	15.23720	16.84221	18.39770	19.91048	21.38584	22.82799
1.631	13.28325	14.91126	16.48194	18.00415	19.48458	20.92838	22.33967
1.608	13.23645	14.85873	16.42387	17.94072	19.41593	20.85464	22.26096
1.430	12.85428	14.42971	15.94967	17.42273	18.85534	20.25250	21.61823
1.275	12.49098	14.02189	15.49889	16.93031	18.32243	19.68011	21.00725
1.135	12.13382	13.62096	15.05572	16.44621	17.79852	19.11739	20.40657
1.011	11.78668	13.23127	14.62498	15.97570	17.28932	18.57045	19.82275

6.3.4. Negative and Zero Sequence Unbalances:

As a result of the geometric dissimilarity, in addition to ground displacement another two unbalances exist such as negative and zero sequence unbalances. These unbalance factors are defined in terms of mutual sequence potential coefficients, given by⁽⁹⁾

$$P_{11} = P_{22} = 5.3342 \times 10^6 \text{ Log } \frac{D_{aa} D_{bb} D_{cc} d_{bc} d_{ac} d_{ab}}{R_c^3 D_{bc} D_{ac} D_{ab}} \text{ Farads/Km.}$$

$$P_{21} = 5.3342 \times 10^6 \left[\text{Log } \frac{D_{aa} D_{bc}^2 d_{ac} d_{ab}}{D_{bb} D_{cc} d_{bc}^2 D_{ac} D_{ab}} + j0.866 \text{ Log } \frac{D_{bb} D_{ac}^2 d_{ab}^2}{d_{cc} d_{ac}^2 D_{ab}^2} \right] \text{ Farads/Km.}$$

$$P_{01} = 5.3342 \times 10^6 \left[\text{Log } \frac{D_{aa} d_{bc}}{D_{bb} D_{cc} D_{bc}} \sqrt{\frac{D_{ac} D_{ab}}{d_{ac} d_{ab}}} + j0.866 \text{ Log } \frac{D_{cc} D_{ac} D_{ab}}{D_{bb} d_{ac} D_{ab}} \right] \text{ Farads/Km.}$$

$$P_{00} = 5.3342 \times 10^6 \left[\text{Log } \frac{D_{aa} D_{bb} D_{cc} D_{ab}^2 D_{bc}^2 D_{ac}^2}{R_c^3 d_{ab}^2 d_{bc}^2 d_{ac}^2} \right] \text{ Farads/Km.}$$

The sequence unbalances are defined by-

$$d_2 = - \frac{P_{21}}{P_{22}} \quad \text{and} \quad d'_0 = - \frac{P_{01}}{P_{00}}$$

Fig.6.1. illustrates the result of the computer calculations of d_2 and d'_0 . The following facts are highlighted from this figure. Ground displacement factor is increased by reducing the intra-conductor separation. On the contrary d_0 is small at smaller conductor heights. Increase in phase separation further reduces this factor. For EHV lines in practice the factor can vary between 4-11 percent.

The zero sequence electrostatic unbalance factor on the other hand is not effected by height. The calculations indicated that at greater heights than those used in practice (about 30m or

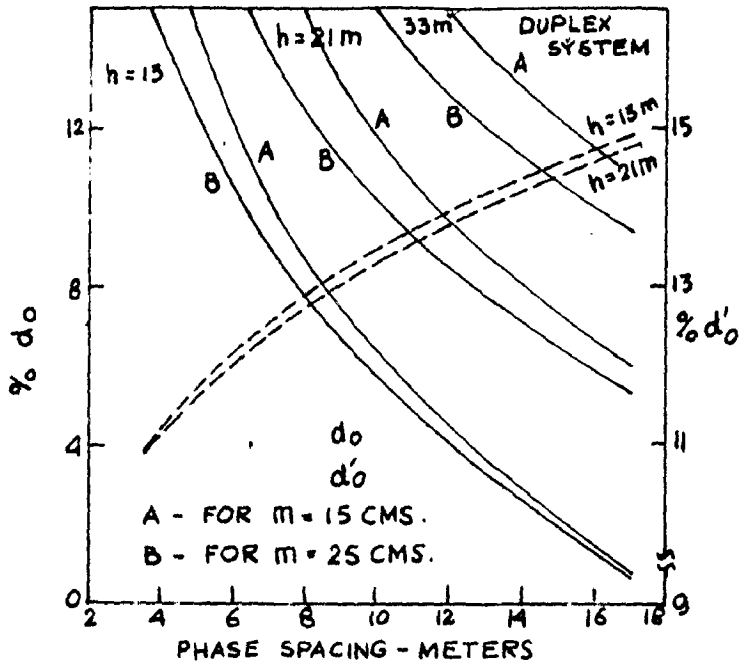


FIG. 6.1 ELECTRO STATIC UNBALANCE OF A DUPLEX SYSTEM WITH NO GROUND WIRES

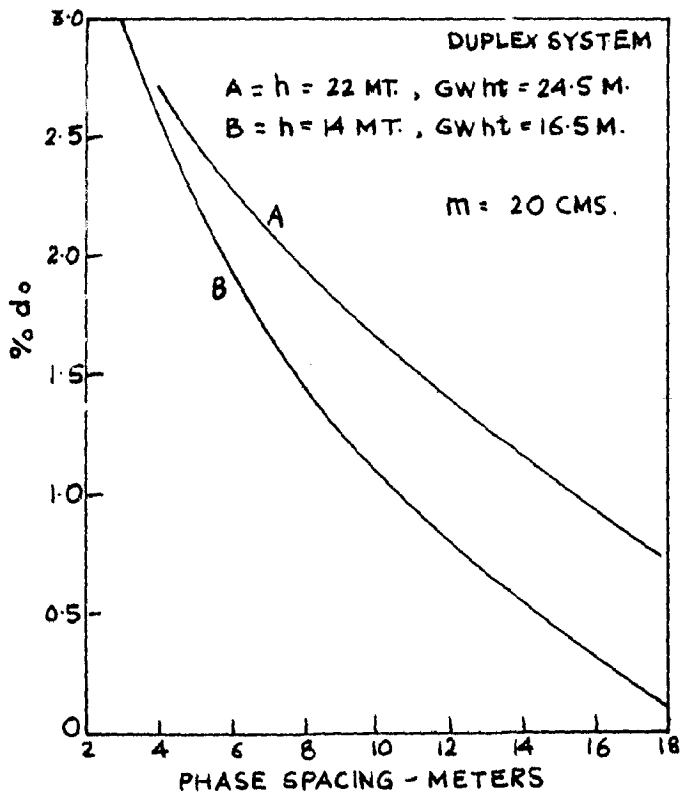


FIG. 6.2 ELECTRO STATIC UNBALANCE WITH TWO G.W.

conductor separation excepting for very slight differences. Contrary to d_0 , d_0' increases with phase separation. For typical lines in practice this is about 14 percent.

6.3.5. Line with Two Ground Wires:

For a line with two ground wires equation (3) can be written as-

$$\begin{bmatrix} V_a \\ V_b \\ V_c \\ 0 \\ 0 \end{bmatrix} = \begin{bmatrix} P_{aa} & P_{ab} & P_{ac} & P_{aw} & P_{ax} \\ P_{ba} & P_{bb} & P_{bc} & P_{bw} & P_{bx} \\ P_{ca} & P_{cb} & P_{cc} & P_{cw} & P_{cx} \\ P_{wa} & P_{wb} & P_{wc} & P_{ww} & P_{wx} \\ P_{xa} & P_{xb} & P_{xc} & P_{xw} & P_{xx} \end{bmatrix} \begin{bmatrix} Q_a \\ Q_b \\ Q_c \\ Q_w \\ Q_x \end{bmatrix} \quad (9)$$

A single circuit horizontal line will have-

$$\begin{aligned} P_{aa} &= P_{bb} = P_{cc} & P_{ab} &= P_{ba} = P_{bc} = P_{cb} \\ P_{aw} &= P_{bx} = P_{cx} = P_{bw} & P_{ww} &= P_{xx} = P_{GG} \\ P_{ax} &= P_{cw} & P_{wx} &= P_{xw} \end{aligned}$$

Substituting these into equation (7) and defining the equivalent coefficients after eliminating the last two rows

$$\begin{bmatrix} V_a \\ V_b \\ V_c \end{bmatrix} = \begin{bmatrix} P'_{aa} & P'_{ab} & P'_{ac} \\ P'_{ab} & P'_{aa} & P'_{ab} \\ P'_{ac} & P'_{ab} & P'_{aa} \end{bmatrix} \begin{bmatrix} Q'_a \\ Q'_b \\ Q'_c \end{bmatrix}$$

where,

$$P'_{ii} = P_{ii} + \frac{2P_{iw} P_{ix} P_{wx} - P_{GG}(P_{iw}^2 + P_{ix}^2)}{P_{GG}^2 - P_{wx}^2}$$

$$\text{and } P'_{ij} = P_{ij} + \frac{P_{iw}(P_{ix} P_{wx} - P_{jw} P_{GG})}{P_{GG}^2 - P_{wx}^2} + \frac{P_{ix}(P_{jw} P_{wx} - P_{jx} P_{GG})}{P_{GG}^2 - P_{wx}^2}$$

It is evident that the effect of ground wires is to introduce correction factors depending on disposition of ground wires.

$$d_{owx} = \frac{P'_{ab} - P'_{ac}}{3P'_{aa} - 2P'_{ab} - P'_{ac}} \quad (10)$$

The sequence unbalance factors are given as-

$$d_{2wx} = -\frac{P_{21wx}}{P_{22wx}} \quad \text{and} \quad d'_{owx} = -\frac{P_{01wx}}{P_{22wx}}$$

However unbalance factor given by equation (10) only was calculated.

Fig.(6.2) shows the ground displacement factor on a single circuit duplex line with two g.w. comparison with Fig.(6.1) shows that the ground displacement factor has greatly reduced. Thus the presence of ground wires reduce the unbalance of the system. The ground wire was maintained at a constant height of 2.5m. The comments regarding variation of the displacement factor with height and phase spacing without ground wire hold good for the case with ground wires also. Evidently a thorough calculation is necessary to study the effect of other variables such as conductor dimension, intra-conductor spacing, conductor disposition, phase spacing, ground wire height etc. The/author proposes such thorough calculation as an extension of this work.

6.4. Electromagnetic Unbalance:

6.4.1. Line with no Ground Wires:

Inherent geometric unbalances of a transmission system give rise to mutual-sequence impedances, not present in the balanced system. Because of the existence of these mutual sequence impedances, the respective sequence currents circulate in the line. The unbalance factors F_2 and F_0 are defined for a line without ground wires as follows,

$$F_2 = \frac{I_{a2}}{I_{a1}} = -\frac{Z_{21}}{Z_{22}} = -\frac{Z_{21}}{Z_{11}} ; F_0 = \frac{I_{a0}}{I_{a1}} = -\frac{Z_{01}}{Z_{00}} \quad (11)$$

where I_{a1} , I_{a2} and I_{a0} are positive, negative and zero sequence

defined as follows,

$$\begin{aligned} Z_{11} &= \frac{1}{3} (Z_{aa} + Z_{bb} + Z_{cc}) - \frac{1}{3} (Z_{ab} + Z_{ac} + Z_{bc}) \\ Z_{00} &= \frac{1}{3} (Z_{aa} + Z_{bb} + Z_{cc}) - \frac{2}{3} (Z_{ab} + Z_{ac} + Z_{bc}) \\ Z_{21} &= \frac{1}{3} (Z_{aa} + aZ_{bb} + a^2Z_{cc}) + \frac{2}{3} (a^2Z_{ab} + aZ_{ac} + Z_{bc}) \\ Z_{01} &= \frac{1}{3} (Z_{aa} + a^2Z_{bb} + aZ_{cc}) - \frac{1}{3} (aZ_{ab} + a^2Z_{ac} + Z_{bc}) \\ Z_{00} - Z_{11} &= Z_{00} - Z_{22} = (Z_{ab} + Z_{ac} + Z_{bc}) \\ Z_{11} &= Z_{22} = Z_1 = Z_2; \quad Z_{00} = Z_0 \end{aligned} \quad (12)$$

and

$$\begin{aligned} Z_{1j} &= R + \frac{1}{3} R_e + j(X_a + \frac{1}{3} X_c) \text{ ohms/Km.} \\ &\quad 1, j = a, b \text{ or } c \\ Z_{1j} &= \frac{1}{3} R_e + j[\frac{1}{3} X_e - X_d(1j)] \text{ ohms/km.} \end{aligned} \quad (13)$$

In equation (13),

$$R_e = 0.002978f = 0.1489 \text{ ohms/km at 50 cycles}$$

$$X_e = 0.008732f \text{ Log} (2162 \sqrt{\frac{\rho}{f}}) = 1.3030 \text{ ohms/Km. at 50 cycles}$$

and $\rho = 100$, earth resistivity in ohms per m^3 .

$$X_a = 0.1446 \text{ Log} \frac{1}{\text{GMR} \cdot m_{12} \cdot m_{13} \cdots m_{1n}} \text{ ohms/Km. at 50 cycles.}$$

$$X_d(1j) = 0.1446 \text{ log} (D_{1j}) \text{ ohms/Km. at 50 cycles.}$$

Certain simplifications in equation (13) result in due to inherent characteristics of the line such as, similarity of conductors, same geometric mean radii and same resistance per conductor per kilometer. This leads to-

$$\begin{aligned} Z_{01} &= \frac{1}{3} (a X_{ab} + a^2 X_{ac} + X_{bc}) \\ &= 0.289 (X_{ac} - X_{ab}) + \frac{1}{3} (X_{bc} - 0.5X_{ab} - 0.5X_{ac}) \\ &= 0.04179 \text{ Log} \frac{D_{bc}}{D_{ab}} - j0.0723 \text{ Log} \frac{\text{GMD}}{D_{ac}} \end{aligned}$$

.GMD .

$$Z_{21} = j0.1446 \text{ Log } \left(\frac{\text{GMD}}{D_{ac}} \right) \quad (15)$$

An obvious result of equations (14) and (15) is-

$$Z_{21} = 2Z_{01}$$

So also the positive, negative and zero sequence impedances can be simplified and the corrected expressions for bundle conductor lines are as follows, ⁽⁸⁷⁾

$$Z_1 = Z_2 = \frac{R}{n} + j0.1446 \text{ Log} \left(\frac{\text{GMD}}{\text{GMR} \cdot m_{12} \cdot m_{1n}} \right) \text{ ohms/km.} \quad (16)$$

$$Z_0 = \frac{R}{n} + 0.1489 + j \{ 1.3030 - 0.1446n \log (\text{GMD}^2 \cdot \text{GMR} \cdot m_{12} \cdot m_{1n}) \} \text{ ohms/km.} \quad (17)$$

The calculation of the two unbalance factors are done with the help of IBM 1620. The results are plotted in Fig.(6.3)& (6.4). The variables considered are indicated ^{ln} the respective figures. It is to be noted that the magnetic unbalance without ground wires is essentially independent of ^{the height of the} conductor on the lines in practice. The following facts are evident from the figures. The zero sequence unbalance decreases with the increase in number of conductors, maximum being on duplex line. Increase in intra-conductor spacing further decreases the zero sequence unbalance factor. However the range of reduction is same for all arrangements duplex, triplex and quadruplex lines.

Negative sequence unbalance slightly increases with the number of conductors. And also increase in intra conductor-spacing increases the unbalance. The difference in increase of unbalance factor however seems to be almost same on all arrangements.

The intra-phase spacing in general decreases the unbalance in a logarithmic manner in both the cases .

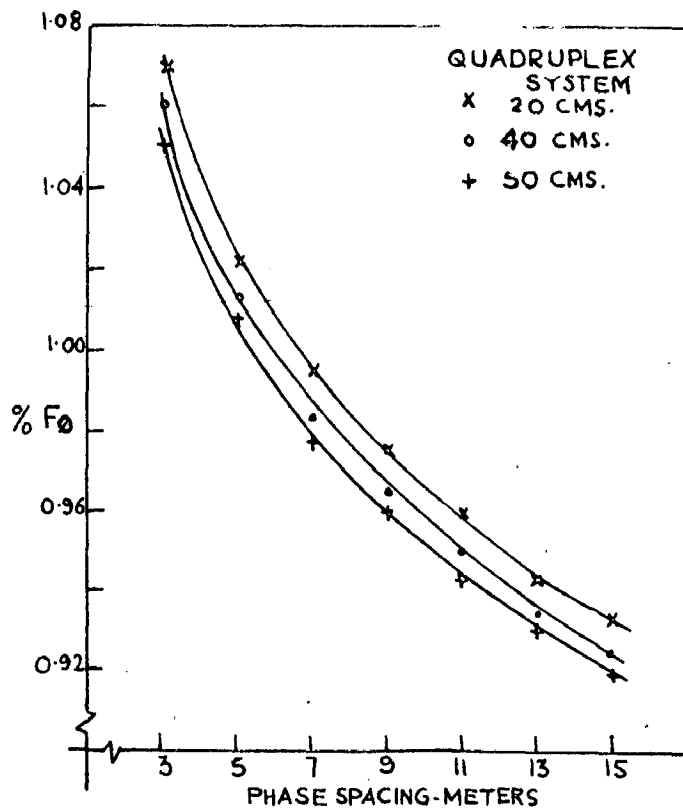
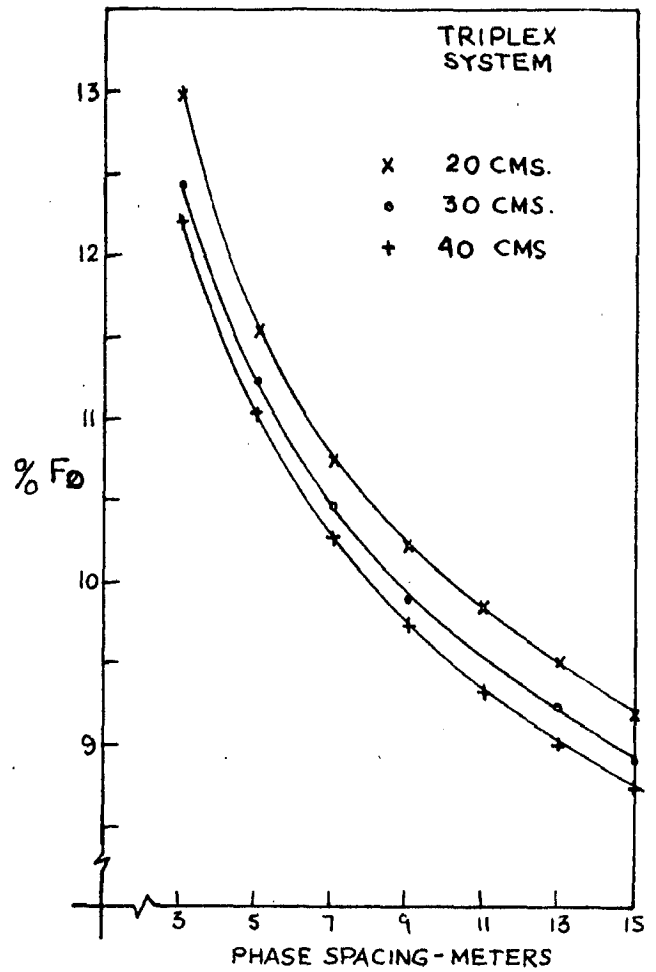
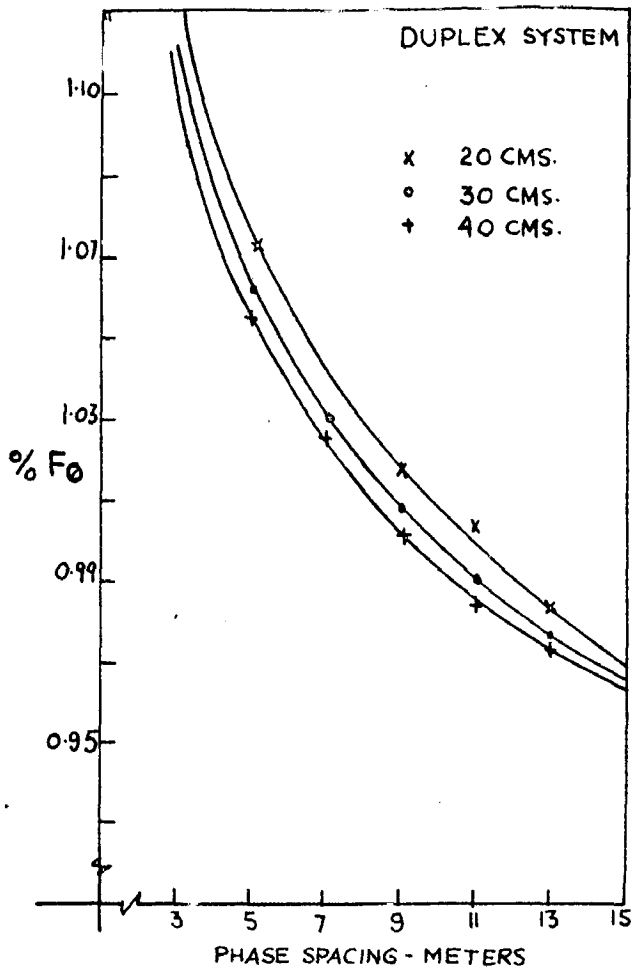


FIG. 6.3 ZERO SEQUENCE UNBALANCE FACTOR
 (ELECTROMAGNETIC UNBALANCE OF HOR. SINGLE CKT. LINES WITH NO G.W.)

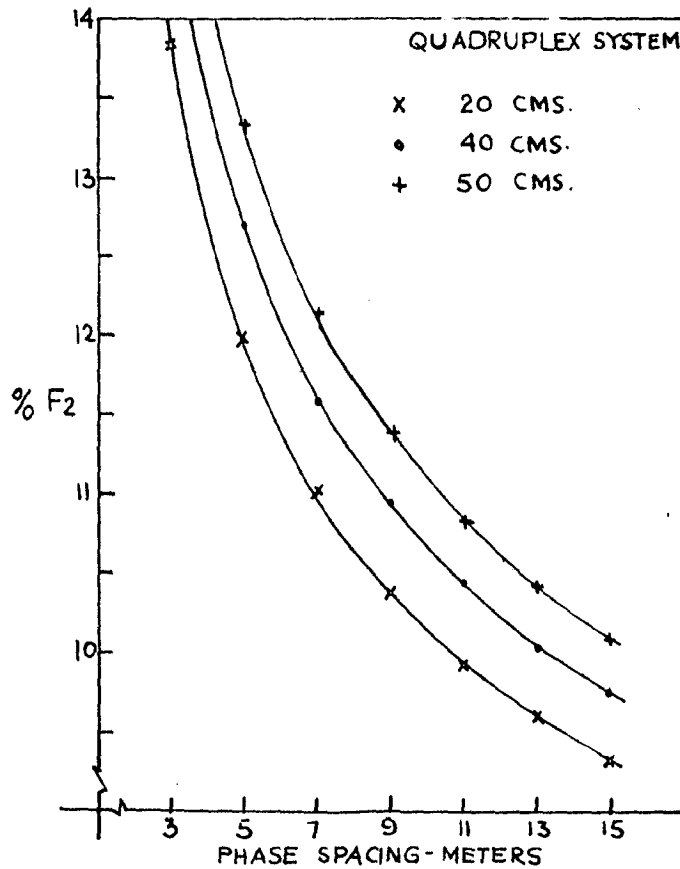
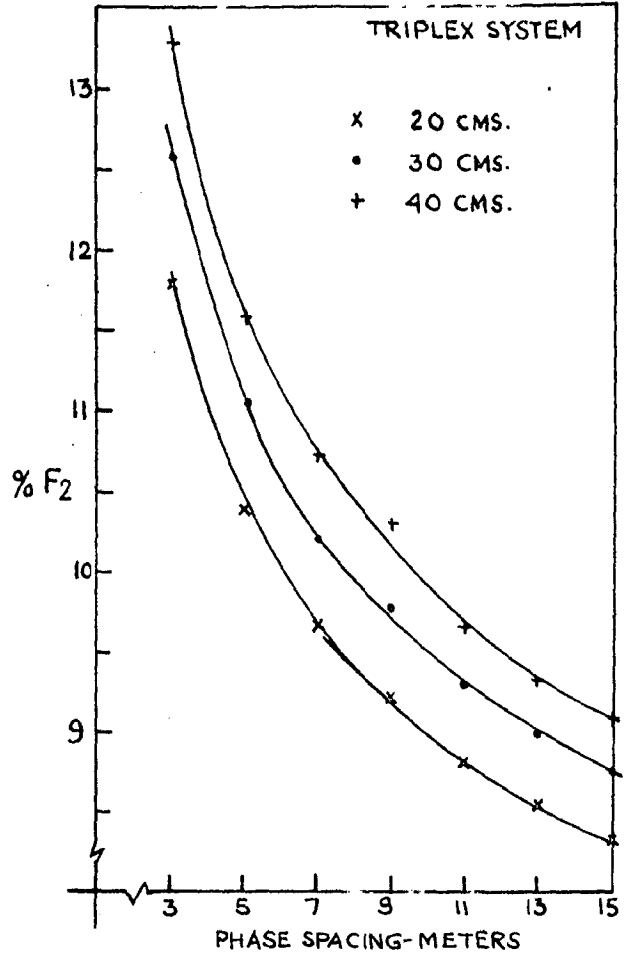
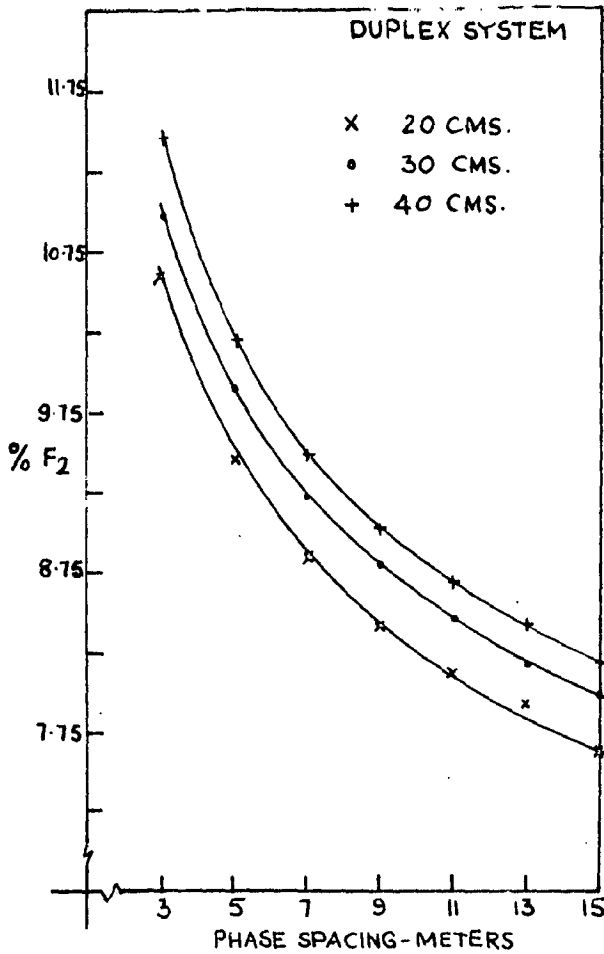


FIG.6.4 NEGATIVE SEQUENCE UNBALANCE FACTOR
 (ELECTROMAGNETIC UNBALANCE OF HOR. SINGLE CKT. LINES WITH NO G.W.)

impedances. Thus the unbalance factors can be defined for lines with ground wires as follows-

$$F_{2wx} = \frac{I_{a2}}{I_{a1}} = - \frac{Z_{21wx}}{Z_{2wx}} = - \frac{Z_{21wx}}{Z_{1wx}}$$

$$\text{and } F_{0wx} = \frac{I_{a0}}{I_{a1}} = - \frac{Z_{01wx}}{Z_{0wx}} \quad \dots (18)$$

For a horizontal ^{Line} with two ground wires having 30° protective angle, $D_{aw} = D_{bw} = D_{bx} = D_{cx}$, where W and X are ground wires, a, b & c are phases in order from left to right.

With the help of the above equality, the sequence impedances of a line with ground wires can be written as ⁽⁹⁾

$$Z_{01wx} = Z_{01} - \frac{2}{3} \frac{b_2}{a_4^2 + b_4^2} (a_1 b_4 - a_4 b_1) - j \frac{2}{3} \frac{b_2}{a_4^2 + b_4^2} (a_1 a_4 + b_1 b_4)$$

$$Z_{21wx} = Z_{21} - \frac{2}{3} \left(\frac{a_2^2 a_3}{a_3^2 + b_3^2} \right) - \frac{b_2^2 a_4}{a_4^2 + b_4^2} + j \frac{2}{3} \left(\frac{a_2^2 b_3}{a_3^2 + b_3^2} + \frac{b_2^2 b_4}{a_4^2 + b_4^2} \right) I$$

$$Z_{00wx} = C_0 - \frac{2}{3} \frac{a_1^2 a_4 - b_1^2 a_4 + 2a_1 b_1 b_4}{a_4^2 + b_4^2} + j \left(k_0 - \frac{2}{3} (2a_1 a_4 b_1 + b_1^2 b_4 - a_1^2 b_4) \right) I$$

$$Z_{11wx} = C_1 + \frac{2}{3} \left(\frac{a_2^2 a_3}{a_3^2 + b_3^2} + \frac{b_2^2 a_4}{a_4^2 + b_4^2} \right) I + j \left(k_1 - \frac{2}{3} \left(\frac{a_2^2 b_3}{a_3^2 + b_3^2} + \frac{b_2^2 b_4}{a_4^2 + b_4^2} \right) \right) I \quad \dots (19)$$

where,

$$a_1 + j b_1 = Z_{aw} + Z_{bw} + Z_{cw}$$

$$a_2 + j b_2 = Z_{bw} + a Z_{aw} + a^2 Z_{cw}$$

$$a_3 + j b_3 = Z_{ww} - Z_{wx}$$

$$a_4 + j b_4 = Z_{ww} + Z_{wx}$$

$$c_1 + j k_1 = Z_{11}$$

$$c_0 + j k_0 = Z_{00}$$

But, the effect of bundling being only on the self-sequence impedances, with suitable modification for these effects equations (20) can be used on bundle conductor lines with ground wires.

The two unbalance factors for a duplex line are illustrated in Figs.(6.5) and (6.6 A&B). The fact that ground wires reduce the zero sequence magnetic unbalance⁽¹⁰⁵⁾ is evidenced by these figures. Fig.(6.5) shows the variation of zero sequence unbalance factor with ground wire height above the line and with the intra-conductor separation. The effect of ground wires is diminished with increase in their height. Increase in intra-conductor separation displaces the curve to the right thereby increasing the unbalance.

Ground wire presence and its height have very little effect on negative unbalance. However a comparison of Figs.(6.6 A & B) shows that increase in intra-conductor spacing increases the negative sequence unbalance also.

Increased phase separation evidently decreases the unbalance. However, the rate of decrease is less in the case of negative sequence unbalance.

6.5. Reduction of Unbalances:

Unbalances are reduced to a great extent by transpositions. As pointed out earlier too many transpositions may be the source of trouble. A suitable location for transposition is at the series capacitor location. Series capacitor banks are essentially used on long distance power transmission lines for compensation purposes. These may be located in the middle of the line. Three of the possible arrangement of phases with and without transpositions are shown in Fig.(6.7- A,B & C). More adequate balance can be obtained by increasing the number of transpositions to 2 as shown in Fig.(6.8),

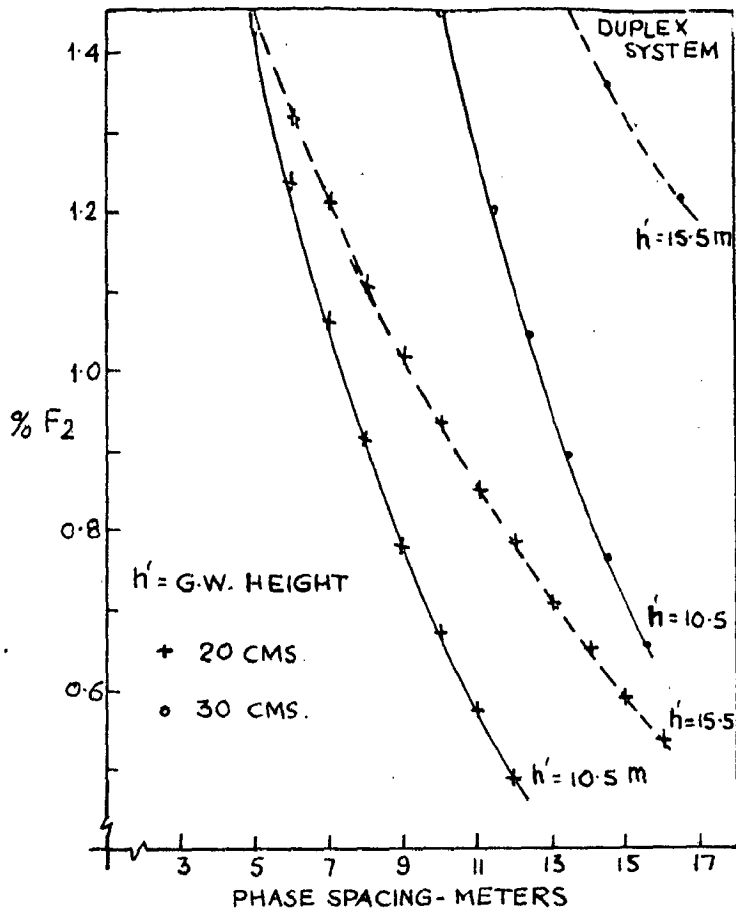


FIG. 6.5 ZERO SEQUENCE MAGNETIC UNBALANCE WITH TWO GROUND WIRES

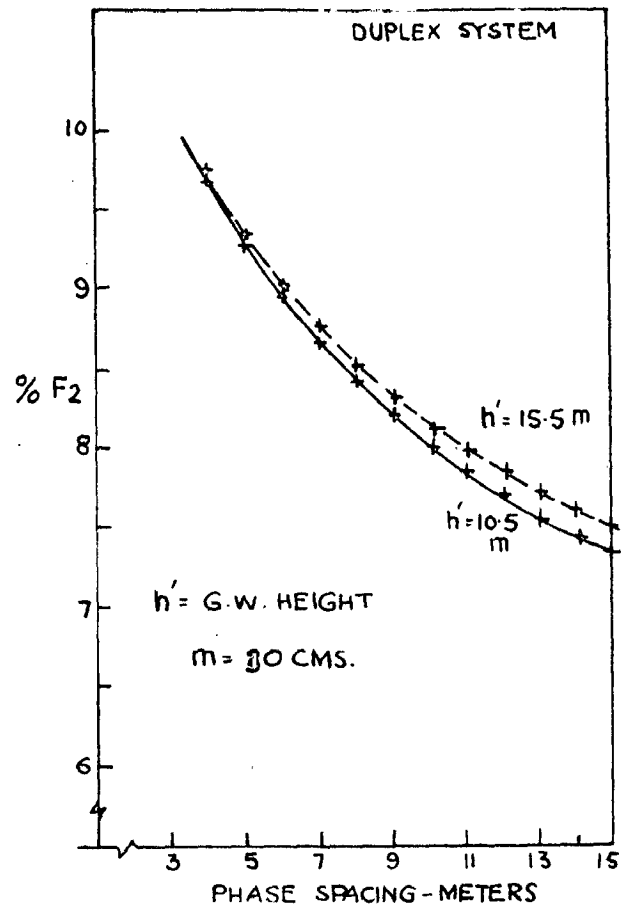
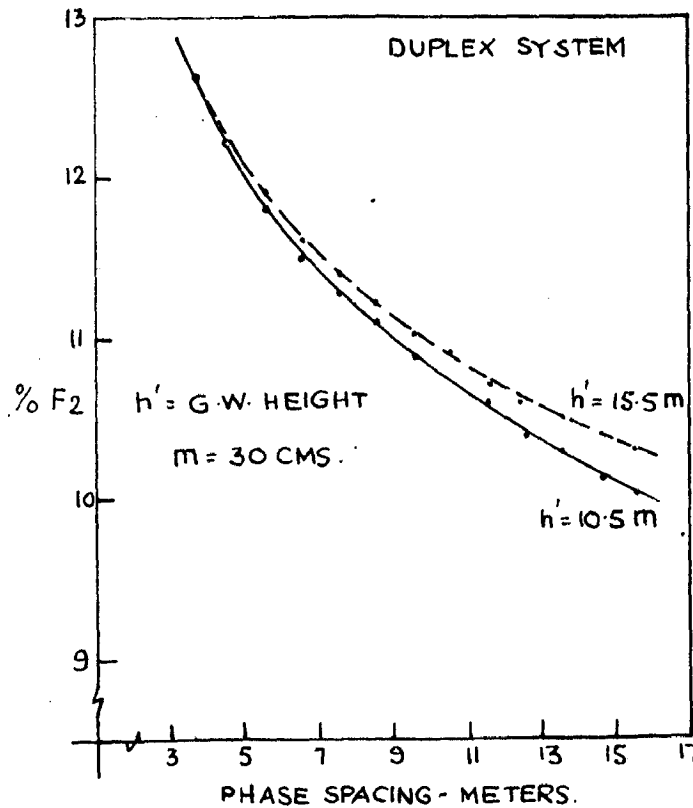


FIG. 6.6 (A)



(B)

FIG. 6.6 NEGATIVE SEQUENCE MAGNETIC UNBALANCE WITH TWO GROUND WIRES

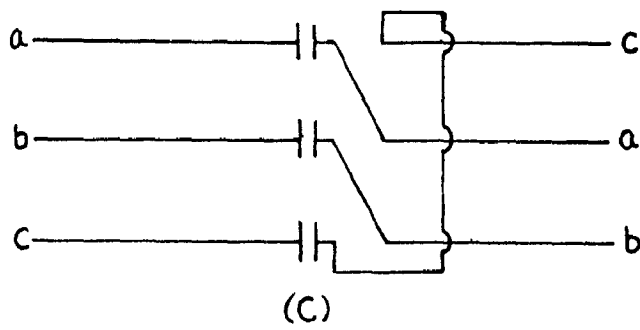
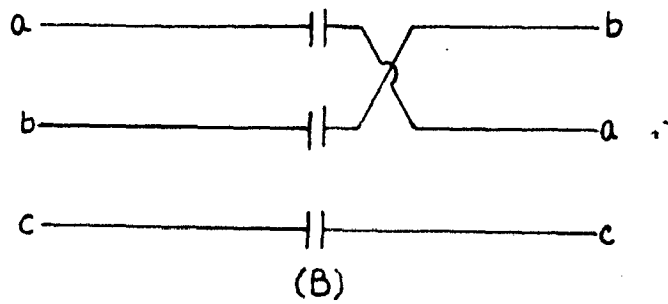
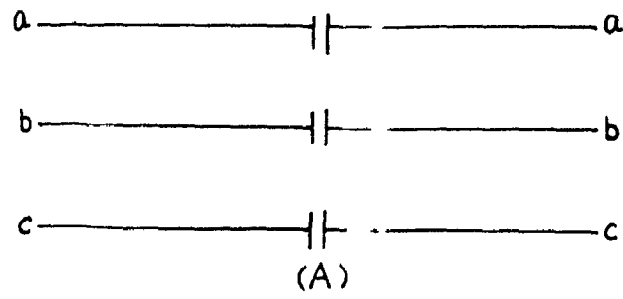


FIG.6.7 TRANSPOSITION IN THE MIDDLE OF THE LINE

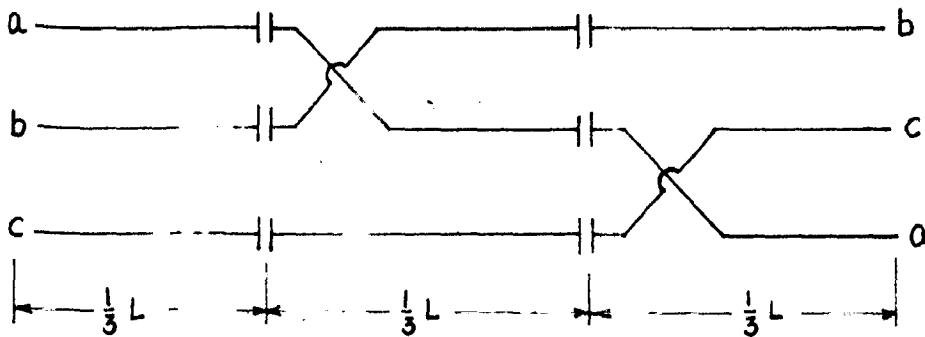


FIG.6.8 TRANSPOSITION AT EACH ONE-THIRD LENGTH

at each one-third length.

Introduction of unequal impedances can reduce the unbalance. By suitably altering the phase voltages at the sending end, with the help of transformer taps can give balanced receiving end voltages.

6.6. Conclusions:

Introductory investigations have been carried out in calculating some of the unbalances on untransposed bundle conductor lines. The study indicates the vast scope for further investigations. A thorough study of all the arrangements of circuits, number of conductors per phase and their disposition is time consuming and is being considered to be undertaken in future.

A method unexploited till now has been used to calculate the ground displacement factor due to electrostatic unbalance. Evidently this method has resulted in a large simplification in the size of the matrix to be solved.

CHAPTER 7

BUNDLE CONDUCTORS FOR DC TRANSMISSION:

7.1. Introduction:

DC transmission is gaining importance due to the inherent advantages over AC power transmission bundle conductors have been used to a limited extent on DC lines. This fact is well illustrated in Table 1.1, of Chapter 1. Till now only duplex arrangement has been used for DC power transmission, either monopolar or Bipolar.

7.2. Voltage Gradients:

Voltage gradient on a monopolar duplex line at a height h is given by-

$$g_{\max} = \frac{1}{r \log_e \frac{(2h)^2}{r \cdot m}} \left(1 + \frac{2r}{m}\right) \text{ KV/cm./KV} \quad (1)$$

voltage gradient for a bipolar duplex line at a height h and intra pole separation D is given by -

$$g_{\max} = \frac{1}{r \log_e \frac{D^2}{rm \left[1 + \left(\frac{D}{2H}\right)^2\right]}} \left(1 + \frac{2r}{m}\right) \text{ KV/cm./KV} \quad (2)$$

7.3. Corona Phenomenon:

The corona phenomenon is different on DC lines from that on AC lines. Each bundle in the case of a DC line is subjected to potential of one polarity only. Each bundle is therefore associated with the particular space charge only, and this space charge hangs on as long as the polarity of the voltage is not changed. Thus a positive space-charge forms on a negative bundle and a negative space charge on positive bundle. Hence the charge released from a bundle must be carried to ground or the conductor of opposite polarity only. This is not the case with AC corona, the space charge changes in sign in each half cycle. Thus the space charge surrounding the conductors in

a bundle of DC transmission line has a suppression effect and thus decreases the potential gradient. This evidently results in a decreased corona loss.

As a result of the difference in ionisation phenomenon around the positive and negative bundles, the corresponding corona is also different. On the bundle at positive polarity the corona pulses are infrequent and are associated with greater charges. The positive corona pulses are of a fraction of microsecond duration. The conductors at negative polarity are associated with negative corona pulses frequent in nature and of relatively small charge. The duration of negative corona pulses are relatively shorter. The colour of positive corona is reddish-orange and gives a cracking sound of low frequency. On the other hand, the negative corona is bluish in colour and produces a hissing noise of relatively high frequency. Farwell⁽⁷⁷⁾ established formulae for critical corona voltage at positive and negative polarities.

$$\text{Critical gradient for positive corona} = 35 \delta + 11.4 / (\delta / d) \text{ KV/cm.} \quad (3)$$

$$\text{Critical gradient for Negative corona} = 31.6 \delta + 11.9 / (\delta / d) \text{ KV/cm.} \quad (4)$$

Under same pressure, temperature and other ambient conditions positive corona/^{forms} first, on conductors of small diameter. However for conductors used in practice negative corona may appear first. Tichodeev⁽⁹⁹⁾ has derived efficiency coefficients for DC bundle conductor lines. Such coefficients have been presented for AC lines in this work.

7.4. Corona Losses on DC Lines:

Relatively not many investigations have been done on the behaviour of bundle conductors. However, time and again, reports have been made of measurement of corona losses and RI.^(74,78,84) Most of these

105156

CENTRAL LIBRARY UNIVERSITY OF INDIA
KORKEE

7.4.1. Effect of Weather on Corona Losses:

The various contingent weather variables have different effect on corona losses of DC bundle conductor lines.

Rain: Rain virtually increase the corona losses on both DC and AC lines. In both cases the increase in loss is due to wetting of the conductor. In the case of DC lines the losses increase only by about 10 times⁽⁷⁴⁾ the fair weather value, as compared to an increase of 100 times⁽⁴¹⁾ on AC lines. Inherently total losses on DC lines will be relatively less than the total losses on three phase AC lines. Fig.(7.1) shows the variation of corona losses on a bipolar duplex line in rain.⁽⁷⁸⁾

Wind: Corona losses are due to eventual drift of ions at different velocities in their respective directions. Under continuous potentials these ions move in one direction only either away or towards the conductor. Hence they are likely to be pushed towards or carried away from the conductor in the presence of wind.

On lines at alternating potentials, ions oscillate within a small distance from the conductor. Whereas, the ions oscillate over the whole distance between the conductors at opposite polarities on DC lines. Hence wind has no effect practically on AC lines as compared to DC lines.

Corona losses on DC lines are increased by wind due to two processes namely ionisation at the conductors and mixing of charge between them. Wind gives rise to both the processes by altering the rate of flow of ions by acceleration. Wind reduces the suppression action of space charge by carrying away some charge from the first conductor encountered and by adding this charge to the other conductor in the leeward direction, at opposite polarity. Thus

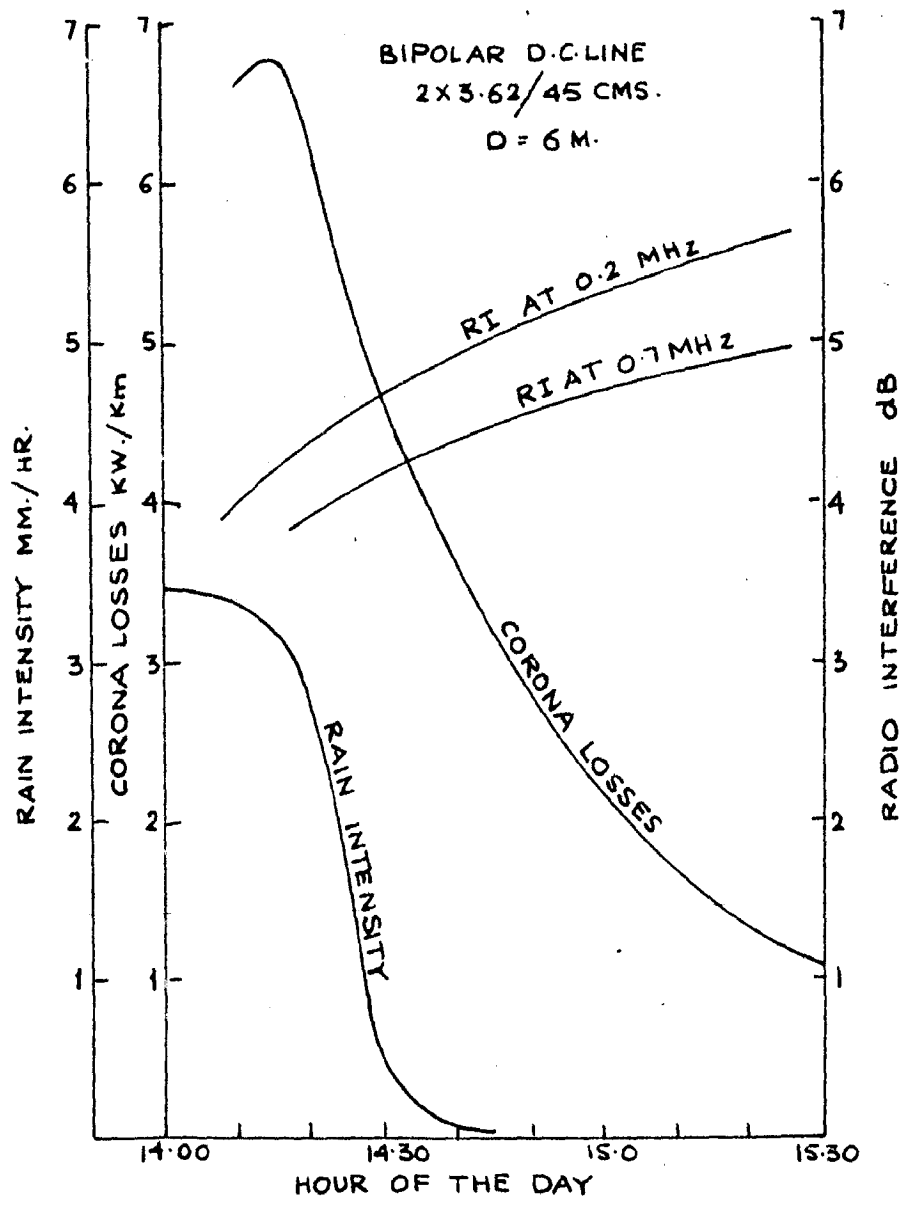


FIG. 7.1 PERFORMANCE OF A BIPOLAR D.C. LINE

In the meanwhile there is a fast intermixing of positive and negative ions which adds to the above process.

On bundle conductors, suppression of space charge on windward conductor is decreased while that on leeward conductor is increased. With a similar process on the bundle of opposite polarity a differential intensive ionisation takes place eventually increasing the losses.

Extensive investigations have not yet been carried on either test lines or actual lines in practice, of bundle conductors so it is not possible at present to give the quantitative analysis of the wind effect. (74)

Other weather variables: Snow increase corona losses in the same manner as rain, on both AC and DC transmission lines. Increase in percent relative humidity increases the losses due to settlement of moisture on conductors. Effect of relative air density on corona of DC transmission lines is not well known.

7.4.2. Effect of Voltage on Corona Losses:

Fig.(7.2B) shows the variation of corona losses at direct potentials. The curve also shows corona losses on AC lines for comparison purposes. Bipolar corona losses are higher than monopolar corona losses as can be expected. Corona losses on monopolar lines at negative potential are more than those at positive potential. The ratio of losses on negative to positive polarity is between 1 and 1.2. (84) The curves represent fair weather corona losses. It is observed that the losses are not as sensitive to voltage as on a three phase AC system. The losses on a DC line can be represented as (84)

$$W = F(g) \cdot n^2 \cdot r^2 \dots \dots (5)$$

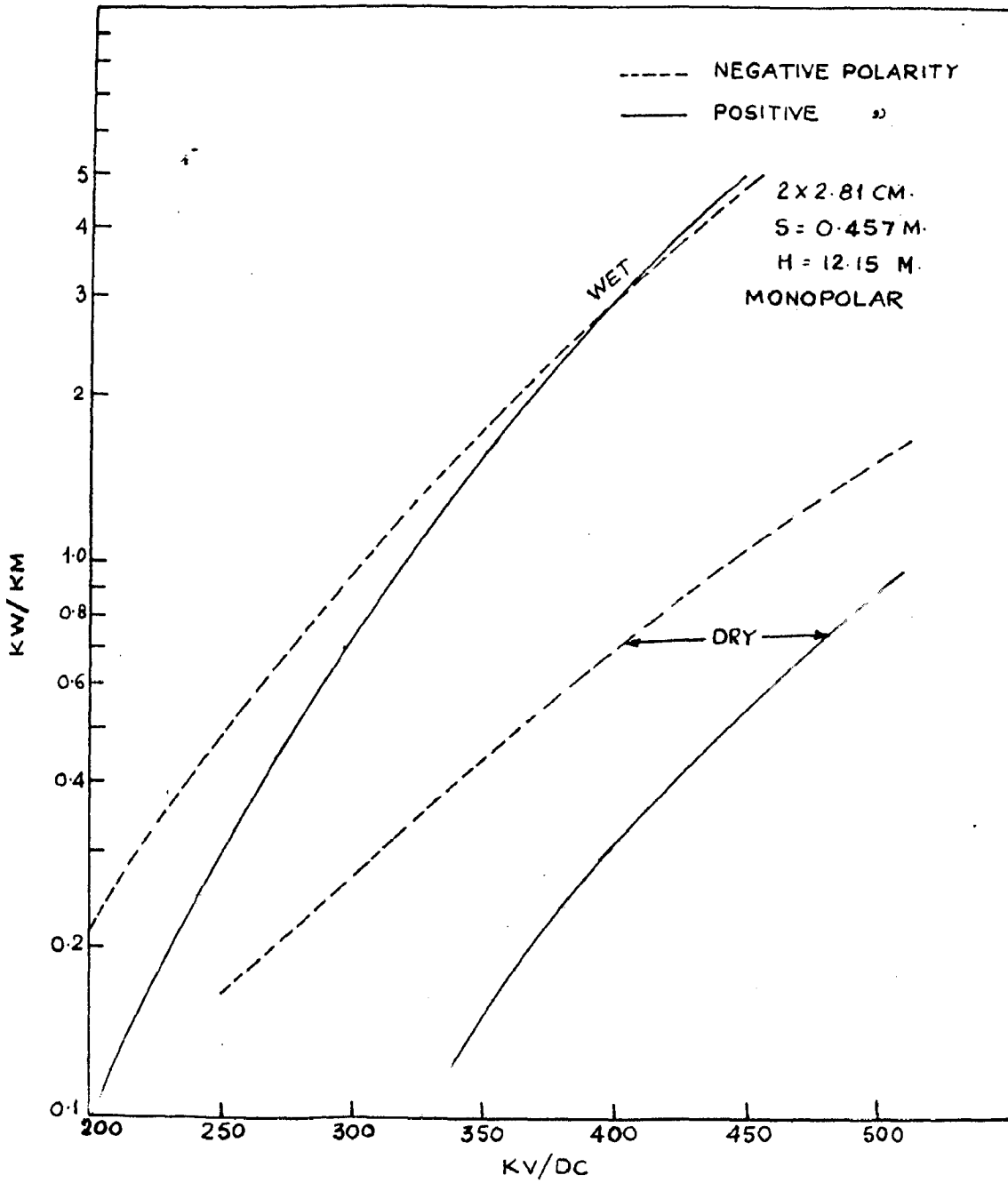
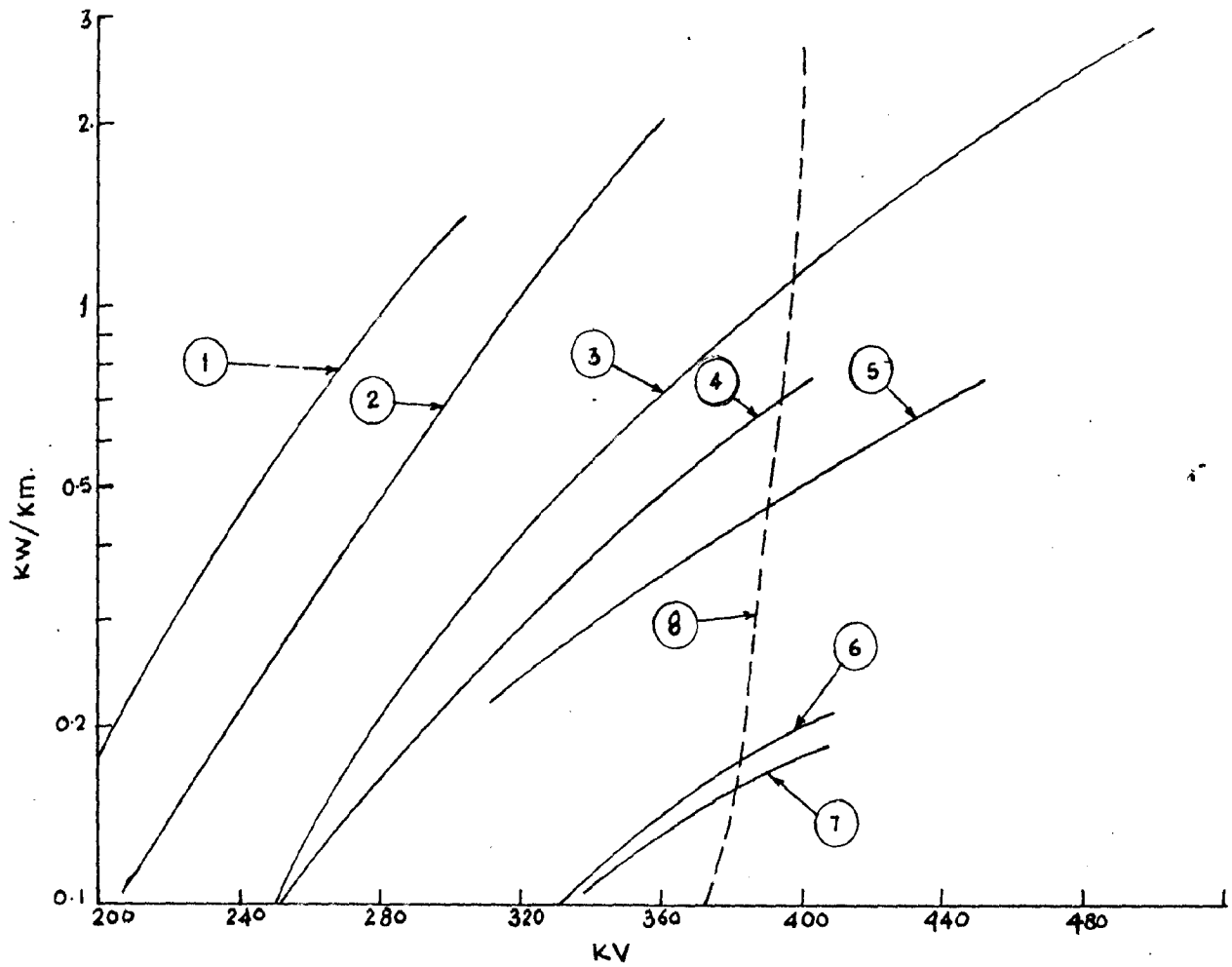


FIG. 7.2 A MONOPOLAR CORONA LOSSES



1. BIPOLAR 2 x 2.93 CM. ; D = 10 M. ; S = 0.4 M. ; H = 15 M.
2. BIPOLAR 2 x 3.17 CM. ; D = 10 M. ; S = 0.45 M. ; H = 13 M.
3. BIPOLAR 2 x 4.62 CM. ; D = 11 M. ; S = 0.457 M. ; H = 23.3 M.
4. MONOPOLAR NEGATIVE 2 x 3.17 CM. ; S = 0.45 M. ; H = 13 M.
5. MONOPOLAR " 2 x 3.77 CM. ; S = 0.45 M. ; H = 13 M.
6. MONOPOLAR POSITIVE 2 x 3.17 CM. ; S = 0.45 M. ; H = 13 M.
7. MONOPOLAR " 2 x 3.77 CM. ; S = 0.45 M. ; H = 13 M.
8. A.C. 3 ϕ ; 2 x 3.56 CM. ; D = 8.5 M.

①, ②, ④ TO ⑦ KOVALASKAYA et. al.

③ GEHRIG et. al.

⑧ ROBERSTON et. al.

FIG: 7.2 B CORONA LOSS VS VOLTAGE

the equations (1) and (2). This suggests the reduction of losses on bundled lines indirect proportion to the square of the number of subconductors. This however, is an optimistic value.⁽⁸⁴⁾

Fig.(7.2A) illustrates a different comparison. The curves show only monopolar losses, both at positive and negative potentials under dry as well as wet weather conditions. These curves show the losses on unweathered conductors. With aging the losses will still be lower. The losses are shown to increase with voltage both in fair and foul weathers, but, the incremental rates differ for both dry and wet losses. On monopolar lines the losses in wet condition may be as high as 10 times that in dry weather.

7.5. RI from DC Lines:

7.5.1. RI Generations:

EHV lines DC or AC are invariably associated with the high frequency interference, such as RI and TVI. EHV DC transmission line gives rise to RI in three ways.

- (1) By pulses, conducted from the converter station.
- (ii) By corona pulses on the line.
- and(iii) By partial discharges on insulators and associated hardware.

While, by proper screening the former can be completely eliminated,^(71,76) the other two modes of generation need consideration. However, RI from line conductors is discussed here.

Experiments⁽⁷⁸⁾ show that only RI from positive line is of some importance, where as that due to negative line is relatively of no importance and hence can altogether be neglected till a certain voltage level is reached. Same is the case on AC lines in the negative half cycle.⁽⁴¹⁾

7.5.2. Measurement of RI:

measure the RI. Any of the two specifications viz. CISPR⁽⁷³⁾ and USASI⁽⁹²⁾ or any variant thereof is used in measurement. Inherent errors such as pointed out in Chapter 5 may be neglected considering the variations in RI values under essentially similar conditions.

7.5.3. Short Line Test Results and Long Line Predictions:

It is convenient to conduct tests on short test lines while studying the effect of the inherent variables. The frequency spectra of such short test lines is characterised by peaks and valleys due to multiple reflections. It has been analytically shown that geometric mean value of such spectra gives the long line frequency spectrum.⁽³⁶⁾ The noise level throughout the length of the line may not be same due to inherent variation in weather conditions. A slightly higher value as was suggested for AC lines may be used.

7.5.4. SNR on DC and AC Lines:

Table 7.1 lists the values of SNR on a \pm 550KV duplex DC line (2 x 4.62mm., D = 10.05m) and a 345 KV AC line (1x4.07 cm.) operated under same conditions.⁽⁷⁴⁾ The table shows that- comparatively higher

TABLE 7.1
SNR ON AC AND DC LINES
(Measured with Rod antenna at 0.834 MHz)

Type of Reception	SNR on	
	DC line	AC line
Background not detectable	14.0	46.0
Background detectable	8.5	23.0
Background evident	4.0	13.0
Background objectionable	2.0	6.5
Difficult to understand	1.0	4.0
Unintelligible	0.55	0.9

AC lines, under similar operating conditions. An SNR of 9 to 1 gives a good reception on DC lines as against 25 to 1 on AC lines. (74)

However, on bundle conductor AC and DC bipolar lines in fair weather then there is very little difference in noise level. (78)

7.5.5. RI and Weather:

Rain: Fig.(7.1) shows the typical test results of bipolar duplex line at two frequencies, at 0.2MHz and 0.7MHz. As indicated RI drops down during rain, and as the rain stops and the conductors get dry RI increases to fair weather value. Similar behaviour is also exhibited in snowy conditions. This is in contradiction to the performance of AC lines. This is an additional advantage of DC lines. Bundle conductor lines have lower fair weather RI levels than single conductor lines. Hence Bundle conductor DC lines are the most suitable method of power transmission in cold regions. RI in foul ^{weather} is steady wrt frequency than in fair weather. (84)

Wind: The effect of wind on DC EHV lines was indicated while discussing corona losses. The ion drift and intermixing cause the difference in performance of DC lines as against AC lines. During windy weather not only are corona losses but also the RI levels are increased. No investigation has yet been made of the performance of bundle DC lines. (74)

7.5.6. Influence of the Line Voltage:

Fig.(7.3) illustrates the effect of the pertinent system variable viz., line voltage. Radio interference increases with the voltage as indicated. Evidently the RI level on bundle conductor line is less than that on single conductor line, for the same operating conditions. RI curves for DC lines are relatively smooth upto about $\pm 550KV$. Over and above this voltage line hardware contributes greatly to the overall RI level of the line. (74) The maximum RI

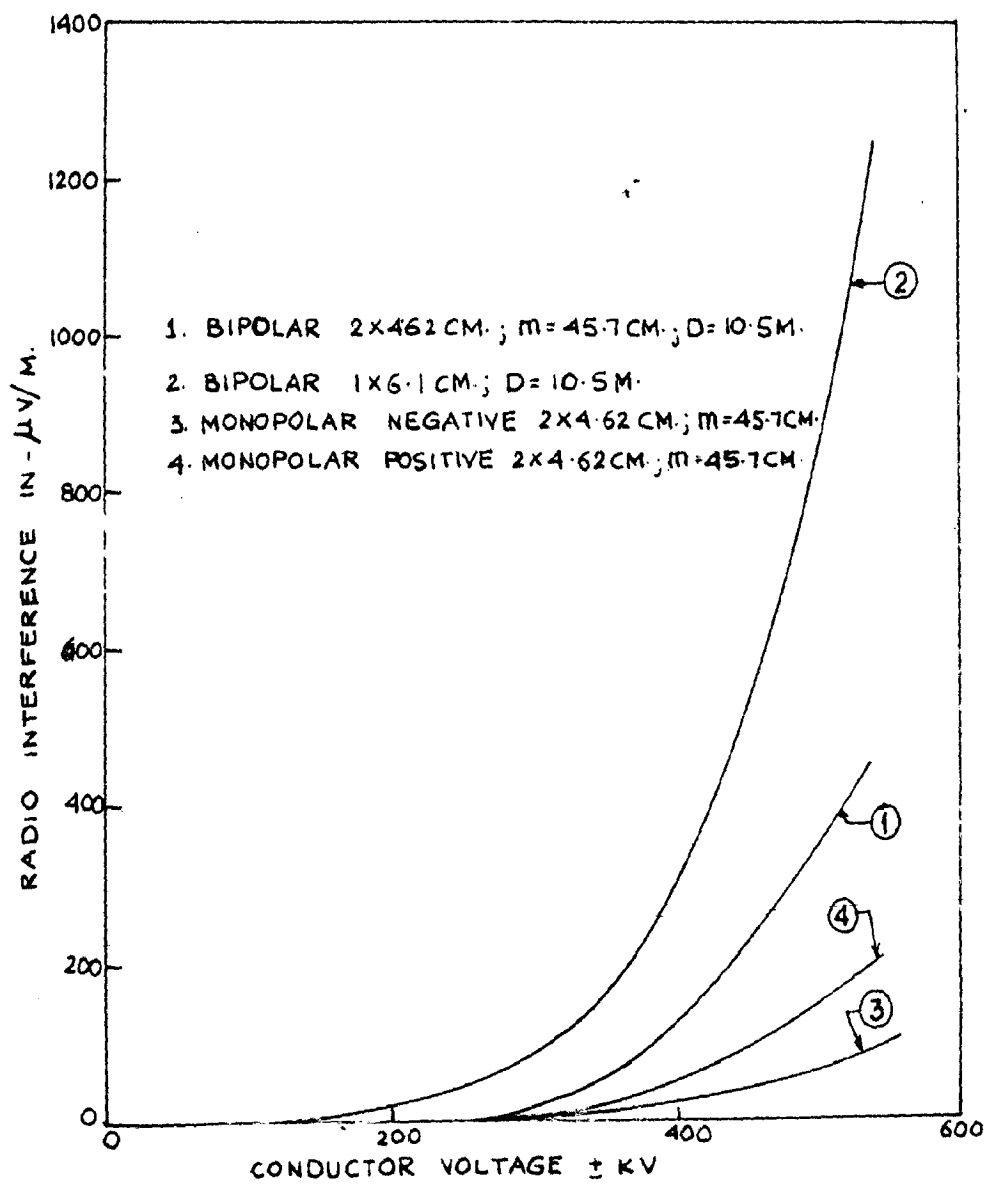


FIG. 7.3 EFFECT OF VOLTAGE ON RI

levels have a ratio of 2 to 1 for positive and negative conductors. Therefore as far as acceptance levels of RI is concerned it is enough if only the RI due to positive pole is considered in the case of bipolar DC lines. The RI for a monopolar (positive) line is about half that of bipolar line.

Experiments⁽⁷⁴⁾ have lead to a formula for predetermination of RI level on bundles DC line.

$$RI = k e^{ng} d^2 \quad \mu V/m \quad (6)$$

where,
 $k = 0.85$

7.6. Conclusions:

Bundle conductors on DC lines have the same advantages as that of AC lines, in addition the RI level under foul weather conditions are lower than under fair weather conditions. Fair weather RI levels are nearly the same as on AC lines. Definitely corona losses and RI levels on bundle conductor lines are lower than on single conductor lines.

Mostly duplex lines have been used in practice. Corona losses under foul weather increase by about 10 times where as on AC lines it may be as much as 100 times.

Losses on a bundle at negative potential are greater than on those at positive potential. Losses on DC lines are not as sensitive to voltage as on AC lines. The dominating influence of space charge produces this effect.

Bipolar RI and corona losses are greater than those on monopolar lines. Bipolar corona losses can be as much as 3 to 5 times higher than the sum of the corresponding monopolar losses. Drift of ions from one pole to the other causes this effect. Evidently the increase

same RI level on corresponding AC lines at same voltage to ground.

Much is to be investigated about the performance of DC bundle lines in foul weather, especially that in wind. Relations are yet to be established about the effect of relative humidity and relative air density factor.

CHAPTER 8

CONCLUSIONS AND PROPOSALS FOR FURTHER STUDY:

8.1. Conclusions:

(1) Bundle conductors are being used extensively throughout the world, for large blocks of power transmission at EHV over long distances. Practical limitations of the diameters that can be handled, in accordance with Kelvin's law led the power engineers to adopt the ingenious method of splitting the conductor into many subconductors. Most of the advantages materialise with the splitting of the single conductor into two sub conductors. Any further increase in the number of conductors will only add a little more to these advantages. Bundle conductor lines have less inductive reactance and proportionately increased capacitance. This leads to increased power transmission capability for example an increase of 30 percent capability is obtained by increasing the number of conductors from one to two. Triplex and quadruplex lines have an increase in capability of 40 and 50 percent respectively. In addition to increase in capability, for essentially the same area of cross section, the operating voltage level is also substantially increased as shown in Table 1.2.

(2) Voltage gradients around bundle conductors are less than those on the corresponding single conductor lines. The characteristic feature of the gradients around bundle conductors is their non-uniformity, around the surface. It is often enough to determine the maximum gradient on the bundle in outer as well as center phases for the determination of corona losses as well as radio interference. Intra-conductor spacing in practice is usually 15 to 20 percent higher than that defined by the minimum of maximum surface gradient, due to mechanical problems, such as maintaining adequate and constant

calculation have been compared in the Chapter on voltage gradients. There exists a difference in the gradient on each sub-conductor and this has been computed with the help of the IBM 1620 and is presented in Appendix B. Ground wires are usually neglected in the calculation of the gradients. This fact is substantially evident from the above calculations.

(3) Inductance of bundle lines decreases while the capacitance increases. The usual method of calculation of these quantities is illustrated and tables have been prepared for ready use for the three configurations-double circuit, single circuit horizontal and triangular. Graphs show the relative increases and thus provides a comparison of bundle conductors and single conductors.

(4) Corona on bundle conductors in fair weather is delayed to a much higher voltages due to reduced voltage gradients. Thus corona losses in fair weather are less than those on the single conductor lines. Foul weather losses evidently are lesser. It is possible to reduce or completely eliminate losses on bundle conductor lines in fair weather, by a suitable design. A bundle efficiency coefficient can be defined as the ratio of critical voltage on the bundle to that on single conductor line. Equations for such coefficients are derived for all possible arrangements of circuits as well as bundles. The equation for critical corona voltage due to Crary has been modified to take into account the separations and heights used in practice. Loss measurement techniques have been classified and compared. The loss variations on bundle conductor lines are studied and substantiated by the results obtained from test projects.

(5) Radio interference level of bundle conductor/is less than
 that of the single conductor line

SNR is different for same RI level in urban and rural areas. A suitable design can provide the required SNR. SNR for various classes of reception of radio signals and those allowable on transmission lines are tabulated. RI decreases lateral to the line with the square of the distance. The RI level at 30m from right of way is of interest as the radio receivers which usually are located in the vicinity are greatly affected, in comparison with receivers farther away. The formulae in use for estimation of RI level on transmission lines have been tabulated. There is very little difference in the formulae, even though they were formulated to suit the conditions existing in the respective countries. Once the test results are available, these formulae can be modified suitably to take into account the existing conditions in our country. The variation of RI levels with weather is illustrated with the help of the typical test results from the test projects. The analytical methods so far developed such as that of Adams are based on the rms value of the RI voltage generated. But, measurements all over the world have been done with quasi-peak meters because of their commercial availability and simplicity. It is necessary to take into account this fact, while correlating the determined levels from such analytical methods with those measured on the lines. Results from short test lines can be used to predict the frequency spectra of long lines by considering the geometric mean of the maximum and minimum of the frequency spectra on short lines. By plotting the signal strengths and RI levels at the particular frequencies, the frequencies affected by RI can be determined. Thus, by suitably limiting the RI level the required class of reception can be obtained. It is possible to attenuate the RI at any frequency using auxiliary conductors of quarter wave length connected to main

locating it at a considerable distance it is possible to relieve the listener of this nuisance factor.

(6) The modern trend in power transmission is to avoid transpositions, the transpositions if employed are the major sources of frequent faults and with bundle conductors, especially they are not only expensive but are also cumbersome. Avoiding transpositions causes electrostatic and electromagnetic unbalances. Computation of unbalances of bundle conductor lines is tedious because of the many variables involved. A brief treatment of the general calculations has been presented. A more thorough and extensive calculation is proposed to be carried out. A method hitherto unexploited for calculation of ground displacement factor with or without ground wires has been used (Chapter 6). This reduces the tedium of calculation to a great extent. This method while maintaining the accuracy, provides quick evaluation of the ground displacement factor. However, it is worth pointing out that in the formula for calculation of the equivalent conductor of the same total capacitance, the influence of ground wires - a factor which often not known is neglected. The unbalances of current distribution among sub-conductors is very small viz. about 1.5%.

(7) Bundle conductors are being used on HVDC lines also. They have the same advantages as on AC lines. Their performance in windy weather is greatly different from that of AC lines. RI and corona losses increase greatly, especially on positive poles. However, experimental determinations of the performance of bundle conductor lines is necessary before any conclusion is drawn from the often tested single conductor lines. Foul weather RI is less than that in fair weather. This is an added advantage of bundle conductors on HVDC lines, which supports their use in countries

(8) It is also worth pointing that there are not only advantages but many disadvantages also. For instance, the mechanical problems are greatly increased. Twisting and rotation under snow loads, frequent intra-conductor contacts due to vibrations, and serious intra-conductor contacts during short circuits cause much damage to the conductors. Spring loaded spacers are widely used on bundle conductor lines, but these often suffer premature failure due to the frequent electro-mechanical forces, corrosion etc. Though all the conductors in a particular bundle are maintained at the same potential at the sending end, due to inherent differences in conductors used, there is a potential across the spacers which further enhances chances of their failure. Proposals are made in the field, to adopt insulated bundle conductor system for carrier current propagation. This in addition is expected to reduce RI further by about 5 dB*. There are however controversies about this point. IBS (insulated bundle conductor system) is already in practice to a limited extent in countries like Japan. The fact that investment on bundle conductors is higher, is worth mentioning. It remains, to weight the advantages obtainable with increase in investment (about 13 percent for duplex systems) before deciding upon the method of transmission. However, at voltages at and above 400 KV bundle conductors are inevitable.

8.2: Proposals for Further Study:

(1) Corona gives rise to space charge around the bundle. Thus the capacitance of the bundle is increased. This leads to an increase in flux and a change in gradient from that of the bundle without corona. A mathematical base can be worked out to compute the above changes, by considering the virtual increase in conductor diameter. This, the author hopes, will lead to the exact analysis of the

performance of bundle conductor lines in corona and leads to correct assessment of corona losses and RI.

(2) In our country, power demand is rising greatly. This has led to exploitation of all possible power sources. This necessitates long distance power transmission at EHV. It is thus necessary to predetermine the performance of a bundle conductor line in our environments. A test line can be set up and studied under all the weather conditions and other pertinent system variables. Corona loss and RI levels can be assessed.

(3) The calculation of unbalances of untransposed lines are tedious and consume much time. The study of these unbalances can be split up into four parts viz. (i) electrostatic unbalance of single circuit lines (ii) electrostatic unbalance of double circuit lines (iii) electromagnetic unbalance of single circuit lines and (iv) electromagnetic unbalance of double circuit lines. This splitting in the opinion of author will lead to a more thorough study of the effect of the variables and will form guide lines to reduce or if possible completely eliminate these unbalances.

(4) The author proposes to set up field or Laboratory test project to study the behaviour of HVDC lines using bundle conductors, as it has been observed that RI decreases and corona losses increase on a HVDC line with single conductor per pole under windy conditions. A study, therefore, is justified to observe the behaviour of bundle conductor line under these conditions.

APPENDIX A

Conformal transformation allows folding or expanding a given region, in a plane, to a related region in another plane. This indicates the possibility of decreasing the complexity in determining the potential on and around the subconductors in a bundle. For instance a transformation of the form-

$$z^n = W$$

expands n times the given region (in W plane) to a related region (in W plane). So, the region in the vicinity of a conductor of an n conductor system (in W plane) can be represented by a complete plane (W plane), whence the problem becomes simple, as now only one conductor is considered. In reality a fictitious conductor of radius r is considered in W plane and its image (real conductor) is obtained in Z plane. Image of the field around the single fictitious conductor is obtained. Successive required number of mirrorings provides the actual field system in Z plane.

Fig.A.1 shows the transformation $z^2 = W$ and the changes in angle and magnitude. Fig.A.2 shows the same transformation from W plane (of a fictitious conductor) to Z plane (to the real conductor). For convenience the fictitious conductor is assumed to be located at $(-1, j0)$. Evidently the bundle circle radius R_m is given by-

$$R_m = \frac{1}{2} (\sqrt{1+r} + \sqrt{1-r}) -$$

and radius of the transmission line conductor

$$r = \frac{1}{2} (\sqrt{1+r} - \sqrt{1-r})$$

Intra-conductor separation is given by

$$m = 2 R_m$$

$$\text{So, } \frac{m}{r} = \frac{\frac{\sqrt{1+r} + \sqrt{1-r}}{2} + \frac{\sqrt{1+r} - \sqrt{1-r}}{2}}{\frac{\sqrt{1+r} - \sqrt{1-r}}{2}} = \frac{4r}{m}$$

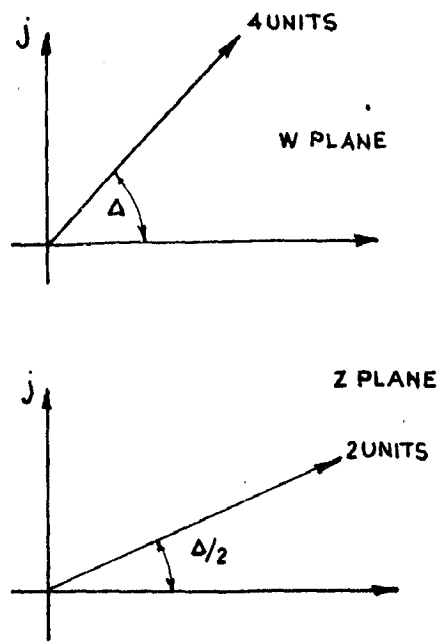


FIG. A.1 CONFORMAL TRANSFORMATION $Z^2 = W$

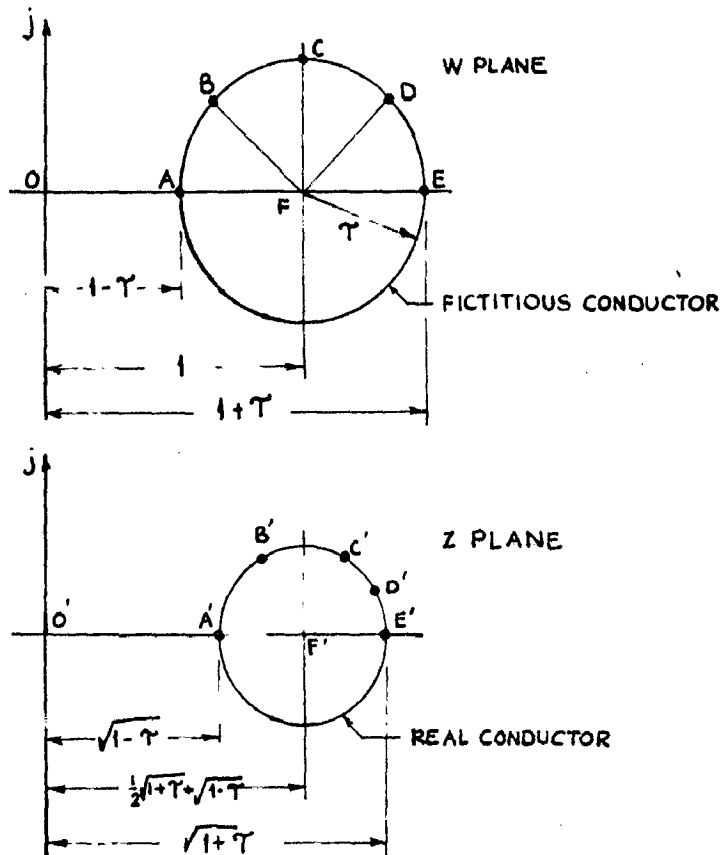


FIG. A.2 APPLICATION OF THE TRANSFORMATION $Z^2 = W$

APPENDIX - B

Due to inherent geometric dispositions of individual conductors of a bundle conductor transmission line, there exists a difference in gradient- instantaneous or maximum- on each subconductor. To consider each individual conductor, the only possible solution is that using Maxwells equations. It can be shown that the gradient factor can be obtained from the relation.

$$[P] [G] = [V]$$

where,

- [P] potential coefficient matrix, of order nxn, n is the number of conductors in the system including ground wires,
- [G] Column matrix of gradient factors,
- [V] Column matrix of voltages.

To assess the difference in gradient on each individual conductor a system shown in Fig.B.1 was considered. First, the voltage on centre phase conductors was assumed to be unity, in which case the voltage on the other two phases will be -0.5 p.u. The gradient factors were evaluated. Then, the voltage on left hand phase conductors was considered to be unity, and that on the central and right hand phase -0.5 p.u. Again the gradient factors were evaluated. The calculations performed on IBM 1620, using Gauss method of elimination are listed in Table B.1. In these calculations the voltage on ground wires (if present) was assumed to be 10^{-5} p.u.

This is pessimistically in conformity with the existing conditions on the system. However a sample calculation with the voltage of ground wire as zero, reveals that there is no significant difference in the gradient factor. The following conclusions can be drawn from the Table B.1.

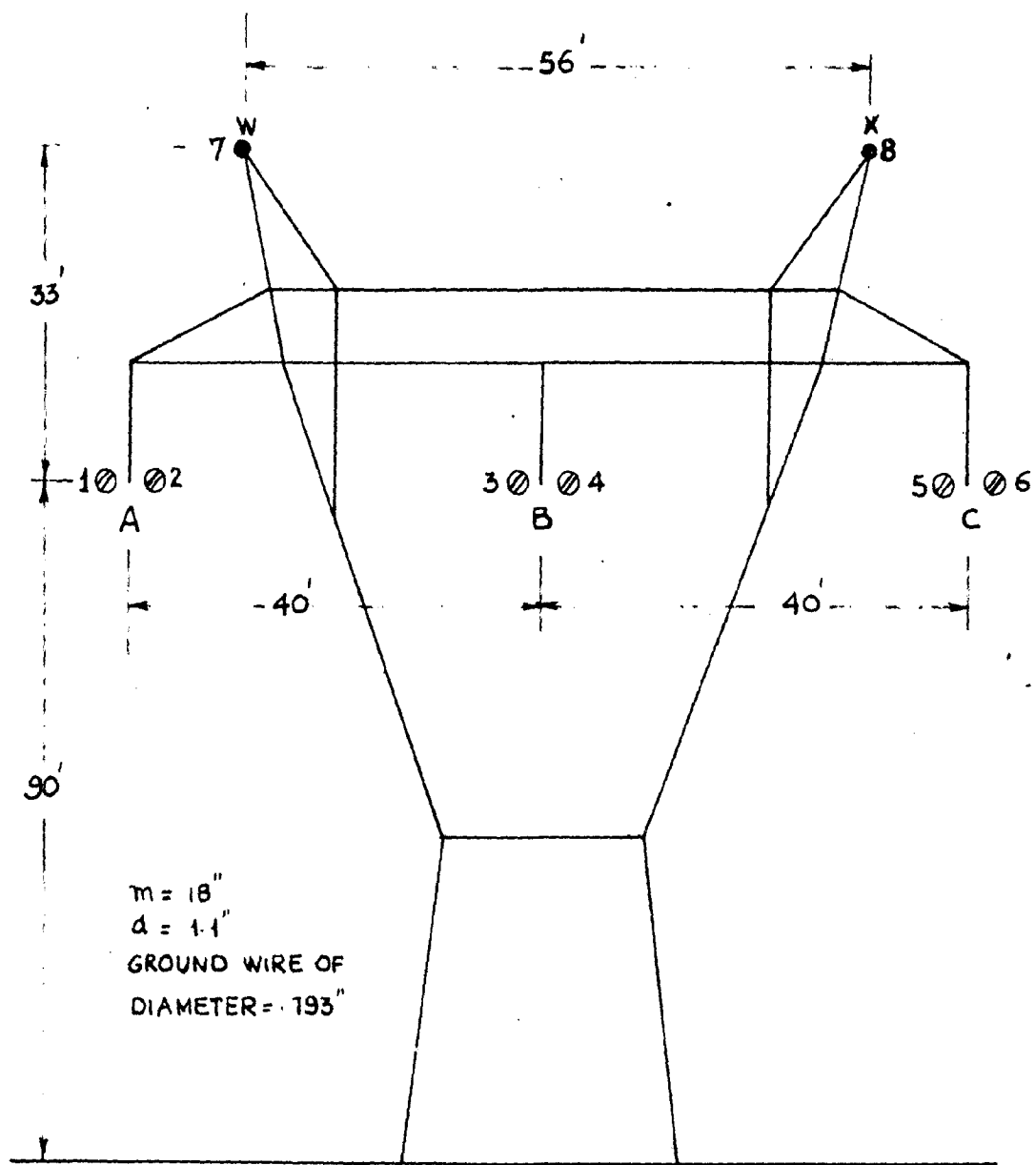


FIG. B.1 500 KV LINE STUDIED

(i) There is some difference in the gradient on each sub-conductor in outer phases of a horizontal single circuit line, and is about .15 percent. But these differences can be neglected in practice.

(ii) The maximum surface gradient on centre phase is greater than that on outer phases by about .7 percent.

(iii) Ground wires decrease the gradients. Reduction in gradient with two ground wires is more than with one ground wire.

and (iv) The gradient on ground wire fluctuates over a wide range depending upon the voltages on individual phases.

TABLE B-1

Studies of Voltage Gradients on Individual Conductors*

A - No ground wires; B-one ground wire on LHS; C- two ground wires.

Con- duc- tor.	Phase	Case 1 Voltage on			Case 2 Voltage on L.H		
		Centre phase	1.0 p.u.		phase	1.0 p.u.	
		A	B	C	A	B	C
1	Left hand	-.05315	-.05300	-.05295	.09235	.09351	.09305
2		-.05458	-.05442	-.05438	.09358	.09476	.09428
3	Centre	.10067	.10079	.10088	-.05155	-.050639	-.05160
4		.10067	.10078	.10088	-.04913	-.048249	-.04928
5	Right hand	-.05469	-.05451	-.05438	-.03883	-.038850	-.03991
6		-.05309	-.05309	-.05295	-.03930	-.03872	-.04010
7	(W)		-.004471	-.00134		-.01078	-.01212
8	Ground wires (X)			-.00134			-.01346

*System Configuration is shown in Fig.B.1.

REFERENCES

1. "Twin conductoring is adopted for 250 mile, 220KV Terni Genoa (Italy) line",
Electrical World, Jan.4, 1954, pp.47-48.
2. F. Cahen,
"Results of tests carried out at the 500KV experimental station of Chevilly (France) especially on corona behaviour of bundle conductors",
Tr AIEE, Vol.67, 1948, p.1118.
3. A. Rusk, Bo.G. Rathsman,
"Series capacitors and double conductors in Swedish transmission system",
Elect.Engg., Vol.69, 1950, pp.53-57.
4. I.W. Gross et.al.
"Corona investigation on extra-high-voltage lines 500KV test project of the American Gas and Electric Company",
Tr AIEE, Vol.70, 1951, p.75 and p.496.
5. M. Temoshok,
"Relative surface voltage gradients of grouped conductors",
Tr.AIEE, Vol.67, 1948, p.1583.
6. J.S. Carrol, M.M. Rockwell,
"Empirical method of calculating corona loss from HV transmission lines",
Tr AIEE, Vol.56, 1937, p.558.
7. E. Hazan,
"EHV single and twin bundle conductors-characteristics and selection",
Tr AIEE, Vol.78, Dec.1959, p.1425.
8. L.N. Stone,
"EHV single and twin bundle conductors- Influence of diameter",
Tr AIEE, Vol.78, Dec.1959, p.1434.
9. M. V. Rao,
"Unbalance of untransposed lines",
ME Thesis submitted to University of Roorkee, 1966.
10. F.G. Heyman,
"Geleierbundels vir Transmissielyne",
Tr.South African Inst.of Electrical Engineers, Vol.57,
May 1966, pp.85-100.
11. V.D. Kravencho, V.I. Levito V and V.I. Popkov,
"Measuring of corona losses on operating 400-500 lines",
Report no.407, CIGRE 1962.
12. P.A. Abetti, C.G. Lindh, H.O. Simmons (Jr.),
"Economics of single and bundle conductors for EHV transmission"
Tr AIEE, Vol.79, Pt.3, 1960, p.138.

13. G.E. Adams,
"Voltage gradients on HV transmission lines",
Tr AIEE, Vol.74, pt.3, 1955, p5.
14. G.E. Adams,
"The calculation of RIL of transmission lines caused by
corona discharges",
Tr AIEE, Vol.75, Pt.3, 1956, pp.411-19.
15. C.J. Miller,
"The calculation of Radio and corona characteristics of
transmission line conductors",
Tr AIEE, Vol.76, Pt.3, 1957, p.461.
16. H.B. Dwight,
"Surface voltage gradients of power transmission lines",
Tr AIEE, Vol.76, Pt.3, 1957, p.1217.
17. G.E. Adams,
"RI from HV transmission lines as influenced by the line
design",
Tr AIEE, Vol.77, Pt.3, 1958, p.54.
18. J. Reichman,
"Bundled conductor Voltage gradient calculations",
Tr AIEE, Vol.78, Pt.3, 1959, p.598.
19. N.B. Bogdanova et.al.
"Research in USSR",
Report no.411, CIGRE 1958.
20. L.B. Loeb,
"Electrical Coronas" (Book),
University of California Press, Berkely, 1965.
21. H.V. Gopalakrishna,
"RI parameter design of EHV transmission line",
J.I.E.(India), Vol.45, April 1965, p.163.
22. K. Schmidt,
"Chart showing gradient around sub-conductors",
Electrical world, April 1963, p.98.
23. P.A. Abetti et.al.
"Data gathering and transmission system for project EHV",
Tr AIEE, Vol. C & E 80, July 1961, pp.272-81.
24. Jack Davey et.al.
"Effect of station RN sources on transmission line noise
levels-experimental results",
Tr AIEE, Vol.PAS-86, Aug.1957, p.1007.
25. E.T.B. Gross, W. Chin,
"Electrostatic unbalance of untransposed single circuit
lines",
Tr IEEE, Vol.PAS-87, Jan.1968, pp.24-34.

26. C.J. Miller,
"Mathematical prediction of Radio and corona characteristics of smooth bundled conductors",
Tr AIEE, Vol.75, pt.3, Oct.1956, p.1029.
27. G.E. Adams,
"Analysis of RI characteristics of Bundled conductors",
Tr AIEE, Vol.75, Pt.3, Feb.1957,p.1569.
28. Gabrielle, Marchenko, Vassel,
"Bundled conductor transmission lines",
Tr IEEE, Vol.PAS-82, Jan.64, p.78.
29. G. Quileo,
"On equivalent diameter and the surface electric gradients of twin conductors",
Report no.214, CIGRE 1956.
30. O. Nigol,
"Analysis of RN from HV lines I: Meter response to corona pulses",
Tr IEEE, Vol.PAS-83, May 1964, pp.533-41.
31. O. Nigol,
"Analysis of RN from HV lines II: Distribution and correlation",
Tr IEEE, Vol.PAS-83, May 1964, pp.533-41.
32. H. Holley, D. Coleman, R.B. Shipley,
"Untransposed EHV line computations",
Tr.IEEE,Vol.PAS-83, March 1964, pp.291-6.
33. S.Y. King,
"An improved solution for the field near the bundle conductors",
Proc.I.E.E., Vol.110, June 1963, pp.1044-50.
34. A. Timaschef,
"Equipgradient lines in the vicinity of bundle conductors",
Tr IEEE, Vol.PAS-82, April 1963, pp.104-10.
35. W.C. Guykar et.al.
"Right of way and conductor selection for the Allegheny power system - 500KV transmission system",
Tr IEEE, Vol.PAS-85, June 1966, pp.624-32.
36. C.W. Helstrom,
"The spectrum of corona noise near a power transmission line"
Tr AIEE, Vol.PAS 80, 1961, pp.1-5.
37. R.L. Thompson et.al.
"500KV line design III- conductors",
Tr IEEE, Vol.PAS-82, Aug 1963, pp.587-97.
38. O. Nigol, J.G. Cassan,
"Corona loss research at ontorio hydro cold-water project",
Tr AIEE, Vol.80, June 1961, pp.304-13.

39. J. Reichman, J.R. Leslie,
"A summary of RI studies applied to EHV lines",
Tr IEEE, Vol.PAS-83, March 1964, pp.223-8.
40. G.A. Mackie, W.A.R. Lemire,
"Construction aspects of the Pinnard Hammer 500KV transmission
line",
Tr IEEE, Vol.PAS-83, March 1964, pp.205-14.
41. J.J. La Forest et.al.
"RN and corona loss results from project EHV",
Tr IEEE, Vol. PAS-82, Oct.1963, p.735.
42. M.H. Hesse,
"Electromagnetic and Electrostatic transmission line para-
meters by digital computer",
Tr IEEE, Vol.PAS-82, June 1963, pp.282-91.
43. H.B. Dwight, E.B. Farmer,
"Double conductors for transmission lines",
Tr AIEE, Vol.51, Sept.1932, pp.803-8.
44. E. Clarke,
"Three phase multiple conductor circuits",
Tr AIEE, Vol.51, 1932, pp.809-20.
45. S.B. Crary,
"Appendix C to Ref.44,
Tr AIEE, Vol.51, 1932, pp.820-21.
46. A.K. Abboushi, L.O. Barthold,
"Digital calculation of RN levels",
Tr AIEE, Vol.80, Dec.1961, pp.841-7.
47. IEEE Committee Report,
"Correlation of various RI meters and reading comparison of
RI meter operators on a 735 KV lines",
Tr IEEE, Vol.PAS-87, May 1968, pp.124-59.
48. W.J. La Forest, E.A. Whempley,
"R.N. aging characteristics of small aluminium conductors",
Tr AIEE, Vol.PAS-81, Oct.1962, pp.424-28.
49. E.T.B. Gross, W.J. Mc Nutt,
"Electrostatic unbalance to ground of twin conductors",
Tr AIEE, Vol.72, 1953, pp.1288-97.
50. W.H. Lewis,
"Some transmission line tests",
Tr AIEE, Vol.40, 1921, pp.1079.
51. S. Mutto,
"Sticking phenomena of double conductor transmission line and
mechanical vibration by corona",
Jl. IEE, Vol.74, 1954, pp.686-91.
52. E. Fritz,
"Conductor bundling may end"

53. N.H. Erlandson,
"Bundle reconductor combination Pays off",
Electrical world, 1954, pp.1906-7.
54. G.E. Adams,
"Voltage gradients on HV transmission lines",
Tr AIEE, Vol.74, 1954, pp.5-11.
55. C.J. Miller,
"Characteristics of smooth bundled conductor",
Ele.Engg.April 1956, p.598.
56. V.V. Burgsdorf, A. Ya. Liberman, V.K. Meshkov,
"Conductor Vibration and dancing on EHV transmission
lines employing bundle conductors",
Report no.219, CIGRE 1964.
57. W.E. Pakala, E.R. Taylor,
"A method for analysis of RN on HV transmission lines",
Tr IEEE, Vol.PAS-87, Feb.1968, pp.334-45.
58. A.L. Mohmstrom, L.G. Gifford, J.O. Smith,
"Short circuit tests on Bundle conductors",
Tr AIEE, Vol.77, 1958.
59. G.E. Adams,
"Wave propagation along unbalanced HV transmission lines",
Tr AIEE, Vol.78, 1959, pp.637-47.
60. F.M. Cahen, R.A. Tellier,
"Research in France which established 380/420KV AC system",
Elec Engg.April 1959, pp.320-4.
61. T.W. Liao,
"RIV caused by surface imperfections on single and bundle
conductors",
Tr AIEE, Vol.78, 1959, pp.1038-46.
62. J. Prest, R.F. Rissone,
"Bundle conductors on grid lines in England and Wales",
Proc.IEE, Vol.114, Dec.1967, pp.1873-87.
63. R. Bartenstür,
"Predetermination of HF interference level of HV transmission
lines",
Report no.409, CIGRE 1960.
64. M. Knudsen,
"Corona loss and RI measurements at HVAC on test lines in
Sweden",
Report no.411, CIGRE 1964.
65. F.M. Cahen, J.M. Carterton,
"Measurement of Corona losses under normal conditions",
Tr AIEE, Vol.77, Feb.1958, p.1525.
66. G.D. Lippert et.al.
"RI characteristics of bundle and single conductors",
Tr AIEE, Vol.77, Feb.1958, p.1525.

67. G.E. Adams, L.O. Barthold,
"The calculation of attenuation constants for RW analysis
of overhead lines",
Tr AIEE, Vol.PAS-79, 1960, pp.975-81.
68. W.S. Price, S.C. Bartlett, E.S. Zobel,
"Lightning and corona performance of 330KV lines on the
AGE & OVEC systems",
Tr AIEE, Vol.75, 1956, pp.583-92.
69. M. Hoshiai, T. Yamada, N. Mita, S. Yoshino,
"RI research in Japan with special reference to EHV
transmission",
Report no.403, CIGRE 1956.
70. T. Yamada, H. Kondo,
"EHV corona noise in Japan",
Report no.402, CIGRE 1960.
71. T. Yamada, S. Fuji, H. Konado, K. Okubo,
"Experimental investigation of the corona on the 800KV
Tanashi test transmission line",
Report no.404, CIGRE 1964.
72. F. Burlando Borelli,
"Electric conductors of convenient size",
Report no.227, CIGRE 1964.
73. L. Paris, M. Sforzini,
"RI problems in HV line design",
Tr IEEE, Vol.PAS-85, April 1968.
74. E.H. Gehrig et.al.
"BAPA's 1100 KV-DC test project: II RI and Corona loss",
Tr IEEE, Vol.PAS-86, May 1964, pp.278-86.
75. L. Paris, M. Sforzini,
"Energy losses in the economic design of AC transmission
sys-tem",
World power conference, Sept.1964.
76. P.G. Laurent et.al.
"DC interconnectaon between France and Great Britain by
submarine cables",
Report no.331, CIGRE 1962.
77. S.P. Farwell,
"The corona produced at contineous potentials",
Tr AIEE, Vol.33, 1914, p.1631.
78. N. Hyllen- Cavallins et.al.
"Corona losses, RI and Insulator requirements for HVDC
lines, studies regarding insulator interference for
frequencies between 30-1500 Mc/s",
Direct Current, Vol.9, Aug.1964, pp.95-108.
79. L. Boulet, B.J. Jakubzyk,
"AC corona in foul weather - I above freezing point",
Tr IEEE, Vol.PAS-83, May 1964, pp.502-12.

80. L. Boulet, B.J. Jakubzyk,
"AC corona in foul weather- II below freezing point",
JR IEEE, Vol.PAS-85, June 1966, pp.649-56.
81. L.M. Robertson,
"Colorado high altitude corona tests, I, II & III",
Tr AIEE, Vol.76, June 1957.
82. B.M. Bailey,
"Progress report on BPA HVDC test line-RN and corona loss",
Tr IEEE, Vol.PAS 86, Oct.1967, p.1411.
83. A.A. Akopyan et.al.
"The 750 KV experimental-commercial transmission line
konakovo-Moscow",
Report no,413, CIGRE 1964
84. R.M. Morris, B. Rakoshdas,
"An investigation of corona loss and RI from transmission
line conductors at high direct voltages",
Tr IEEE, Vol.PAS-83, Jan.1964, p.5.
85. G. Jancke,
"The development of the Swedish 400KV network" Tr IEEE,
Tr IEEE, Vol.PAS-83, Mar.1964, pp.197-205.
86. B. Rakoshdas,
"Pulses and RIV of direct voltage",
Tr IEEE, Vol.PAS-83, May 1964, pp.483-91.
87. E.T.B. Gross, M.H. Hesse,
"Electromagnetic unbalance of untransposed lines",
Tr AIEE, Vol.72, Dec.1953, pp.1323-36.
88. J.G. Anderson et.al.
"Corona loss characteristics based on project EHV research",
Tr IEEE, Vol.PAS-85, Dec.1966, p.1196.
89. J.J. LaForest et.al.
"RN levels of EHV transmission lines based on project
EHV research",
Tr IEEE, Vol.PAS-85, Dec.1966, p.1213,
90. E.R. Taylor, W.E. Pakala, N. Kolciko,
"The Apple grove 750KV project- 515KV RI and corona loss
investigations",
Tr IEEE, Vol.PAS-84, July 1965, p.561.
91. E.R. Taylor, W.E. Pakala, N. Kolciko,
".....775KV Project.....",
Tr IEEE, Vol.PAS-84, July 1965, p.573.
92. IEEE Committee Report,
"Transmission system Radio influence",
Tr IEEE, Vol.PAS-84, Aug 1965, p.714.
93. A.T. Edwards, J.M? Boyd,
"Bundle conductor spacer requirements and development of

94. G. Jancke, D. Zetterholm, E. Danielson,
"Bundled conductors meet all Swedish requirements",
Ele.Light and Power, Vol.33, Mar.1955, pp.55-61.
95. T.V. Sreenivasan,
"Potential, potential gradient and evaluation of corona
losses on dual conductor lines",
Jl.IE(India),Vol.40,Part 2, Dec.1960, pp.419-29.
96. A.S. Timaschef,
"Field Patterns of bundle conductors and their electrostatic
properties",
Tr AIEE, Vol.PAS-80, Oct.1961, pp.599-7.
97. L.M. Robertson,
"Testing EHV design at high-attitudes",
Electrical World, Vol.146, July 9, 1956, pp.90-91.
98. E.T.B. Gross and L.R. Stensland,
"Characteristics of twin conductor arrangements",
Tr AIEE, Vol.77, 1958, pp.721-25.
99. C. Adamson and N.G. Hingorani,
"HVDC Transmission" (Book),
Garraway, London, 1960.
100. T.F. Perrine,
Engineering Reference sheet,
Electrical world, Aug.10, 1959, p.49.
101. T.F. Perrine,
Engineering reference sheet,
Electrical world, Aug.24, 1959, p.60.
102. J. Kaminiski, Jr.,
"Development of corona shields for suspension assemblies
of bundled conductor transmission lines",
Tr AIEE, Vol.77, April 1958, pp.88-94.
103. E.L. Peterson et.al.
"Line conductors- Tidd 500KV test lines",
Tr AIEE, Vol.66, 1947, p.1603.
104. C.F. Wagner et.al.
"Corona considerations on HV lines and design features
of Tidd 500 KV test lines",
Tr AIEE, Vol.66, 1947, p.1583.
105. E.T.B. Gross, M.H. Hesse,
"Electromagnetic unbalance of untransposed lines",
Tr AIEE, Vol.PAS-72, 1953, pp.1288-96.
106. J.S. Carrol, B. Cozens, T.M. Blakeslee,
"Corona losses from conductors of 1.4 inch diameter",
Tr AIEE, Vol.53, 1934, p.1727.

107. C. Francis Harding,
"Corona loss between wires at EHV-II",
Tr AIEE, Vol.43, 1924, p.1182.
 108. R.L. Tremaine, G.D. Lippert,
"Instrumentation and measurement-Tidd 500KV test lines",
Tr AIEE, Vol.66, 1947, p.1624.
 109. D. Coleman, F. Watts, R.B. Shipley,
"Digital calculation of overhead transmission line
constants",
Tr AIEE, Vol.PAS-78, Feb.1959, pp.1266-68.
 111. T.S.M. Rao, K.B. Misra, H. Chandra Gupta,
"EHV Transmission line parameter calculations",
Depart, Publ. University of Roorkee, no.3, 1968.
-